

NASA Technical Memorandum 87634

Ground Vibration Test of an F-16 Airplane With Modified Decoupler Pylons

F. W. Cazier, Jr., and M. W. Kehoe

APRIL 1986



NASA Technical Memorandum 87634

Ground Vibration Test of an F-16 Airplane With Modified Decoupler Pylons

F. W. Cazier, Jr.

*Langley Research Center
Hampton, Virginia*

M. W. Kehoe

*Ames Research Center
Dryden Flight Research Facility
Edwards, California*



National Aeronautics
and Space Administration

**Scientific and Technical
Information Branch**

1986

Contents

Summary	1
Introduction	1
Test Configuration	2
Test Equipment	2
Test Procedures	2
Excitation	2
Frequency Sweeps	2
Structural Mode Measurement	3
Pylon Position	3
Pylon Preload	3
Results and Discussion	3
Rigid-Body Modes	3
Structural Modes	3
Correlation of Analytical and Measured Data	4
Comparison With Previous Test	5
Concluding Remarks	5
References	6
Tables	7
Figures	11
Appendix A—Frequency Sweep Data	23
Appendix B—Mode Shape Data	56

PRECEDING PAGE BLANK NOT FILMED

Summary

The decoupler pylon is a passive wing/store flutter suppression device. It was modified to reduce friction following initial flight tests. Prior to flight tests of an F-16 airplane with modified decoupler pylons, a ground vibration test was conducted on an F-16 loaded with the flight test stores configuration. Each wing carried a one-half-full (center bay empty) 370-gal fuel tank mounted on a standard pylon, a GBU-8 store mounted on a decoupler pylon, and an AIM-9J missile mounted on a wingtip launcher. Sinusoidal frequency sweeps were performed, and frequency response functions at several locations on the airplane were measured with the modified decoupler pylon in the centered and nose-up position. In addition, the pylon was tested with an applied side load and yaw moment. The effect of shaker force level on the GBU-8 pitch mode was measured. Rigid-body modes and structural modes were identified. Mode shape data were taken for six symmetric and five antisymmetric structural modes. The modified decoupler pylon was characterized by substantially reduced lateral free play, reduced friction about the pitch axis, and a lowered GBU-8 pitch mode frequency.

Introduction

Modern lightweight fighter airplanes are required to carry many types and combinations of external wing-mounted stores. The carriage of some of these stores can result in wing/store flutter speeds that are within the desired operational envelope of the airplane. If wing/store flutter problems occur, the solution normally requires increasing the structural stiffness, with an accompanying increase in weight, or reducing the airplane envelope. The decoupler pylon is a passive device for suppression of wing/store flutter. In the decoupler pylon concept, described in reference 1, the store is attached to the wing by using a pivoting attachment point, soft spring, and damper such that the pylon pitch frequency is less than the fundamental wing bending frequency. The static pitch deflection of the soft-mounted store due to maneuvers and changing aerodynamic drag forces may be minimized by a low-frequency feedback control system. The results of several wind-tunnel tests using model decoupler pylons on three different flutter models are given in reference 2. In each case, increases in flutter speed in excess of 40 percent were demonstrated with properly designed decoupler pylons.

Because of the success of these wind-tunnel tests and the need to examine parameters that could not be simulated properly in ground tests, such as maneuver loads and turbulence, two flightworthy pylons

for an F-16 airplane were designed and fabricated under contract to the General Dynamics Corporation. The results of the feasibility and conceptual design of these pylons are given in reference 3. The design, manufacture, and ground testing of the decoupler pylons mounted in a test fixture are documented in reference 4. These tests revealed that the pylon was binding in the pylon pivot bushings. The pylon with bushings is referred to in this report as the "initial decoupler pylon." Calculations were made indicating that atmospheric turbulence might be adequate to overcome the friction due to binding and thus allow the pylon to function properly in flight. Therefore, the pylons were not modified at that time. In preparation for flight tests with the initial decoupler pylons, a ground vibration test (GVT) was conducted (documented in ref. 5) on an F-16 with the flight test store configuration. In this configuration each wing carries a one-half-full (center bay empty) 370-gal fuel tank mounted on a standard pylon, a GBU-8 store mounted on a decoupler pylon, and an AIM-9J missile mounted on a wingtip launcher. This configuration exhibits well-defined antisymmetric flutter when the GBU-8 store is carried on a standard pylon. In subsequent flight tests, the initial decoupler pylon did suppress the flutter that occurs with the standard pylon. However, the binding in the pylon pivot bushings prevented the initial decoupler pylon from completely decoupling store and wing motions.

Following the first series of flights, the decoupler pylon was modified to reduce the friction. The modification consisted of replacing the pylon pivot bushings with a combination of roller and thrust bearings. The modification, design, and ground tests of the modified pair of decoupler pylons mounted in a test fixture are described in reference 6.

This report contains the results of a GVT conducted on an F-16 with the flight test store configuration in which the modified decoupler pylon is used to carry the GBU-8 store. This GVT was a joint effort by the Dryden Flight Research Facility of the Ames Research Center (referred to as "Ames-Dryden") and the Langley Research Center, with the General Dynamics Corporation/Fort Worth Division providing technical assistance. The test was performed at Ames-Dryden from August 30 to September 10, 1984.

The objectives of the GVT were as follows:

1. To measure the frequencies of airplane structural modes below 24 Hz.
2. To measure mode shapes for the first three symmetric and antisymmetric structural modes.
3. To study any unusual vibratory motion of the modified decoupler pylon and/or airplane.

4. To assess predictive analysis accuracy by comparing measured modal data with predicted data.
5. To measure the effect of shaker force level on the modal frequencies for the pylon vertical and lateral modes.
6. To measure the pylon pitch frequency with the pylon positioned against its nose-up electrical travel stop.
7. To measure the pylon pitch frequency with a yawing moment and side load applied.

Test Configuration

The F-16 airplane with test stores used in the flight test and ground vibration test is shown in figure 1. The airplane was on its landing gear during the ground vibration test. The landing-gear struts were collapsed to eliminate potential nonlinearities in the oleo strut. The tires were deflated to approximately one-half the normal pressure to provide a soft support. External electrical and hydraulic power were supplied to the airplane. The control system was initially turned on to trim the control surfaces to their neutral position. Once the control surfaces were trimmed, the flight control system was turned off electrically.

The airplane fuel loading for the test was full fuselage tanks, empty wing tanks, and one-half-full (center bay empty) 370-gal external fuel tanks. As a safety measure, the fuel tanks were pressurized with nitrogen gas to provide an inert atmosphere.

The decoupler pylon, as illustrated in figure 2, incorporates an upper part fixed to the wing and a movable lower part to which the store is attached. Key features of the decoupler pylon are a four-bar-linkage mechanism, a damper, a spring, and an alignment device. The spring stiffness is such that the pylon pitch mode frequency is below the antisymmetric first wing bending mode. Each of the modified pivot joints incorporates roller and thrust bearings to reduce friction and lateral free play. Figure 3 details the bearings in the forward-link upper pivot joint. Also shown for comparison is the pin/bushing forward-link upper pivot joint of the initial decoupler pylon. Ground tests (ref. 6) indicated that the average pitch moment required to overcome friction was reduced 44 percent by the modification. Even with the modified joint, however, the friction forces were sufficiently high that the damper was not required for flight. For this reason, the viscous fluid in the damper was removed. The pylon alignment system consists of an electric motor with a gearbox, on-off switches, and travel limit switches. The alignment system operates only on the static pitch position of the store. The on-off switches activate the alignment motor when the store becomes misaligned from its

nominal position by more than $\pm 0.5^\circ$. The physical pitch limits of the pylon are 3.0° up or down. If the alignment system malfunctions, travel limit switches deactivate the alignment motor prior to contacting the physical limits.

The airplane was tested with the modified pylon and GBU-8 store in the following three different conditions: (1) in the null or trimmed position, (2) positioned against the nose-up electrical stop limit, and (3) in the null or trimmed position with 450-lbf side force applied 34 in. forward of the GBU-8 store center of gravity.

Test Equipment

Ames-Dryden GVT equipment was used for the test. The excitation system consisted of four electrodynamic shakers (two 50 lbf and two 150 lbf), four power amplifiers with independent gain and phase control, and a sweep oscillator for a function generator. Response-measuring equipment consisted of six piezoelectric accelerometers with associated signal conditioning, six tracking filters, and common display and recording devices. A coincident/quadrature (co/quad) analyzer was used for tuning modes.

Test Procedures

Excitation

Single shaker and multishaker techniques were used to excite the airplane rigid-body and elastic modes. Electrodynamic shakers were used to input a sinusoidal forcing function to the structure. The locations at which the shakers were attached and their force ratings are listed in table I, and the actual forces used in testing are indicated in the figures throughout this report. Typical shaker setups are presented in figures 4 and 5.

Each shaker was attached to the airplane by means of a telescoping thrust rod, a force link, and a mechanical fuse. The fuse was attached to a locking ball nut joint, which was either mounted directly to the structure by a threaded stud or bonded to the structure. These components, except the force link, are shown in figure 6.

Frequency Sweeps

The frequency sweeps were performed from 2 to 24 Hz, which encompassed all modes of interest. A logarithmic sweep rate of 0.6 decade per minute was used to adequately concentrate the sweep time at lower frequencies. For the sweeps, accelerometers were placed at several locations and oriented in the vertical and lateral directions. The frequency response plots were recorded on XY plotters.

Structural Mode Measurement

Modal tuning criterion. After the frequency sweeps were completed, each airplane structural mode of interest was finely tuned by using a co/quad analyzer with one acceleration and one force signal as inputs. Each mode was tuned by minimizing the coincident component (in phase) with an accompanying maximization of the quadrature (out of phase) component. Time history traces of acceleration were used to measure phasing between the left and right sides of the airplane. A check of the purity of the modal response was made by terminating electrical power to the shaker and observing the decay of the oscillations for beats. The absence of beats in the decay trace indicates that a mode is properly tuned. In addition, the damping for each mode is calculated from the decay trace.

Modal survey. Once a mode was tuned, a modal survey was performed using the roving accelerometers. The survey points are shown in figures 7 through 9. The point on the structure with the largest amplitude reading was selected as the reference point. The reference was used to normalize all other accelerometer response values and to determine phase relationships with roving accelerometers. Each roving accelerometer was placed at the reference point before the survey. The accelerometer amplifier gains were adjusted as necessary to ensure uniform readings. (Measurements were made in the vertical (V) direction only for symmetric modes and in the vertical and lateral (L) direction as appropriate for the antisymmetric modes.) Some modes were surveyed completely, whereas other modes were surveyed only to the extent that they could be identified.

Pylon Position

Experimental test data from General Dynamics indicated that the pylon pitch stiffness depended on the GBU-8 store position. The position with the pylon nose up against the physical stop was considered the most critical because the pitch stiffness in this position was greater than the stiffness of the production weapons pylon. Subsequent to the General Dynamics tests, however, the alignment system limit switches were set so that the pylon would not contact the physical stops. Thus, for this test, when the pylon was in the nose-up position, it was at its nose-up electrical limit.

Pylon Preload

One of the objectives of the GVT was to determine mode frequencies when the pylon was loaded

with a combined side load and yawing moment. This test was performed to simulate possible flight loads. A combined side load and yawing moment was applied to each GBU-8 store, as shown in figure 10. A 450-lbf load was applied 34 in. forward of the store center of gravity by using a hydraulic ram attached to a 3/8-in. bungee chord. A load cell was used to measure the input force.

Results and Discussion

Rigid-Body Modes

The rigid-body modes of the airplane supported on its landing gear were measured. These modes included pitch, roll, vertical translation, and a combination yaw/roll mode. The lateral and fore-and-aft translation modes were not excited. The measured rigid-body frequencies and damping values are compared with the analytical frequencies from reference 6 in table A.

Table A

Mode	Rigid-body frequency, Hz		Damping coefficient, <i>g</i>
	Analysis (ref. 6)	Measured	
Pitch	1.98	1.83	0.123
Roll	3.00	2.17	0.083
Vertical translation . . .	2.75	2.73	0.054
Yaw/Roll	0.64	0.91	0.097

Structural Modes

Frequency sweeps. Multishaker frequency sweeps were performed at several force levels and with the shakers at several locations. Symmetric and antisymmetric sweeps were performed to identify approximate frequencies of the modes and to ensure that modes were not omitted. Thirty sweeps are given in appendix A.

Mode identification. Structural modes were identified by their frequencies and mode shapes. Tables II and III list the symmetric and antisymmetric modes, respectively, that were identified and give the measured frequencies and damping of the airplane with the pylon in the nominal position, nose-up position, and nominal position with applied preload. A complete or partial modal survey was performed on these modes. The measured mode shapes are presented in appendix B.

Correlation of Analytical and Measured Data

Analytical mode frequencies and mode shapes were available from a vibration analysis in which the airplane was supported on its landing gear and had frictionless decoupler pylons (ref. 6). The fuel loading used in the analysis was the GVT configuration. The analytical mode frequencies are given in tables II and III. In general, correlation of analysis and test data for all structural modes was good, with all modes being within ± 10 percent of the predicted value except for the one mode that was predicted but not found experimentally. Comments on several modes of interest are given in the following sections.

GBU-8 pitch mode. Frequencies for the measured symmetric mode (3.31 Hz) and antisymmetric mode (3.29 Hz) correlated well with the predicted values (3.18 Hz and 3.24 Hz, respectively) for the pylon in the nominal position. Ground tests made at General Dynamics (ref. 6) indicated that the modified pylon had less friction than the initial pylon. Hence, a smaller force would be required to break the pylons out of the friction band. An oscillating shaker force of 35 lbf at the nose of the GBU-8 was required to break the pylons out of the friction band so that the pylons were decoupled. This was one-half the force level required for the initial pylon. The pylons were determined to be decoupled by visually observing motion between the upper and lower portion of each pylon and by observing the presence of the resonance peak in the frequency sweep data. The decay traces for the left and right GBU-8/pylon accelerometer indicated that the damping for each pylon is high and approximately the same. These results correlate with the results obtained at General Dynamics.

With the pylon at its nose-up alignment system limit, the measured pylon pitch frequencies were 4.07 Hz for the symmetric mode and 3.89 Hz for the antisymmetric mode. These measured frequencies were much higher than the frequencies obtained with the GBU-8 centered. The pylon alignment motor travel limit switches had been set such that the nose-up position of the pylon was very close but did not contact a hard travel stop. However, movement of the GBU-8/pylon from this position during shaker excitation caused the pylon to contact the hard travel stop. This introduced nonlinearities into the time history trace of the motion. This mode was not surveyed because of these nonlinearities.

The GBU-8 pitch mode was also measured when the pylon was preloaded by applying a side load and yawing moment. The measured symmetric and antisymmetric frequencies for this condition were 3.41 Hz and 3.20 Hz, respectively. The measured

frequencies indicate that at this position the pylon pitch stiffness was nearly the same as with the pylon centered.

The effect of shaker force on the GBU-8/pylon pitch mode frequency with the pylon in the nominal position is shown in figure 11. In general, the data indicated a slight increase in frequency for the anti-symmetric mode as the force level was increased. No trend was indicated by the data for the symmetric mode.

GBU-8 lateral mode. The GBU-8 lateral mode was excited in the nominal position only. At this position it was noted that the measured symmetric and antisymmetric frequencies for the right pylon agreed very well with analysis. However, the left-pylon symmetric mode frequency was slightly higher than the predicted value and the left-pylon antisymmetric mode frequency was lower than the predicted value. Because of the difference in the frequency of the left and right lateral modes, there was poor phasing between the left and right sides, and each pylon was tuned individually. The free play of each pylon was measured by placing a dial indicator 12 in. aft of the GBU-8 nose. The left-pylon free play was 0.005 in. and the right-pylon free play was 0.008 in. The corresponding free play in the initial decoupler pylons was greater at 0.120 in. and 0.140 in., respectively.

The effect of shaker force level on the lateral frequency of the decoupler pylon in the nominal position is shown in figure 12. The data indicate that as the force level was increased, the frequency of the symmetric mode increased slightly. When the excitation force level was increased on the antisymmetric mode, the difference in frequency between the left and right pylons decreased.

370-gal tank modes. As seen in tables II and III, a different frequency was recorded for the right- and left-tank pitch modes. This was observed for both symmetric and antisymmetric modes with the pylon placed in the nominal position, in the nose-up limit position, and in the nominal position with preload. The frequency difference ranged from 0.48 to 0.67 Hz. The quantity of fuel in each tank was checked. The cockpit fuel gauges indicated 1100 lb of fuel in each tank. The fuel level in each tank bay was visually checked, and it was noted that the fuel level in each bay was very near the filler cap opening. The center bay compartment of each tank was empty. The torque of the bolts securing the fuel tank pylon to the wing was checked and found to be the correct value. Thus, no cause for this difference in frequency was determined.

A frequency difference between the left and right tank of approximately 0.4 Hz was also recorded for the tank yaw mode. This was observed for the symmetric and antisymmetric modes in the nominal position. The tank yaw mode was not excited in the pylon nose-up position or with the pylon preloaded. There was no measurable free play for either fuel tank. The cause of this frequency difference was not determined.

Missing modes. A symmetric missile pitch/wing bending mode at 6.67 Hz and an antisymmetric tip missile pitch/GBU-8 yaw mode at 6.45 Hz were predicted by the analysis. However, these modes were not identified during the test. The frequency range from 6 to 7 Hz was carefully examined for these modes. Although there was significant response, no mode other than tip missile pitch could be properly tuned in this frequency range. It is worth noting that these modes could also not be identified during the GVT of the initial decoupler pylon (ref. 5).

Comparison With Previous Test

Table IV lists the measured mode frequencies from the ground vibration tests of the modified decoupler pylon and the initial decoupler pylon (ref. 5). The reduction in lateral free play in the modified decoupler pylon eliminated the second GBU-8 antisymmetric lateral mode found previously. Significant frequency differences in the GBU-8 pitch, pylon strongback bending, and symmetric first wing bending modes are discussed next.

GBU-8 pitch mode. The frequency of the GBU-8 pitch mode is the most important frequency for proper functioning of the decoupler pylon. The symmetric (3.31 Hz) and antisymmetric (3.29 Hz) GBU-8 pitch of the modified decoupler pylon are lower than the corresponding modes (4.08 Hz and 3.92 Hz, respectively) on the initial pylon. The greater frequency separation between GBU-8 pitch and the antisymmetric tip missile pitch and antisymmetric wing bending modes indicates that the modified decoupler pylon may have better flutter suppression capability than the initial decoupler pylon.

Strongback bending mode. The strongback is the predominant structural member of the upper fixed part of the pylon. The GBU-8 pitch mode involves pivot joint rotation. The strongback bending mode is also a store pitch mode that involves the bending of the upper strongback between the forward and aft attachment points. The strongback bending mode

(4.24 Hz symmetric and 4.30 Hz antisymmetric) obtained on the modified decoupler pylon is reasonably close in frequency to the GBU-8 pitch mode frequencies from the previous test. Only one mode with pitching motion was identified during the initial GVT.

Symmetric wing-bending mode. The symmetric first wing bending mode was obtained at 3.95 Hz versus 3.02 Hz in the initial decoupler pylon GVT. The frequency obtained from the present test agrees with the predicted frequency (4.11 Hz). The current analysis and the modified decoupler pylon GVT were performed with no internal wing fuel. The initial decoupler pylon GVT was performed with full internal wing fuel. The lack of agreement between the two GVT-determined wing bending modes is therefore due to the different wing fuel loading conditions tested.

Concluding Remarks

Flight tests of an F-16 airplane loaded on each wing with a one-half-full (center bay empty) 370-gal tank mounted on a standard pylon, a GBU-8 store mounted on an initial decoupler pylon, and an AIM-9J missile mounted on a wingtip launcher revealed that the decoupler pylon was not free to rotate about its pivot mechanism. Excessive friction existed in the pylon pivot joints because of binding. The initial decoupler pylon was modified by replacing the bushings in the pivot joints with a combination of roller and thrust bearings.

In preparation for flight tests with the modified decoupler pylon, a ground vibration test was conducted on the F-16 with the flight test stores configuration. The F-16 was supported on its landing gear. Sinusoidal frequency sweeps were made from 2 to 24 Hz. Frequency response functions at several locations on the airplane were measured with the modified decoupler pylon in the centered position (with and without a side load and yawing-moment preload) and in a nose-up position.

The structural modes and rigid-body modes of the F-16 on its landing gear were identified. Mode shape data were taken for six symmetric and five antisymmetric modes. All the measured structural mode frequencies were within ± 10 percent of the predicted frequencies. The pylon pitch frequency for the modified decoupler pylon was 3.31 and 3.29 Hz, symmetric and antisymmetric, respectively, versus 4.08 and 3.92 Hz for the initial pylon; this indicated that the modified pylon may suppress flutter more adequately. A second pylon mode, the pylon strongback mode, was found at 4.24 Hz symmetrically and 4.30 Hz antisymmetrically. These values are reasonably close

to the pylon pitch frequencies obtained with the initial pylon that had the binding problem. The pylon pitch frequency increased to 4.07 Hz symmetrically and 3.89 Hz antisymmetrically when the store was nose up at the switch limits of the alignment system. When the pylon was preloaded by applying an external side load and yawing moment, the pylon pitch frequency was essentially unaffected.

The lateral pylon free play was significantly reduced by the installation of bearings in the pylon. However, the lateral pylon modes were characterized by poor left-to-right phasing. As a consequence, each side of the airplane was tuned separately.

Differences in frequency were obtained between the left and right 370-gal tank pitch modes of about 0.6 Hz, and tank yaw modes of about 0.4 Hz. These differences were not a function of pylon position. Fuel quantity, fuel distribution, tank-attachment bolt torque, and free play were checked for both tanks and were found to be proper. Consequently, no cause for the differences in frequency was determined.

Finally, two modes involving missile pitch motion that had been indicated analytically were not found experimentally. These two modes, however, also could not be obtained in the test of the initial pylon.

NASA Langley Research Center
Hampton, VA 23665-5225
January 6, 1986

References

1. Reed, Wilmer H., III; Foughner, Jerome T., Jr.; and Runyan, Harry L., Jr.: Decoupler Pylon: A Simple, Effective Wing/Store Flutter Suppressor. *J. Aircr.*, vol. 17, no. 3, Mar. 1980, pp. 206-211.
2. Reed, Wilmer H., III; Cazier, F. W., Jr.; and Foughner, Jerome T., Jr.: *Passive Control of Wing/Store Flutter*. NASA TM-81865, 1980.
3. Peloubet, R. P., Jr.; Haller, R. L.; and McQuien, L. J.: *Feasibility Study and Conceptual Design for Application of NASA Decoupler Pylon to the F-16*. NASA CR-165834, 1982.
4. Clayton, J. D.; Haller, R. L.; and Hassler, J. M., Jr.: *Design and Fabrication of the NASA Decoupler Pylon for the F-16 Aircraft*. NASA CR-172354, 1985.
5. Cazier, F. W., Jr.; and Kehoe, M. W.: *Ground Vibration Test of F-16 Airplane With Initial Decoupler Pylon*. NASA TM-86259, 1984.
6. Clayton, J. D.; Haller, R. L.; and Hassler, J. M., Jr.: *Design and Fabrication of the NASA Decoupler Pylon for the F-16 Aircraft, Addendum II*. NASA CR-172494, 1985.

TABLE I. SHAKER CONFIGURATIONS

Configuration	Number	Force rating, lbf	Location	Direction
1	1	150	Forward fuselage jack point	Vertical
2	2	50	Wing, aft launcher	Vertical
3	2	150	GBU-8, forward	Vertical
4	{ 2	150	GBU-8, forward	Lateral
	{ 2	50	GBU-8, aft	Lateral

TABLE II. SYMMETRIC MODE FREQUENCIES AND STRUCTURAL DAMPING COEFFICIENTS
AT VARIOUS PYLON POSITIONS

[L denotes left; R denotes right]

Mode	Nominal position			Nose-up switch limit		Nominal position with preload	
	Analysis frequency, Hz	GVT frequency, Hz	Damping coefficient, g	GVT frequency, Hz	Damping coefficient, g	GVT frequency, Hz	Damping coefficient, g
1st wing bending	4.11	3.95	0.041	4.02	0.033	4.04	0.030
2d wing bending	9.82	9.64	.035	9.79	.030	9.71	.044
Tip missile pitch	5.99	6.09	.036	6.29	.043	6.32	.037
Missile pitch/ Wing bending	6.67						
370-gal tank pitch	7.34	$\begin{cases} 6.97 \text{ L} \\ 7.55 \text{ R} \end{cases}$	$\begin{cases} .032 \text{ L} \\ .044 \text{ R} \end{cases}$	$\begin{cases} 7.00 \text{ L} \\ 7.50 \text{ R} \end{cases}$	$\begin{cases} .024 \text{ L} \\ .032 \text{ R} \end{cases}$	$\begin{cases} 7.04 \text{ L} \\ 7.52 \text{ R} \end{cases}$	$\begin{cases} .019 \text{ L} \\ .029 \text{ R} \end{cases}$
370-gal tank yaw	7.92	$\begin{cases} 7.80 \text{ L} \\ 8.17 \text{ R} \end{cases}$	$\begin{cases} .058 \text{ L} \\ .036 \text{ R} \end{cases}$				
GBU-8 pitch	3.18	3.31	.25	4.07	.14	3.41	.29
Pylon strongback bending	4.37	4.24	.091	4.65	.040	4.44	.069
GBU-8 lateral	5.26	$\begin{cases} 5.46 \text{ L} \\ 5.27 \text{ R} \end{cases}$	$\begin{cases} .057 \text{ L} \\ .085 \text{ R} \end{cases}$				

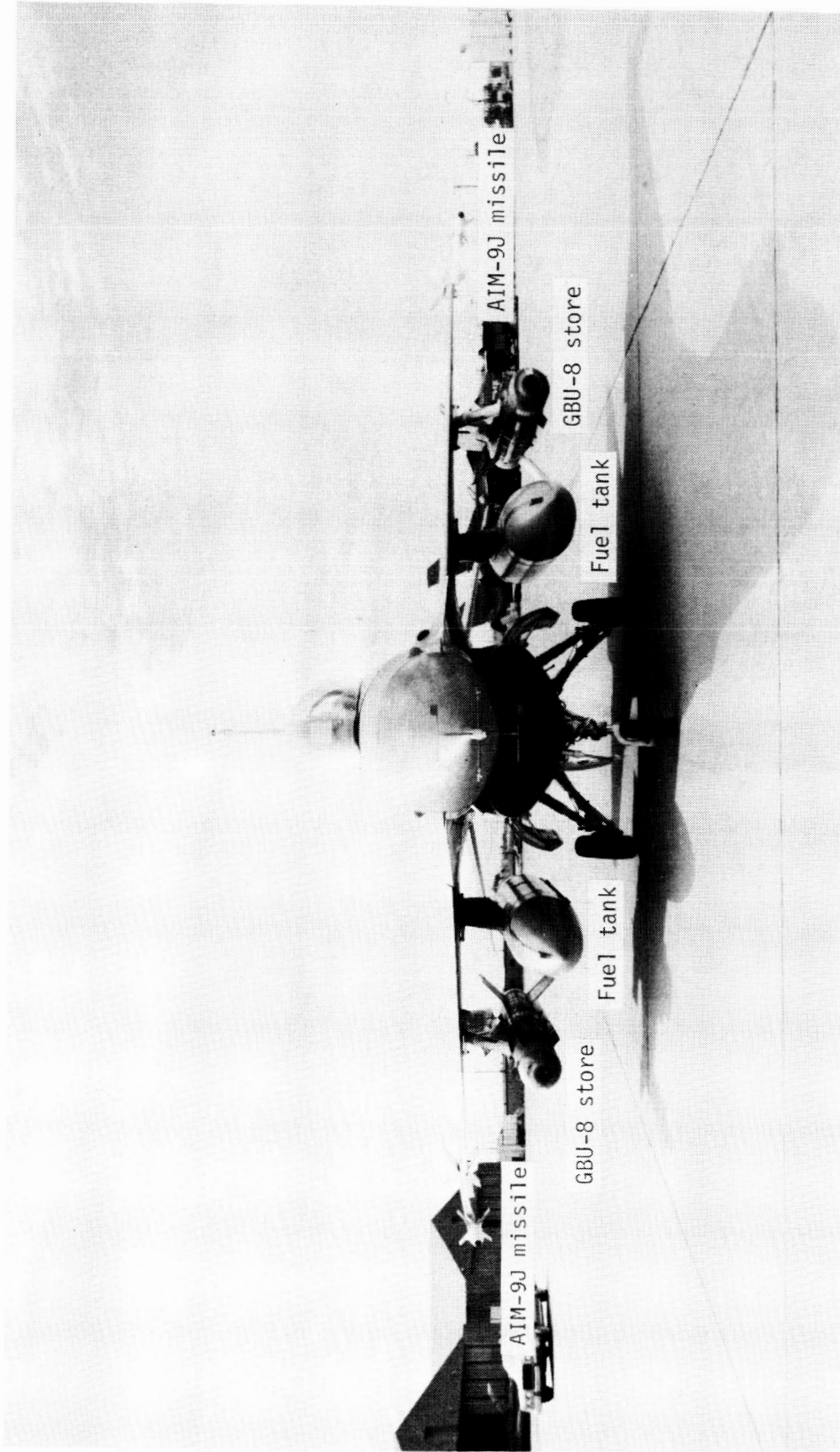
TABLE III. ANTISYMMETRIC MODE FREQUENCIES AND STRUCTURAL DAMPING COEFFICIENTS
AT VARIOUS PYLON POSITIONS

[L denotes left; R denotes right]

Mode	Nominal position			Nose-up switch limit		Nominal position with preload	
	Analysis frequency, Hz	GVT frequency, Hz	Damping coefficient, g	GVT frequency, Hz	Damping coefficient, g	GVT frequency, Hz	Damping coefficient, g
1st wing bending	9.46	8.66	0.046	8.63	0.035	8.71	0.064
Tip missile pitch	5.90	5.53	.067	5.38	.039	5.22	.045
Tip missile pitch/ GBU-8 yaw	6.45						
370-gal tank pitch	7.12	$\left\{ \begin{array}{l} 6.90 \text{ L} \\ 7.57 \text{ R} \end{array} \right\}$	$\left. \begin{array}{l} .037 \text{ L} \\ .060 \text{ R} \end{array} \right\}$	$\left. \begin{array}{l} 6.94 \text{ L} \\ 7.42 \text{ R} \end{array} \right\}$	$\left. \begin{array}{l} .035 \text{ L} \\ .043 \text{ R} \end{array} \right\}$	$\left. \begin{array}{l} 6.99 \text{ L} \\ 7.53 \text{ R} \end{array} \right\}$	$\left. \begin{array}{l} .021 \text{ L} \\ .035 \text{ R} \end{array} \right\}$
370-gal tank yaw	8.06	$\left\{ \begin{array}{l} 7.83 \text{ L} \\ 8.22 \text{ R} \end{array} \right\}$	$\left. \begin{array}{l} .026 \text{ L} \\ .021 \text{ R} \end{array} \right\}$				
Vertical fin bending	12.12	11.81	.024	11.85	.022	11.86	.026
GBU-8 pitch	3.24	3.29	.19	3.89	.070	3.20	.33
Pylon strongback bending	4.61	4.30	.13	4.55	.025	4.30	.026
GBU-8 lateral	5.24	$\left\{ \begin{array}{l} 4.94 \text{ L} \\ 5.18 \text{ R} \end{array} \right\}$	$\left. \begin{array}{l} .065 \text{ L} \\ .069 \text{ R} \end{array} \right\}$				

TABLE IV. COMPARISON OF MEASURED MODE FREQUENCIES OF MODIFIED AND INITIAL PYLONS
 [L denotes left; R denotes right]

Mode	Frequency of modified decoupler pylon, Hz	Frequency of initial decoupler pylon (ref. 5), Hz
Symmetric modes		
GBU-8 pitch	3.31	4.08
Pylon strongback bending	4.24	
GBU-8 lateral	{ 5.46 L 5.27 R	5.26 L 5.21 R
1st wing bending	3.95	3.02
2d wing bending	9.64	9.77
Tip missile pitch	6.09	6.27
370-gal tank pitch	{ 6.97 L 7.55 R	7.49
370-gal tank yaw	{ 7.80 L 8.17 R	
Antisymmetric modes		
GBU-8 pitch	3.29	3.92
Pylon strongback bending	4.30	
GBU-8 lateral	{ 4.94 L 5.18 R	4.75 L 4.82 R
2d GBU-8 lateral/yaw		5.29
1st wing bending	8.66	8.71
Tip missile pitch	5.53	5.32
370-gal tank pitch	{ 6.90 L 7.57 R	7.35
370-gal tank yaw	{ 7.83 L 8.22 R	
Vertical fin bending	11.81	11.91



L-84-103

Figure 1. F-16 airplane with test stores.

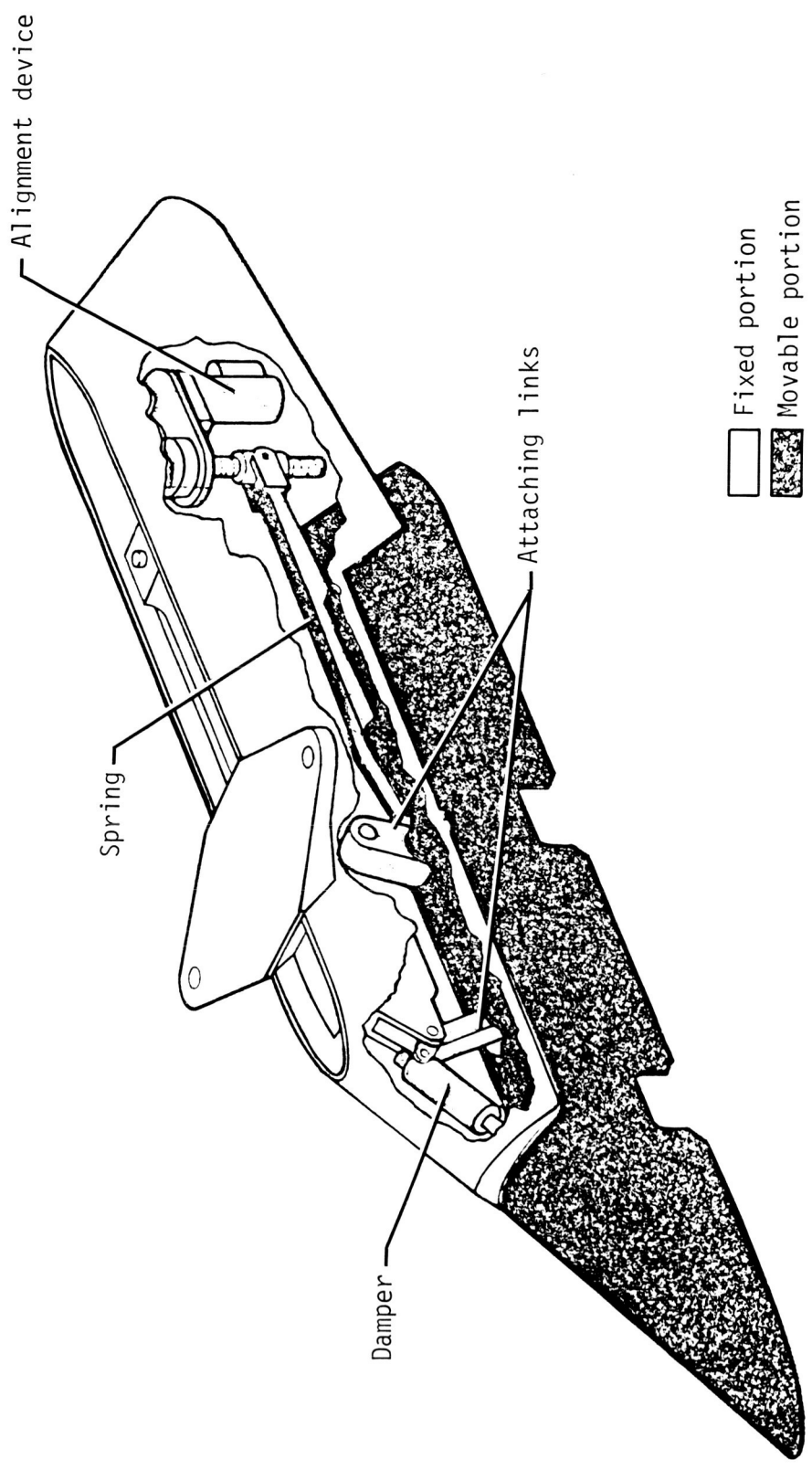
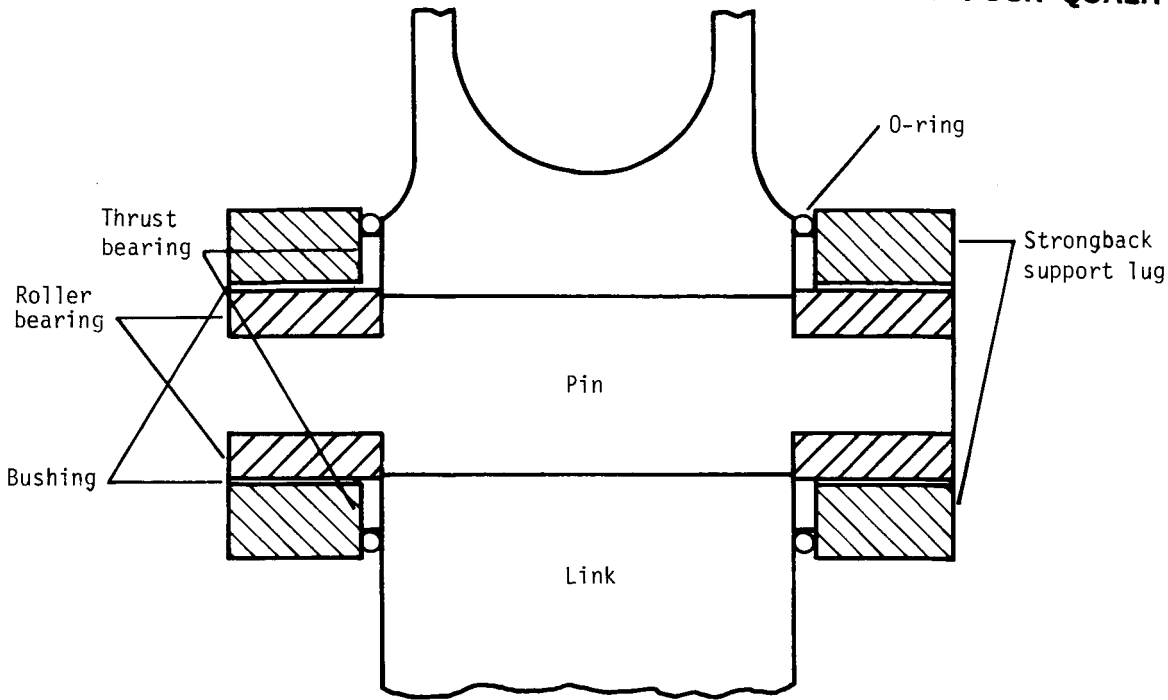
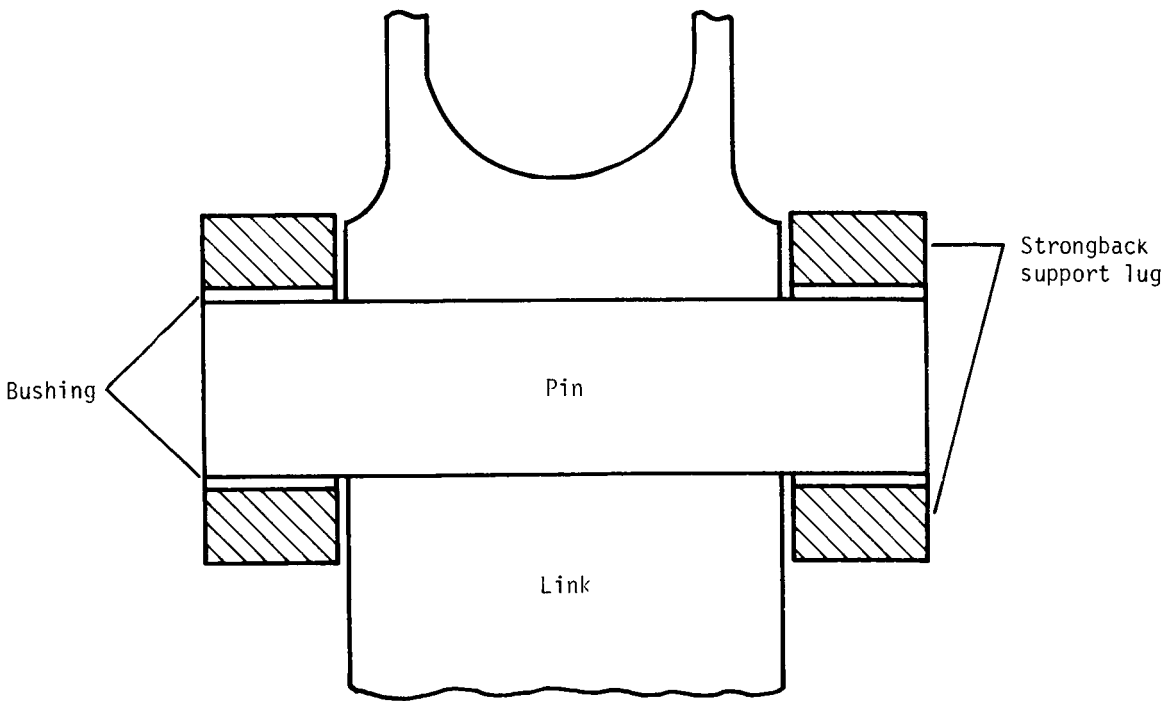


Figure 2. Decoupler pylon components.

ORIGINAL PAGE IS
OF POOR QUALITY



(a) Initial decoupler pylon.



(b) Initial decoupler pylon.

Figure 3. Forward-link upper pivot details.

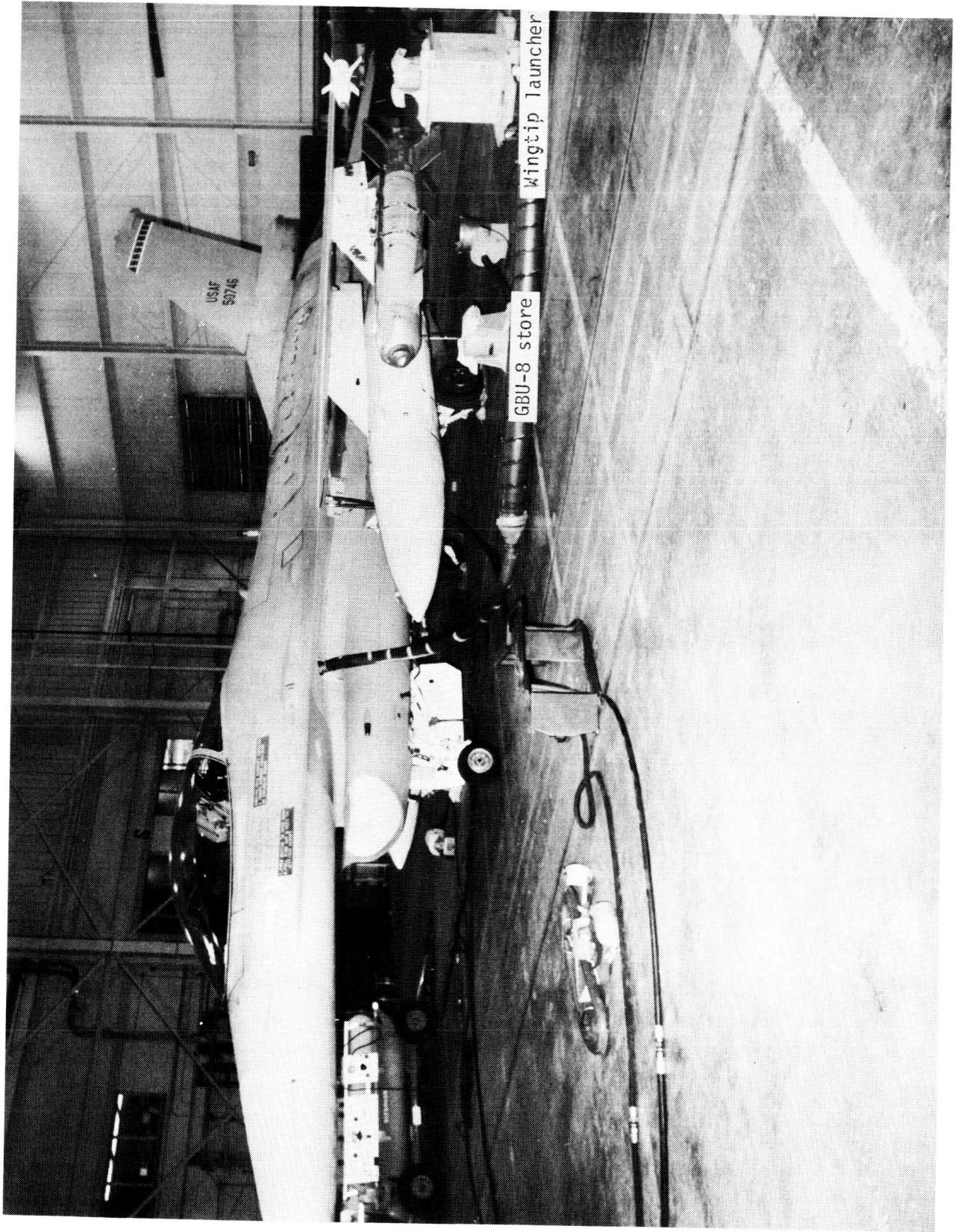
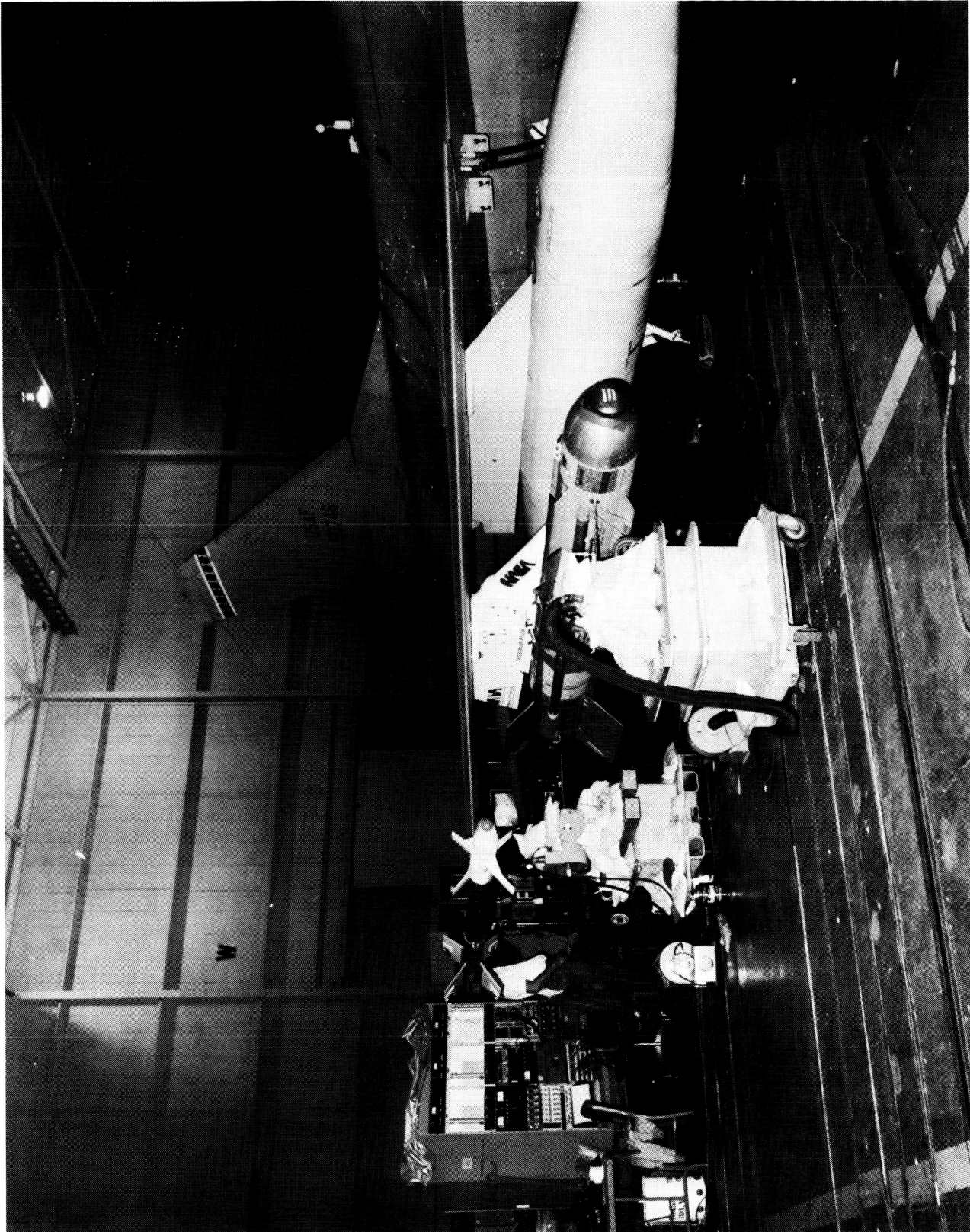


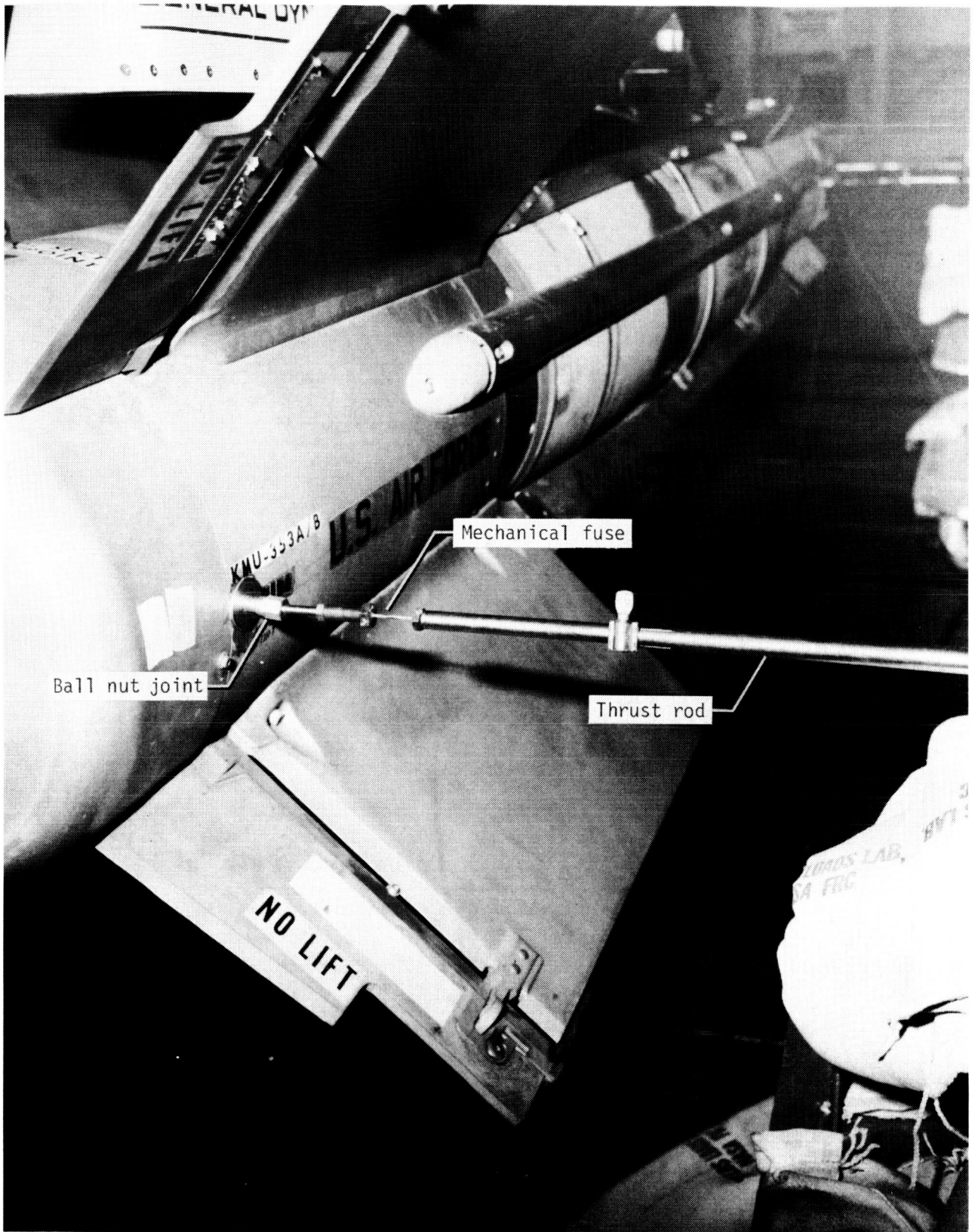
Figure 4. Locations of wingtip missile launcher and GBU-8 store shaker.

L-84-105



L-84-106

Figure 5. Location of GBU-8 store lateral shakers. Configuration 4.



L-84-107

Figure 6. Shaker attachment hardware.

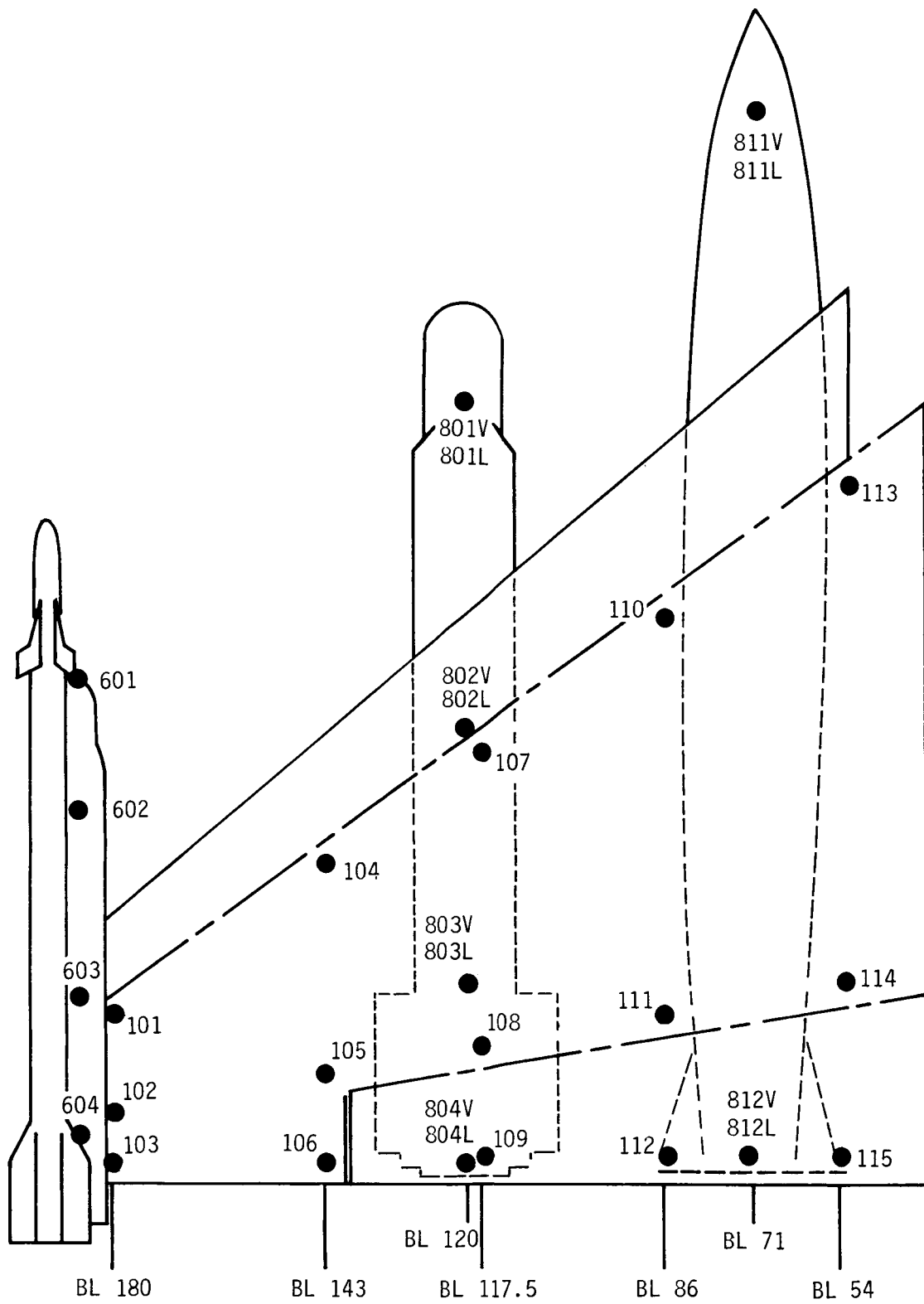


Figure 7. Left-wing survey points. BL denotes buttock line.

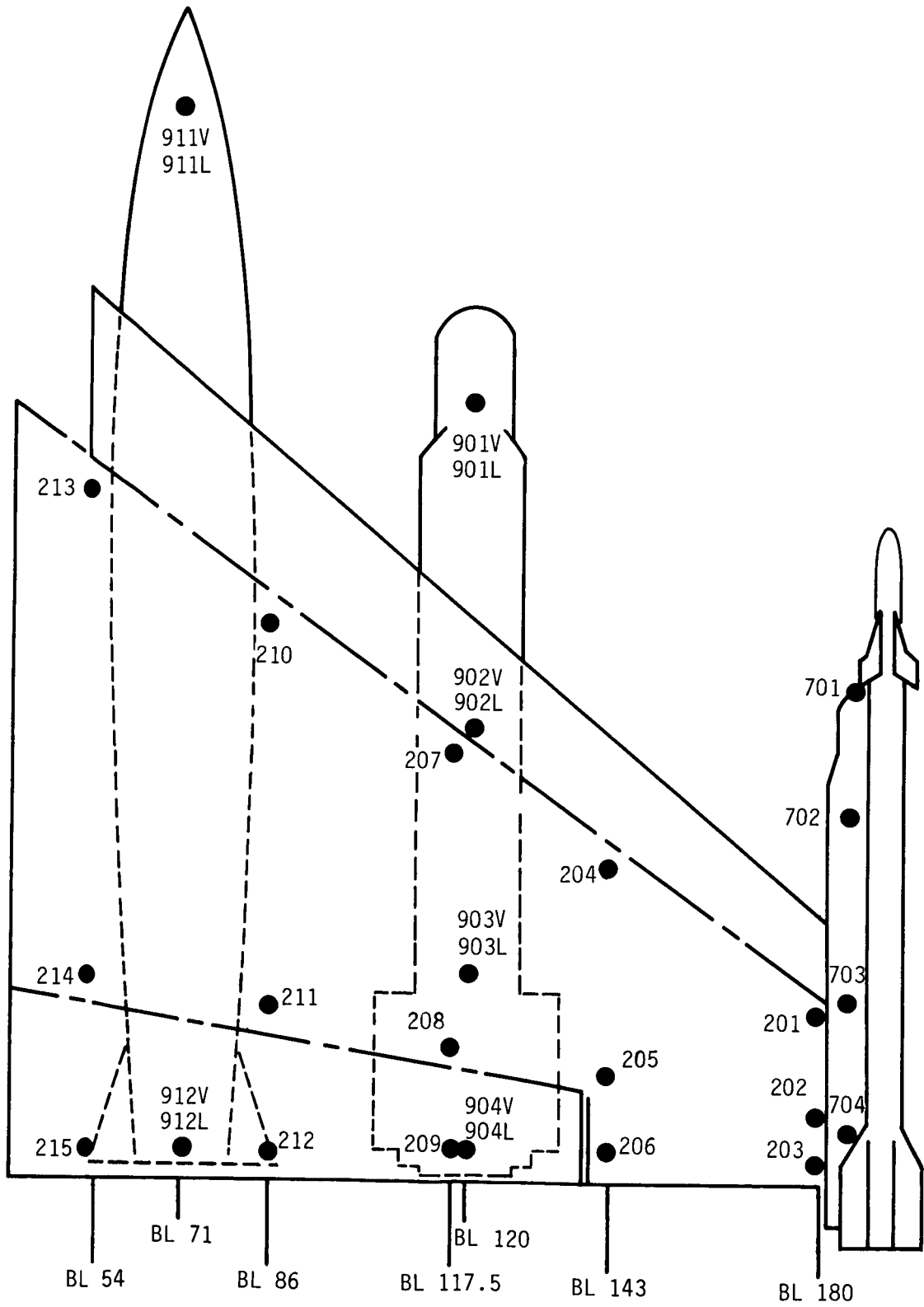


Figure 8. Right-wing survey points.

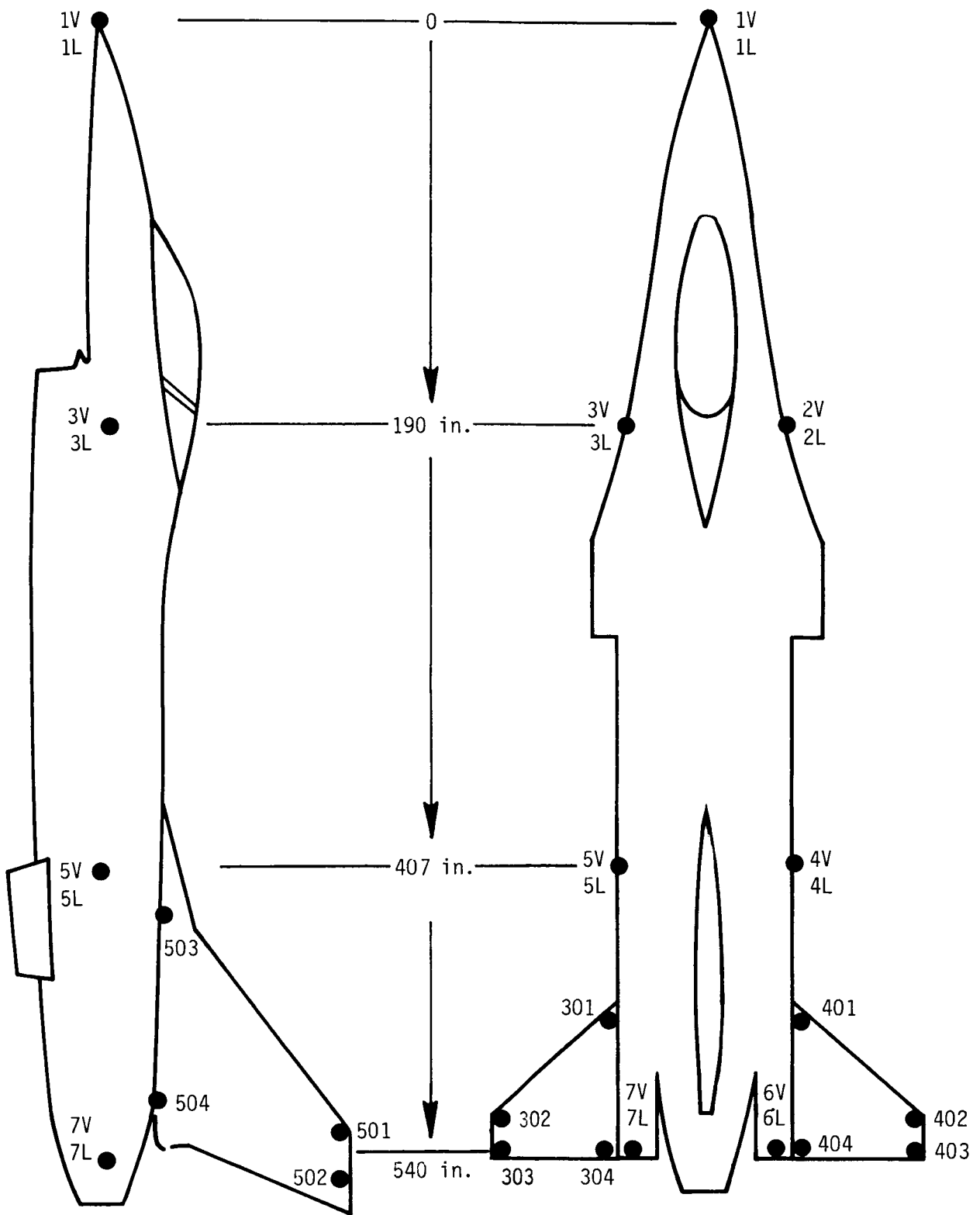
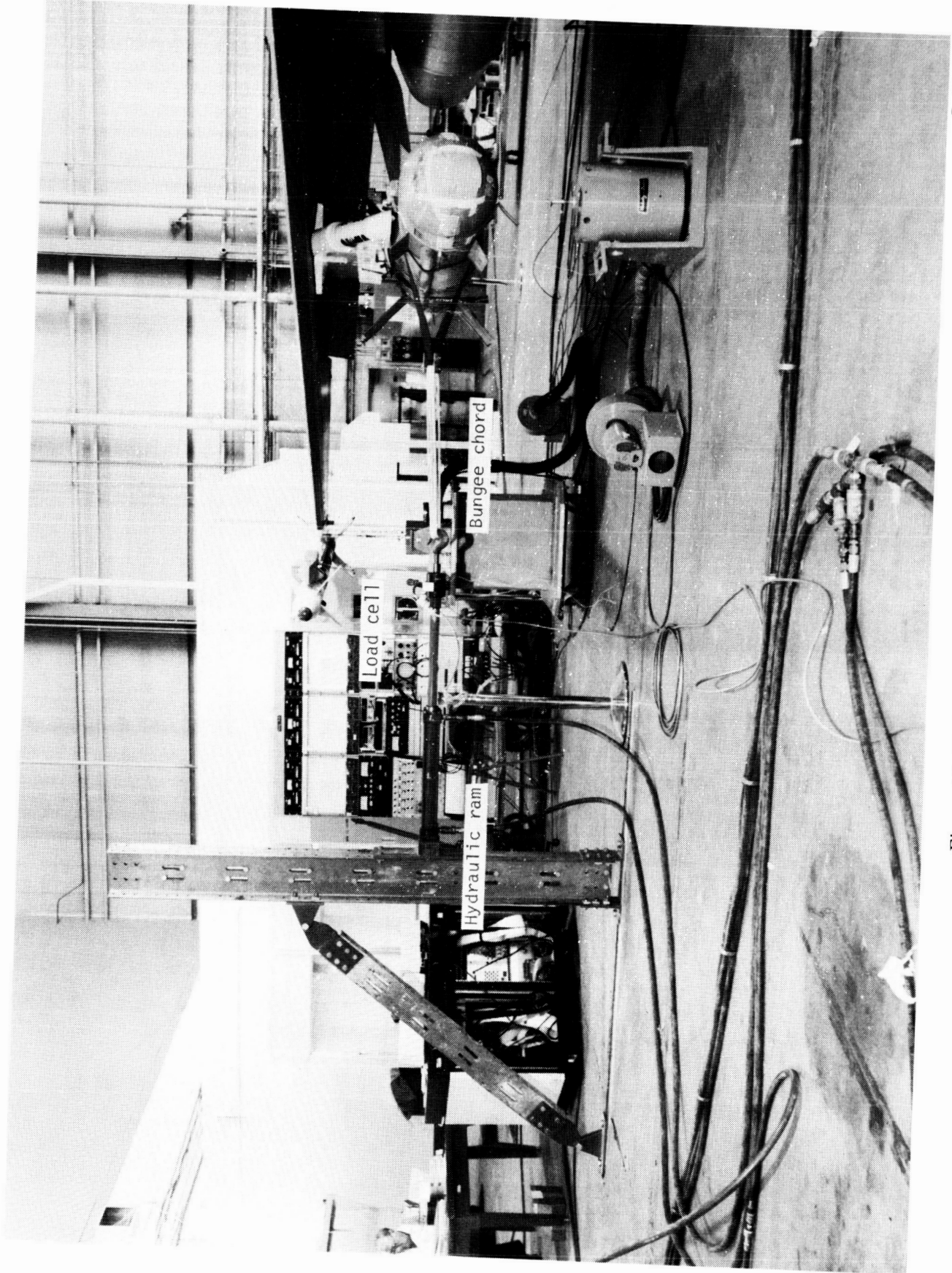
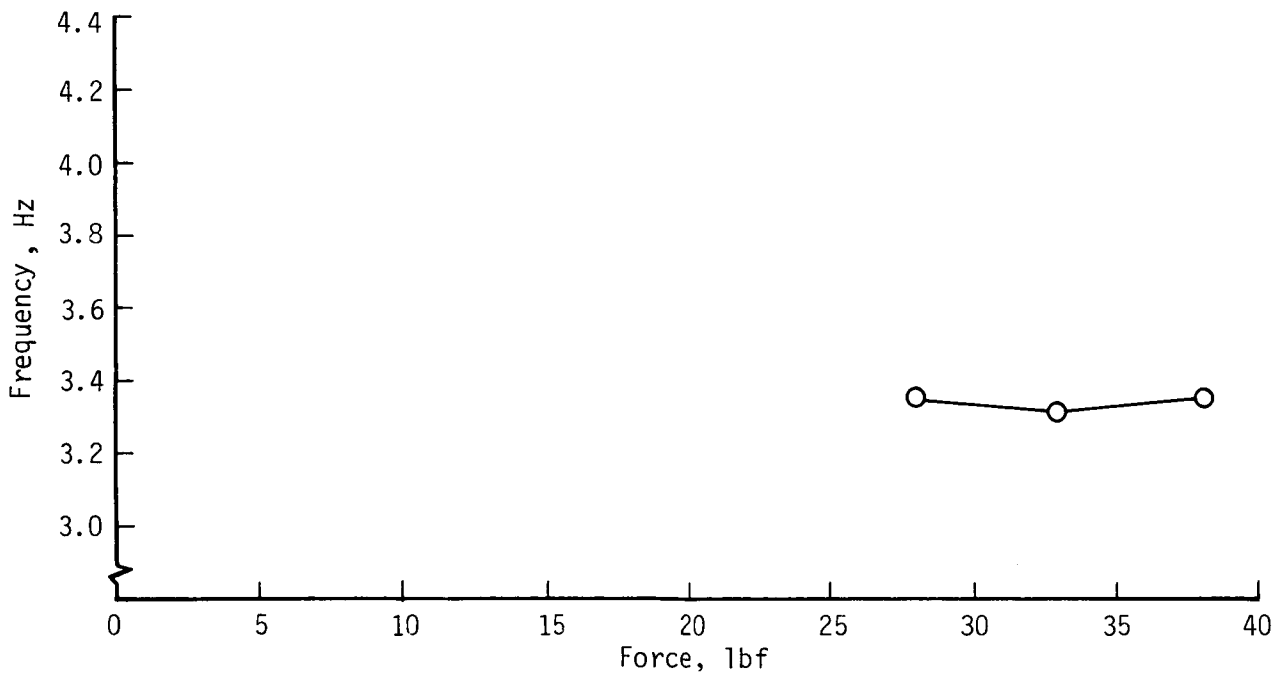


Figure 9. Fuselage survey points.

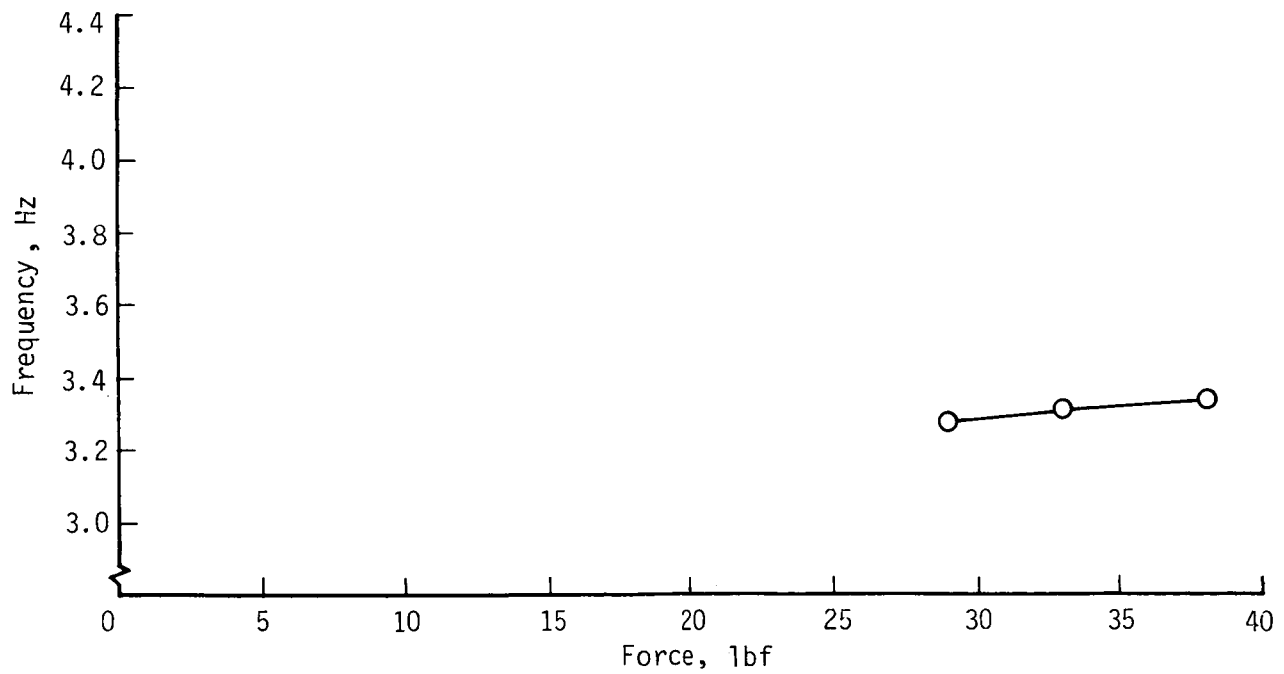


L-85-175

Figure 10. Test setup for pylon preloading.

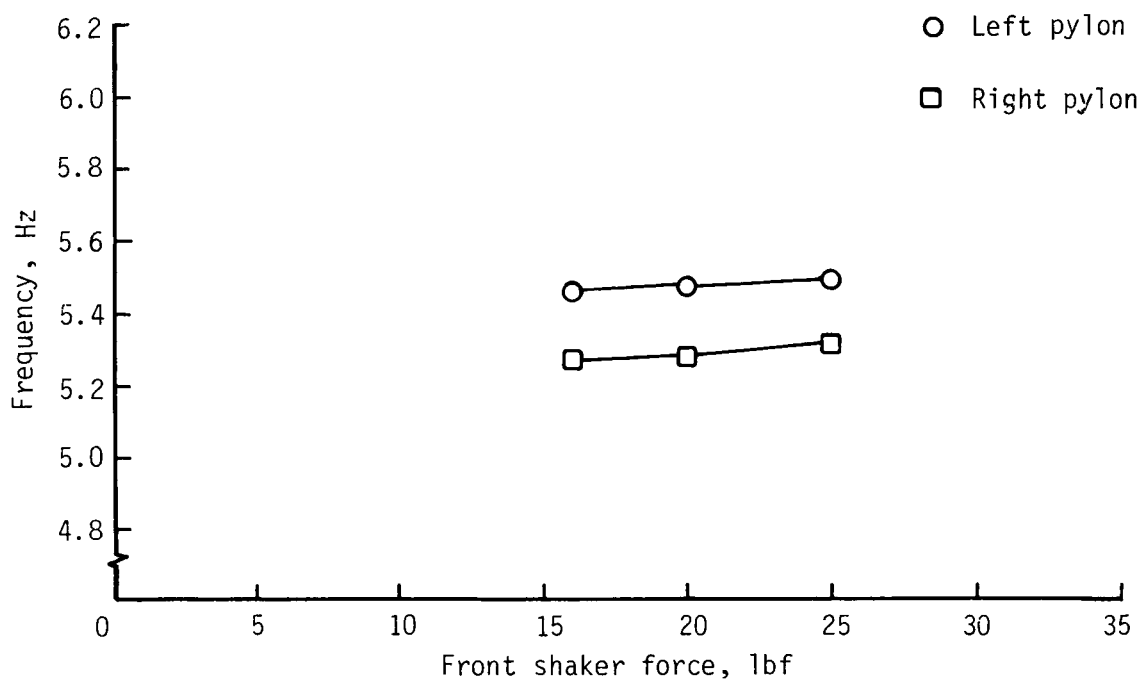


(a) Symmetric mode.

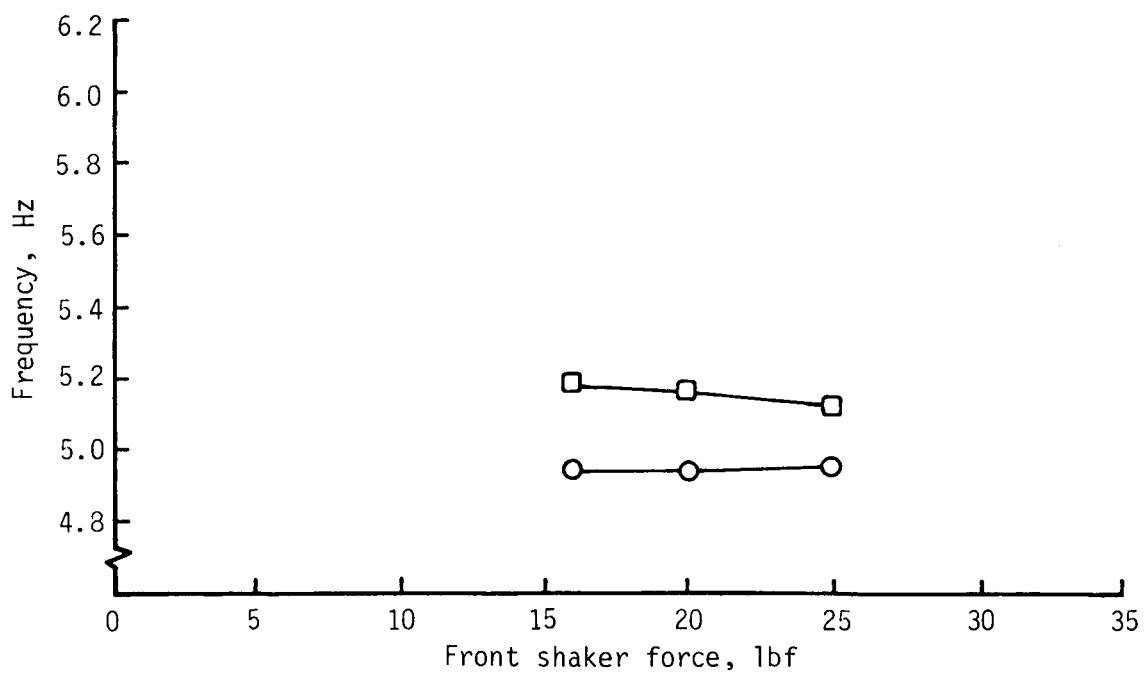


(b) Antisymmetric mode.

Figure 11. Effect of shaker force level on frequency of GBU-8 pitch mode for pylon in nominal position.



(a) Symmetric mode.



(b) Antisymmetric mode.

Figure 12. Effect of shaker force level on frequency of GBU-8 lateral mode for pylon in nominal position.

Appendix A

Frequency Sweep Data

This appendix contains the frequency sweep data for all 30 sweeps obtained during the test. Table AI, which summarizes all the sweeps presented, lists the shaker locations, directions, and forces; the excitation symmetries; the response accelerometer locations; and the pylon configurations. The response

accelerometer locations, shown in figures 7, 8, and 9, are listed in table AII.

The sweeps are contained in figures A1 through A30 in the following sequence. Figures A1 through A15 are the symmetric sweeps, and figures A16 through A30 are the antisymmetric sweeps. The airplane was excited by two shakers for all sweeps except those shown in figures A14, A15, A29, and A30, where all four shakers were used.

TABLE A1. FREQUENCY SWEEP SUMMARY

[V denotes vertical; L denotes lateral; F&A denotes forward and aft]

Figure	Shaker location	Direction	Force, lbf	Excitation	Response accelerometer location (a)	Pylon configuration
A1	GBU-8, forward	Vertical	40	Symmetric	601, 701, 801V, 901V, 811V, 911V 1V, 601, 701, 604, 704, 801V, 901V	Nominal
A2	Launcher, aft		20			
A3	GBU-8, forward	Vertical	25, 35, 45	Symmetric	701	Nominal
A4	GBU-8, forward		25, 35, 45			
A5	GBU-8, forward		25, 35, 45			
A6	GBU-8, forward		15			
A7	GBU-8, forward	Vertical	15, 25, 40	Symmetric	601, 701, 801V, 901V, 811V, 911V	Nose up at limit
A8	GBU-8, forward		15, 25, 40			
A9	Launcher, aft	Vertical	20	Symmetric	601, 701, 801V, 901V, 811V, 911V	Nose up at limit
A10	GBU-8, forward		15			
A11	GBU-8, forward		15, 25, 40			
A12	GBU-8, forward		15, 25, 40			
A13	GBU-8, forward		15, 25, 40			
A14	GBU-8, F&A	Lateral	15	Symmetric roll	601, 701, 801L, 901L, 811L, 911L	Nominal
A15	GBU-8, F&A		Lateral			
A16	GBU-8, forward	Vertical	40	Antisymmetric	601, 701, 801V, 901V, 811V, 911V	Nominal
A17	Launcher, aft		20			
A18	GBU-8, forward	Vertical	25, 35, 45	Antisymmetric	601, 701, 801V, 901V, 811V, 911V	Nominal
A19	GBU-8, forward		25, 35, 45			
A20	GGU-8, forward		25, 35, 45			
A21	GBU-8, forward		15			
A22	GBU-8, forward	Vertical	15, 25, 40	Antisymmetric	601, 701, 801V, 901V, 811V, 911V	Nose up at limit
A23	GBU-8, forward		15, 25, 40			
A24	Launcher, aft	Vertical	20	Antisymmetric	601, 701, 801V, 901V, 811V, 911V	Nose up at limit
A25	GBU-8, forward		15			
A26	GBU-8, forward		15, 25, 40			
A27	GFU-8, forward		15, 25, 40			
A28	GBU-8, forward		15, 25, 40			
A29	GBU-8, F&A	Lateral	15	Antisymmetric roll	601, 701, 801L, 901L, 811L, 911L	Nominal
A30	GBU-8, F&A		Lateral			

^aSee table A11 and figures 7 through 9 for response accelerometer locations.

TABLE AII. RESPONSE ACCELEROMETER LOCATIONS

[V denotes vertical; L denotes lateral]

Survey point number	Airplane component	Direction
1V to 7V	Fuselage	Vertical
1L to 7L	Fuselage	Lateral
101 to 115	Left wing	Vertical
201 to 215	Right wing	Vertical
301 to 304	Left horizontal tail	Vertical
401 to 404	Right horizontal tail	Vertical
501 to 504	Vertical tail	Lateral
601 to 604	Left launcher	Vertical
701 to 704	Right launcher	Vertical
801V to 804V	Left GBU-8	Vertical
801L to 804L	Left GBU-8	Lateral
811V to 812V	Left 370-gal tank	Vertical
811L to 812L	Left 370-gal tank	Lateral
901V to 904V	Right GBU-8	Vertical
901L to 904L	Right GBU-8	Lateral
911V to 912V	Right 370-gal tank	Vertical
911L to 912L	Right 370-gal tank	Lateral

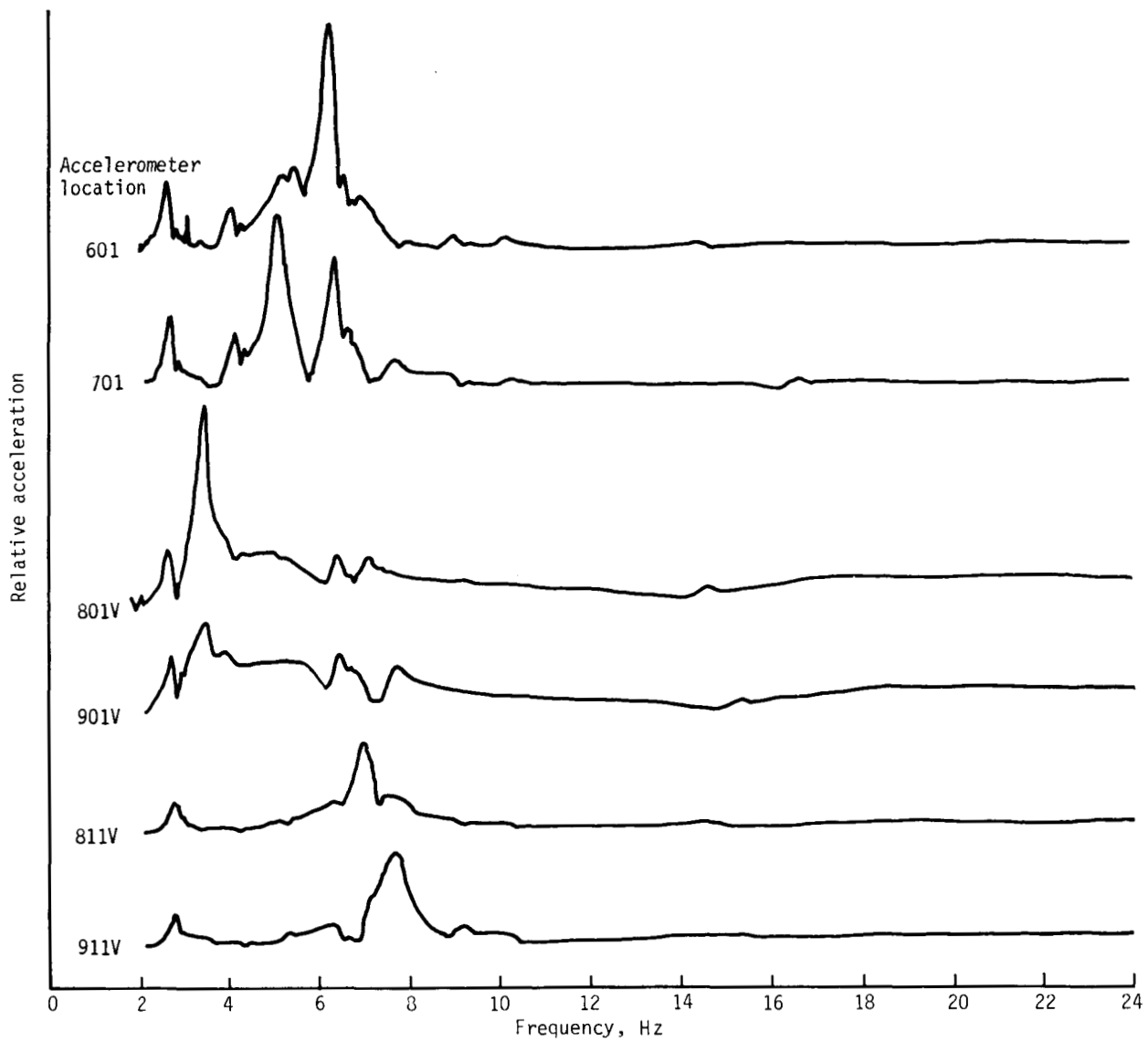


Figure A1. Frequency sweep plot for symmetric vertical excitation, GBU-8 forward shaker location, and force level of 40 lbf.

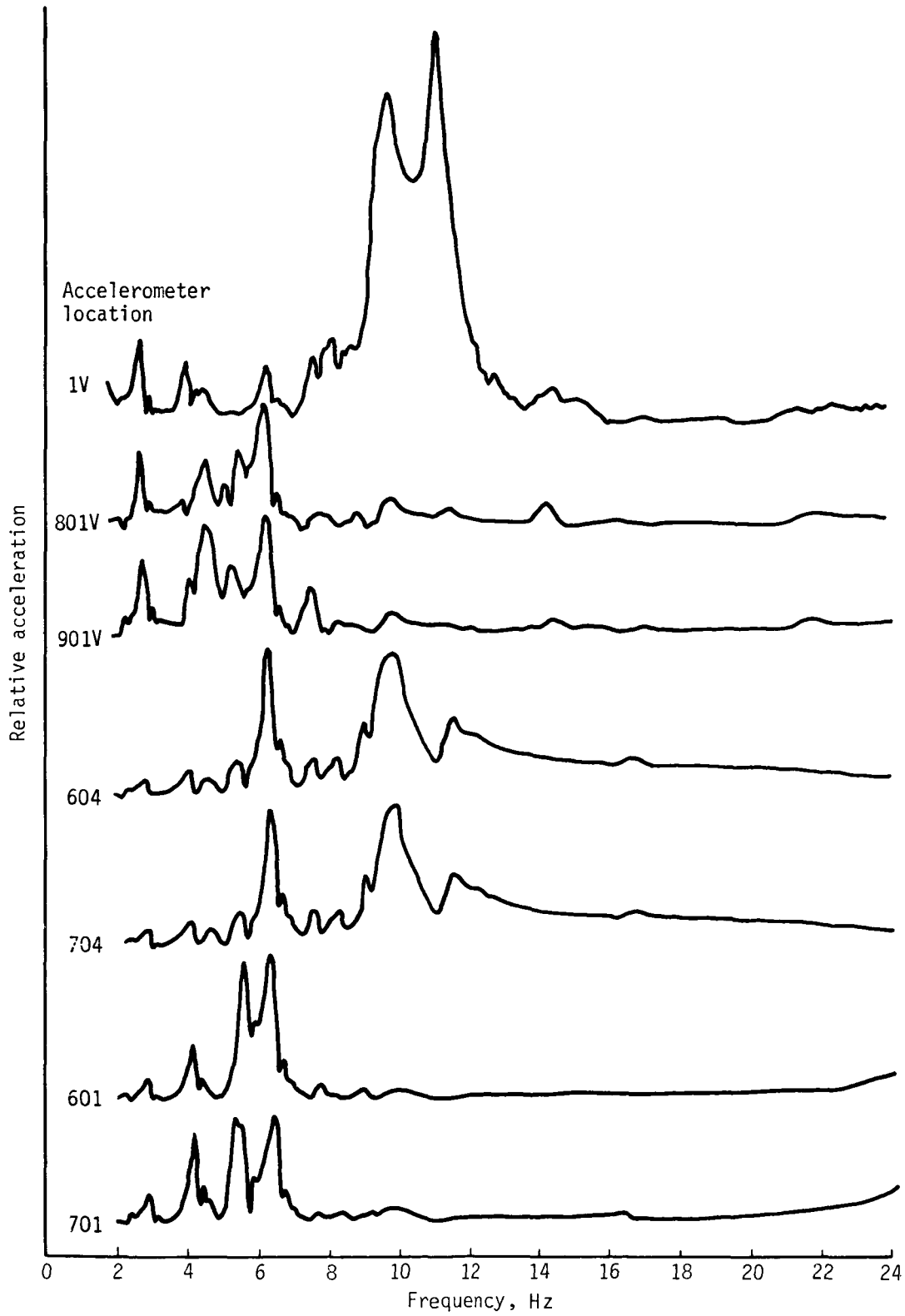


Figure A2. Frequency sweep plot for symmetric vertical excitation, launcher aft shaker location, and force level of 20 lbf.

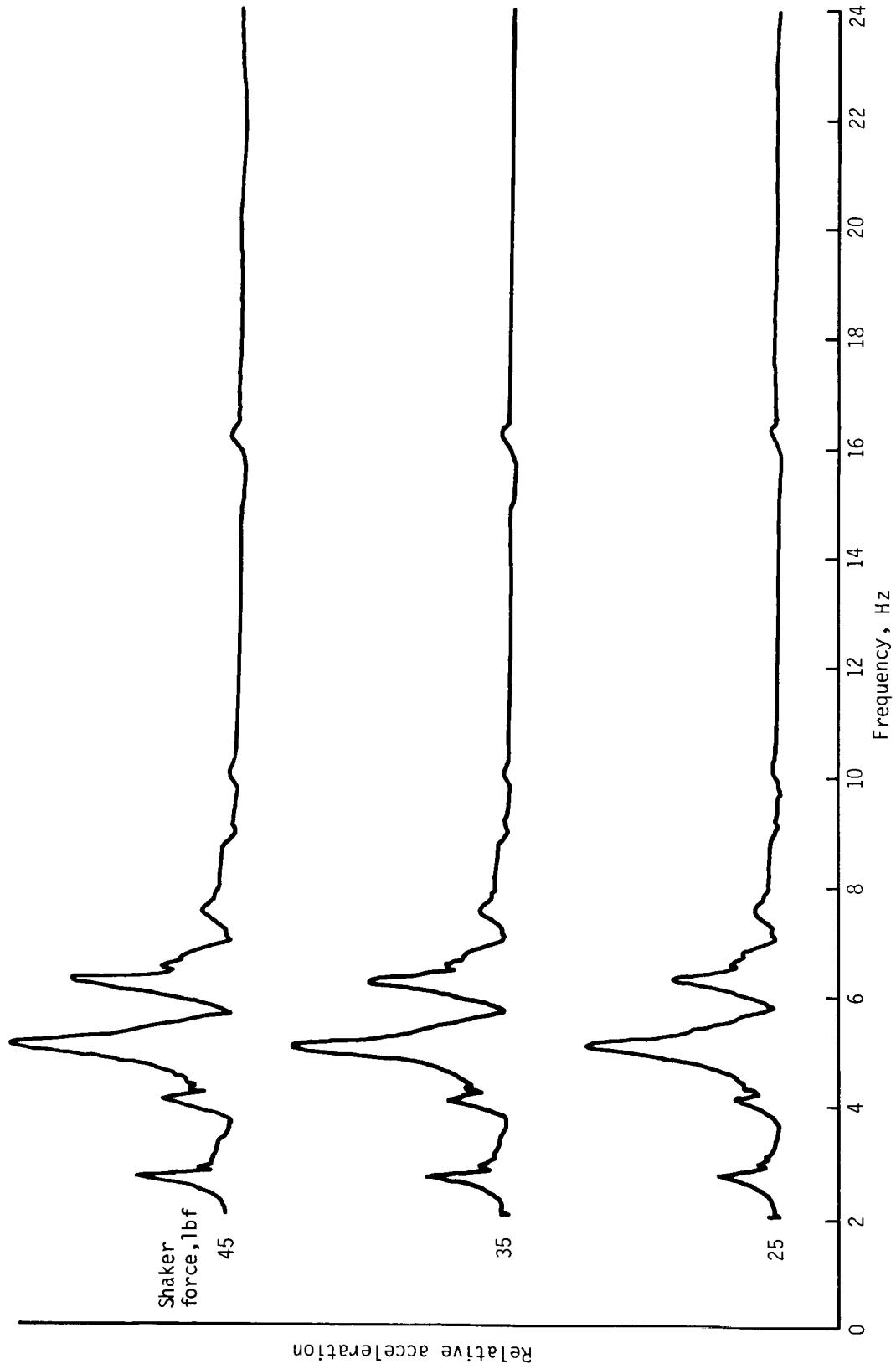


Figure A3. Frequency sweep plot at location 701 for symmetric vertical excitation, GBU-8 forward shaker location, and three force levels.

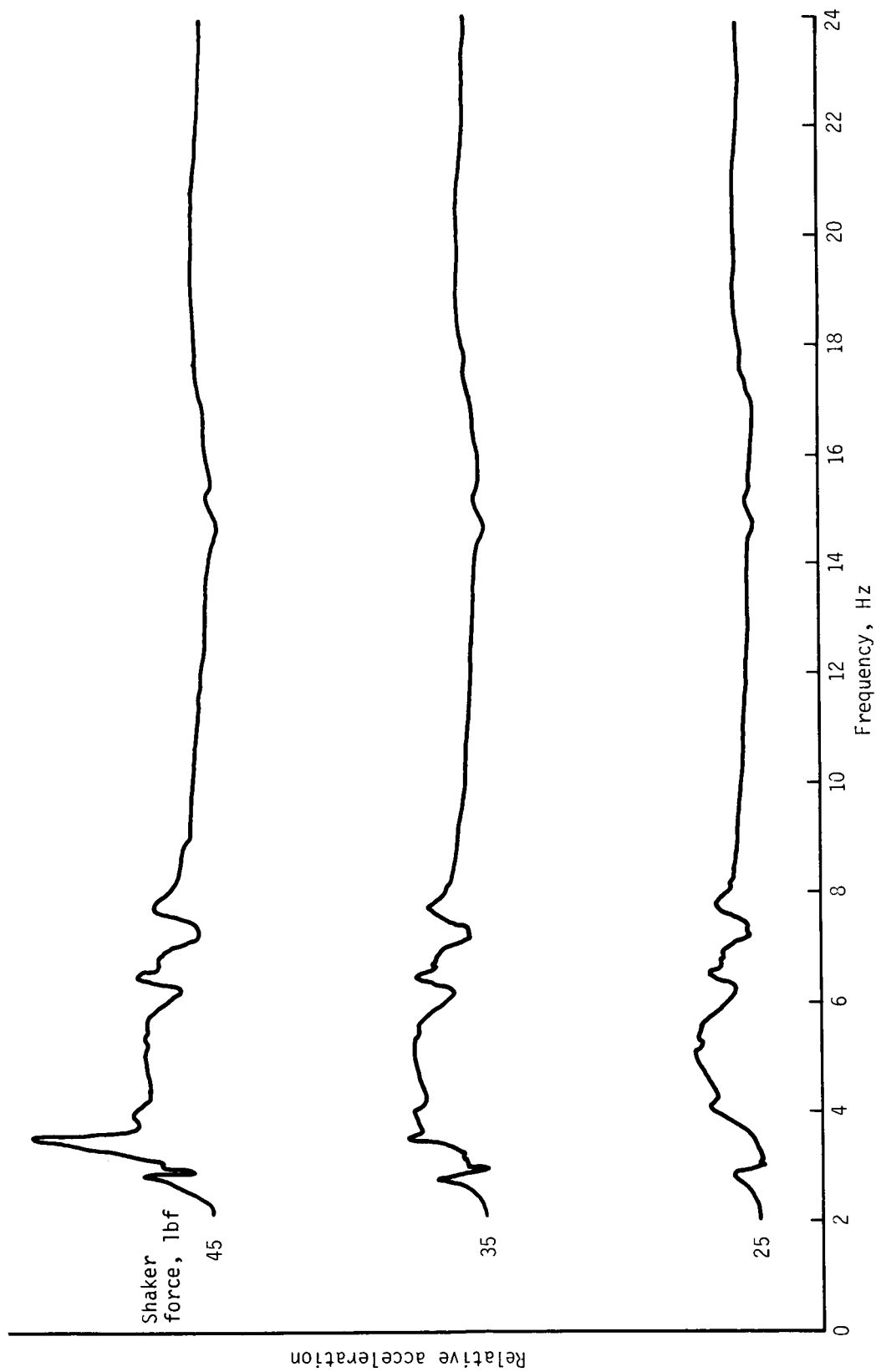


Figure A4. Frequency sweep plot at location 901V for symmetric vertical excitation, GBU-8 forward shaker location, and three force levels.

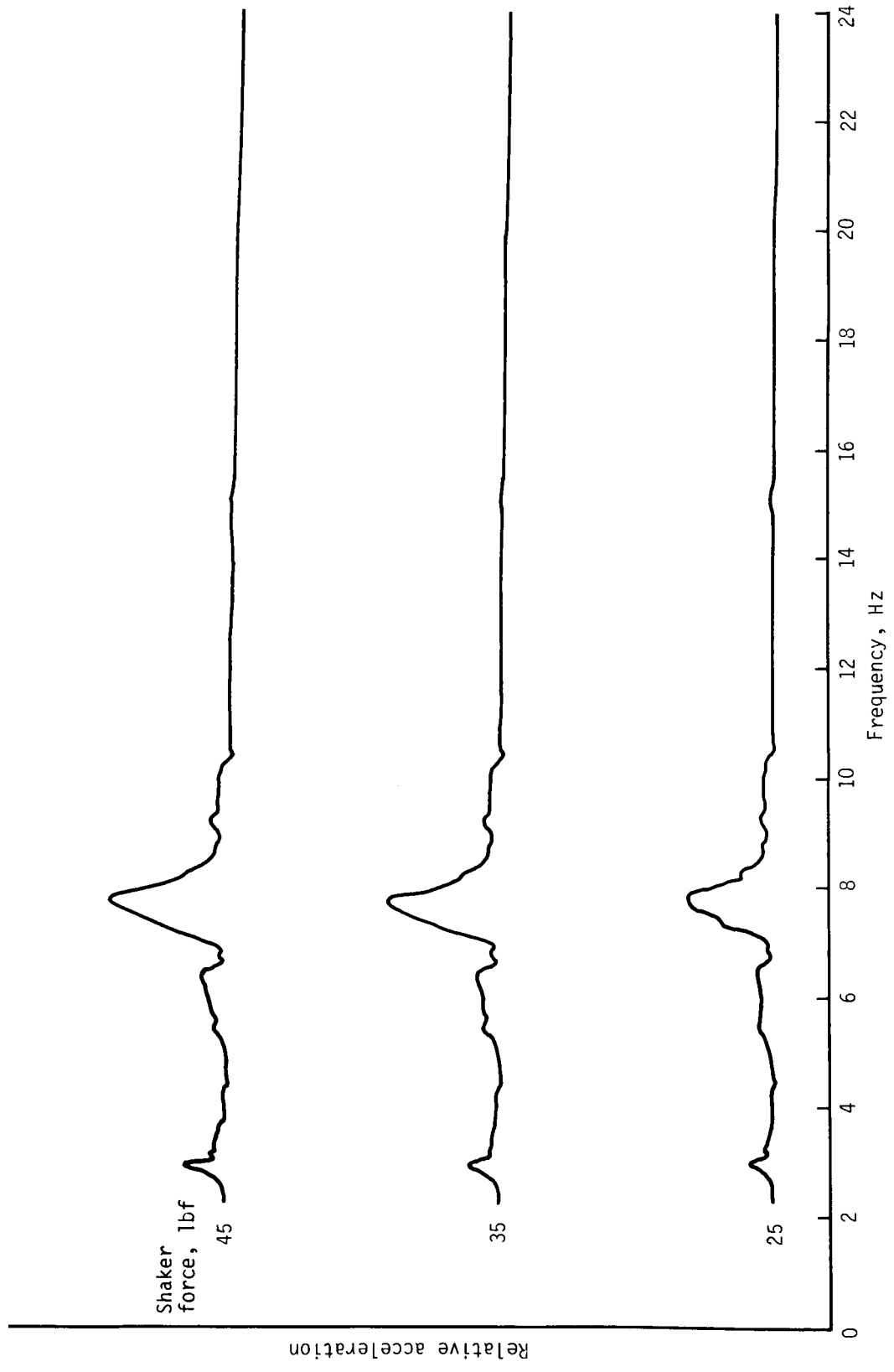


Figure A5. Frequency sweep plot at location 911V for symmetric vertical excitation, GBU-8 forward shaker location, and three force levels.

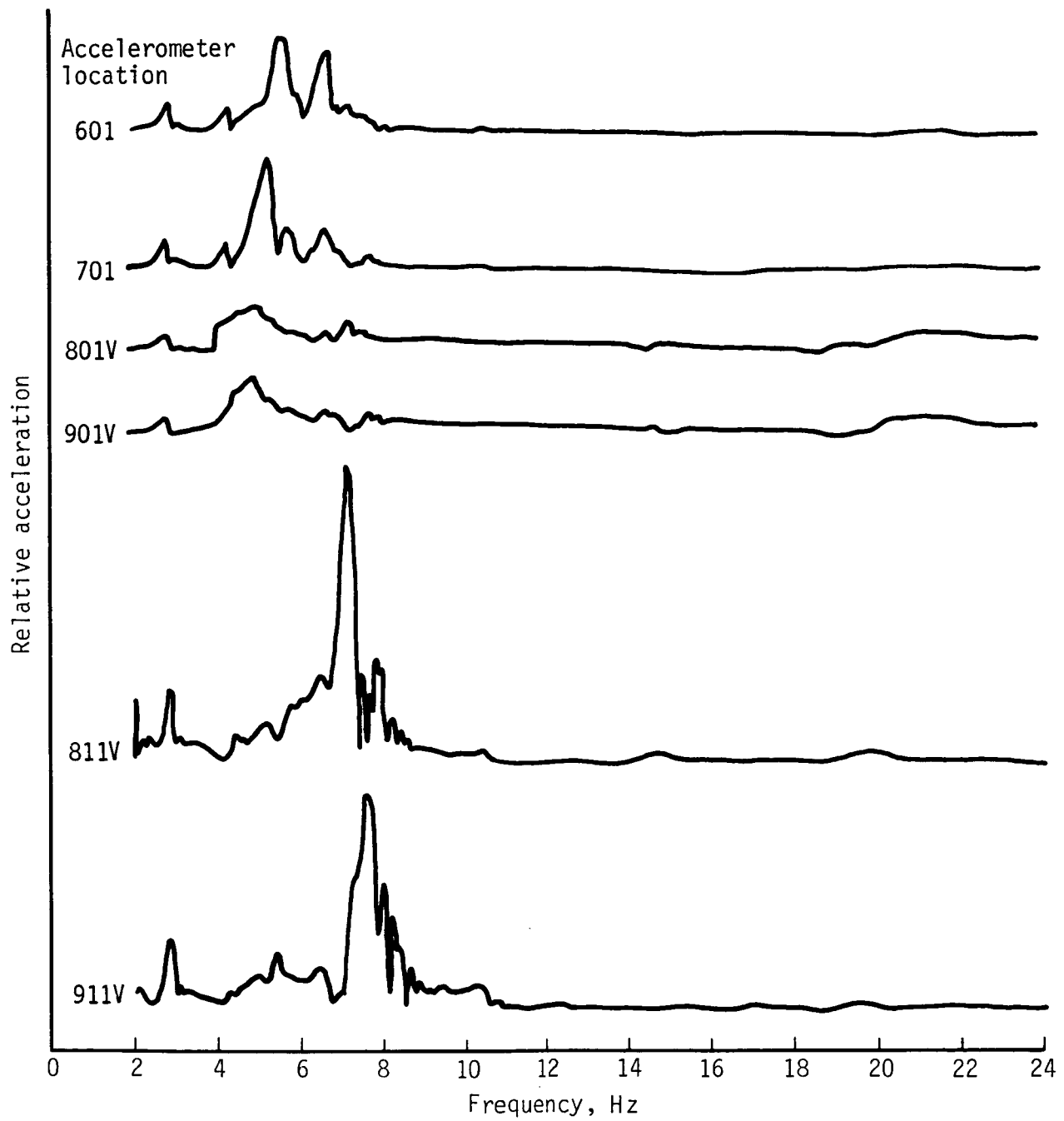


Figure A6. Frequency sweep plot for symmetric vertical excitation, GBU-8 forward shaker location, and force level of 15 lbf. Pylon nose up at limit.

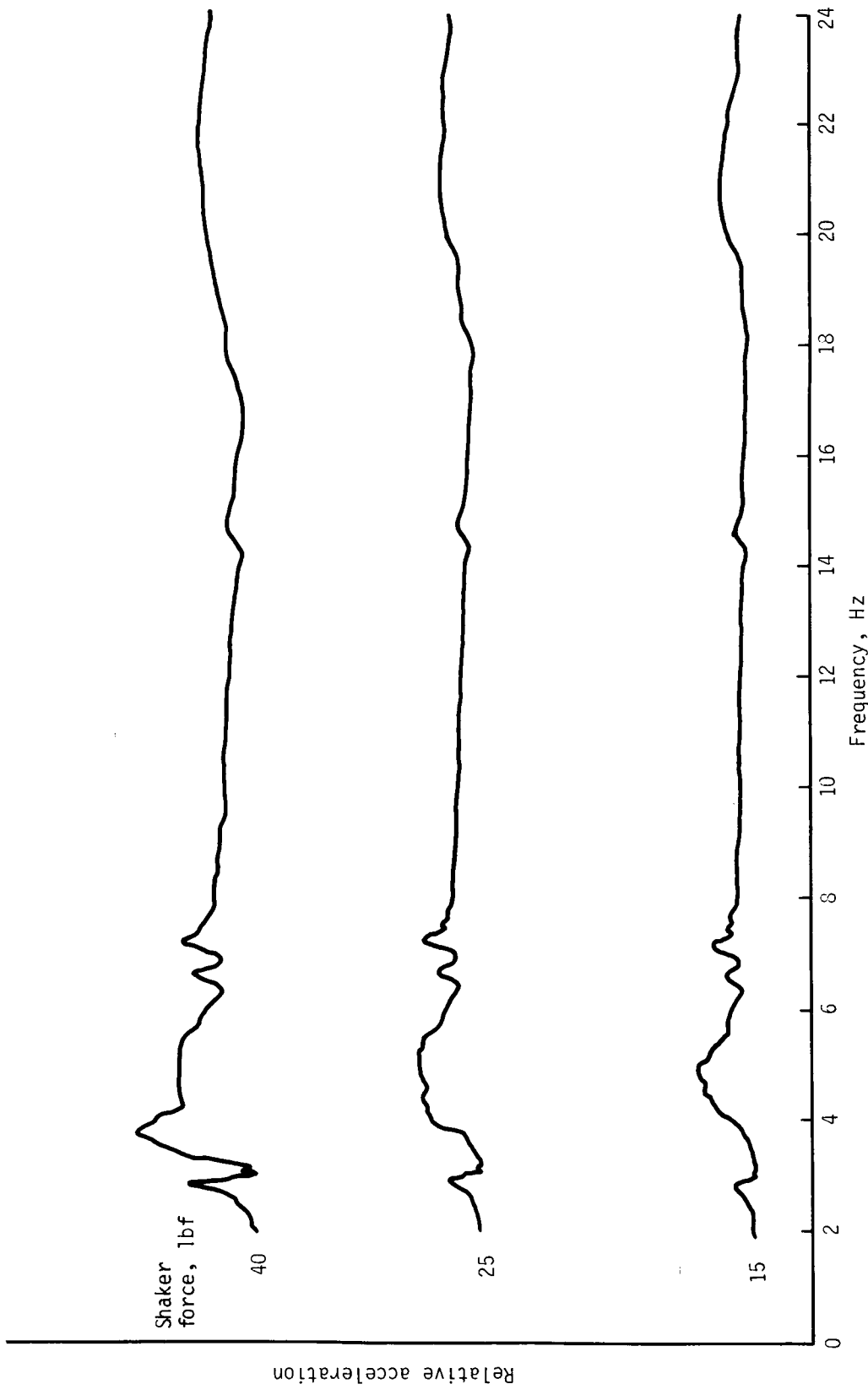


Figure A7. Frequency sweep plot at location 801V for symmetric vertical excitation, GBU-8 forward shaker location, and three force levels. Pylon nose up at limit.

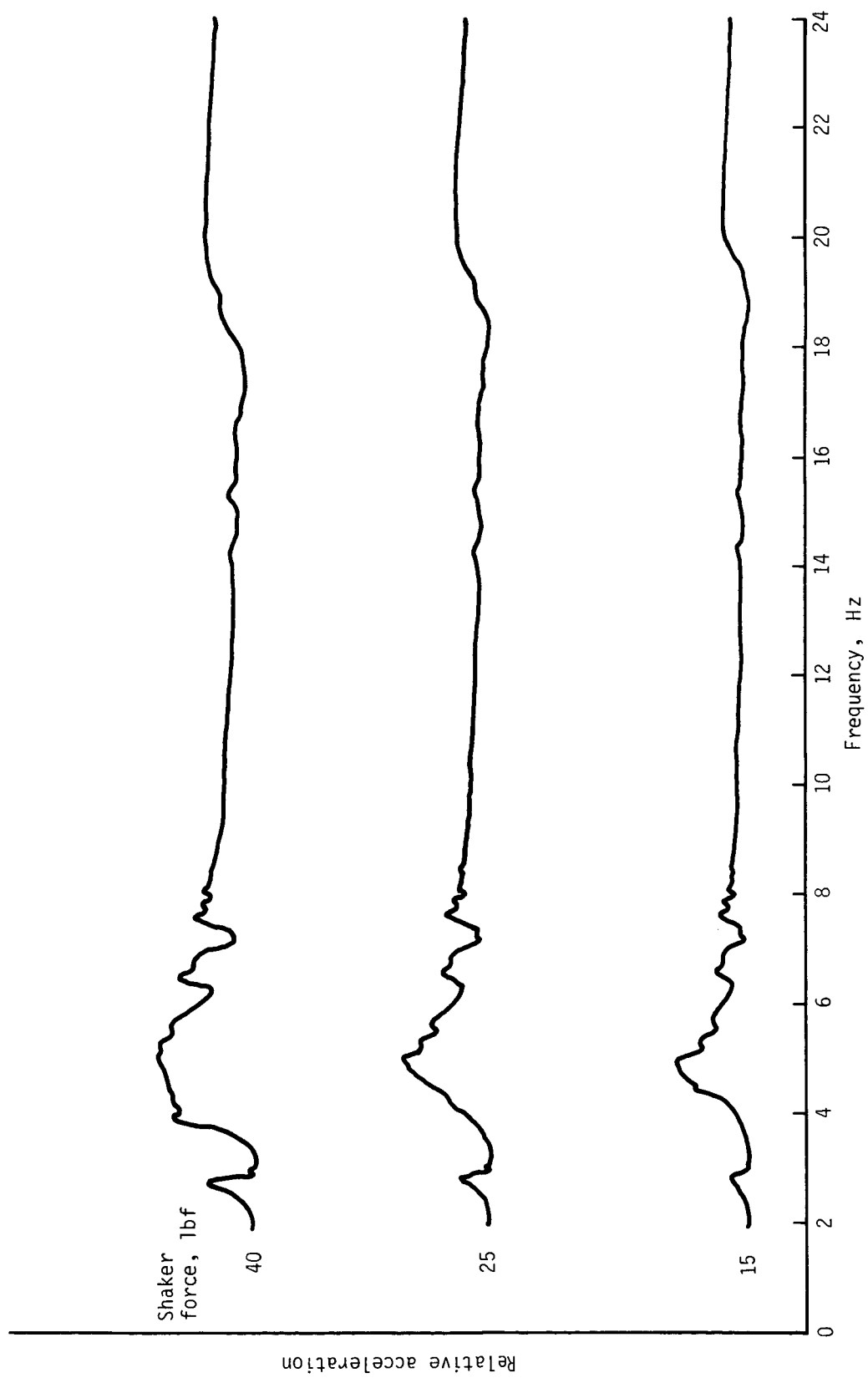


Figure A8. Frequency sweep plot at location 901V for symmetric vertical excitation, GBU-8 forward shaker location, and three force levels. Pylon nose up at limit.

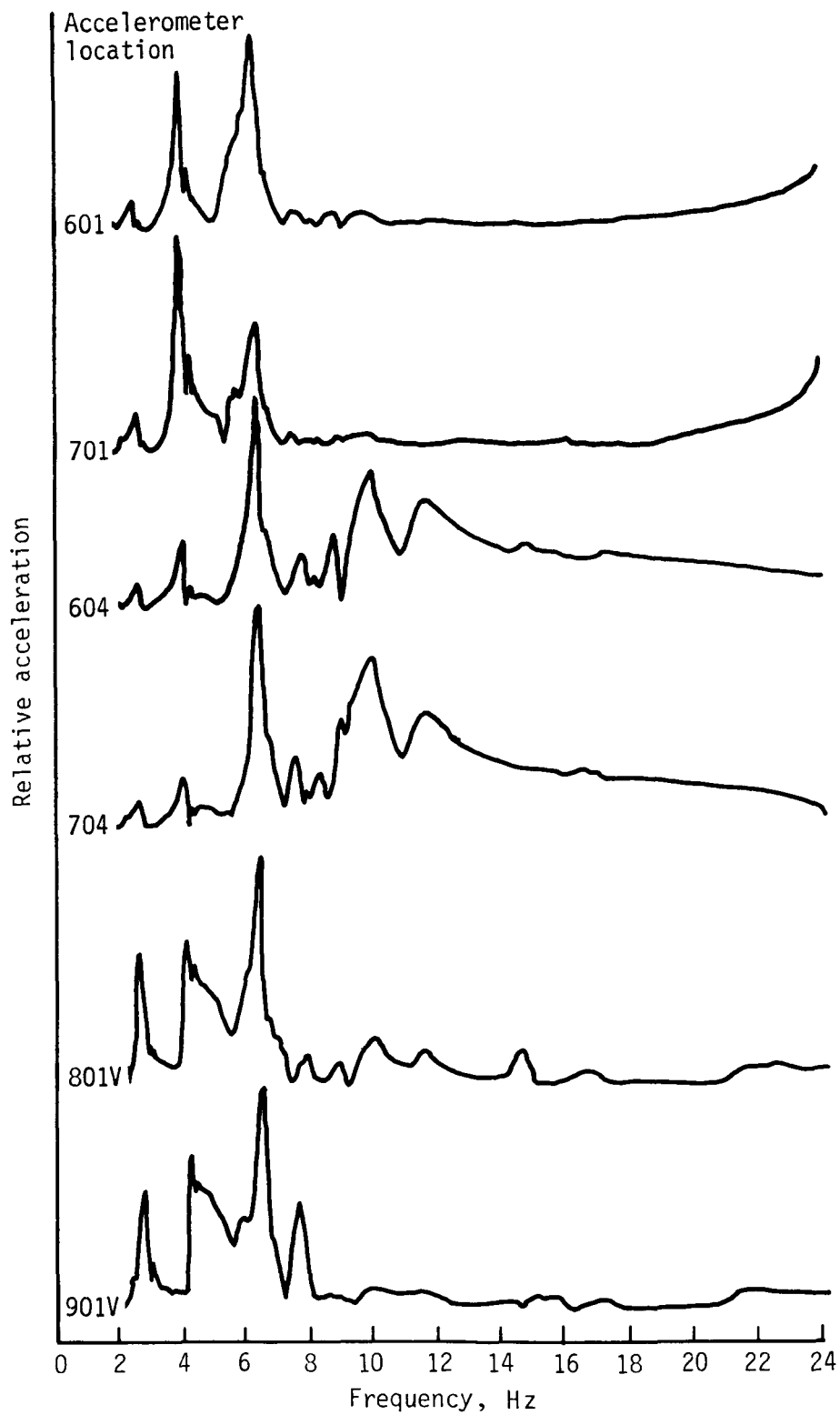


Figure A9. Frequency sweep plot for symmetric vertical excitation, launcher aft shaker location, and force level of 20 lbf. Pylon bound with 450-lbf preload.

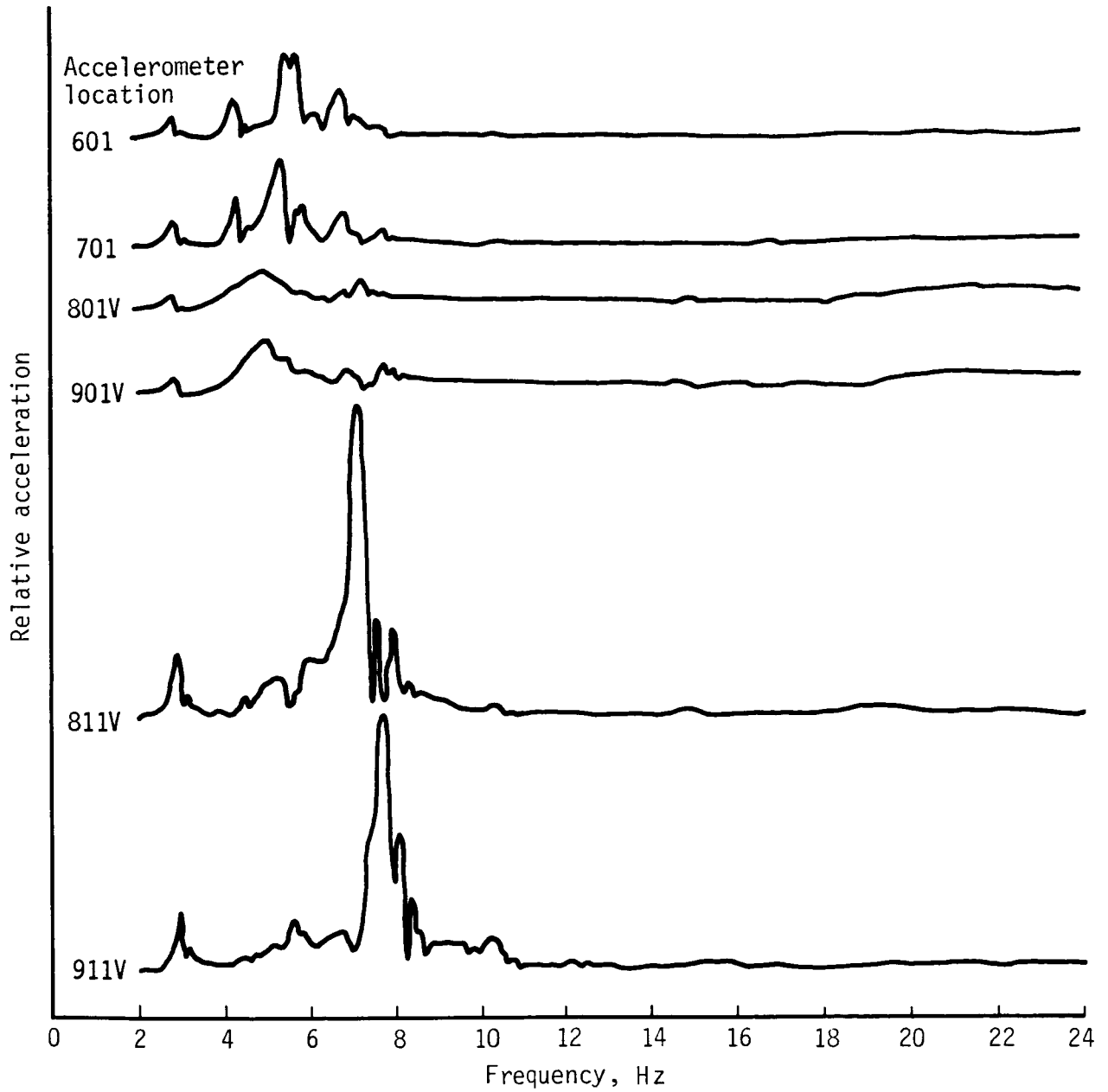


Figure A10. Frequency sweep plot for symmetric vertical excitation, GBU-8 forward shaker location, and force level of 15 lbf. Pylon bound with 450-lbf preload.

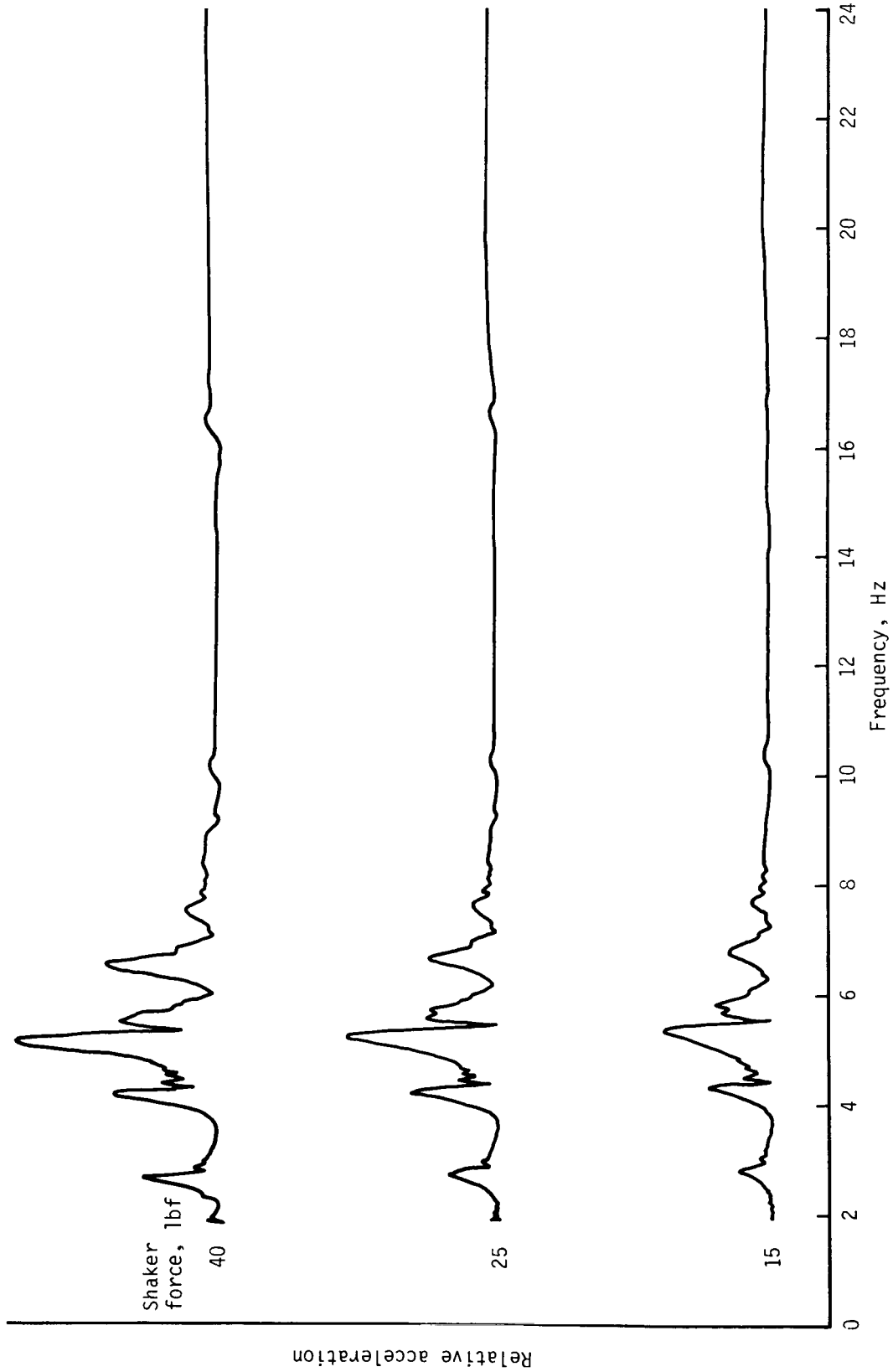


Figure A11. Frequency sweep plot for location 701 for symmetric vertical excitation, GBU-8 forward shaker location, and three force levels. Pylon bound with 450-lbf preload.

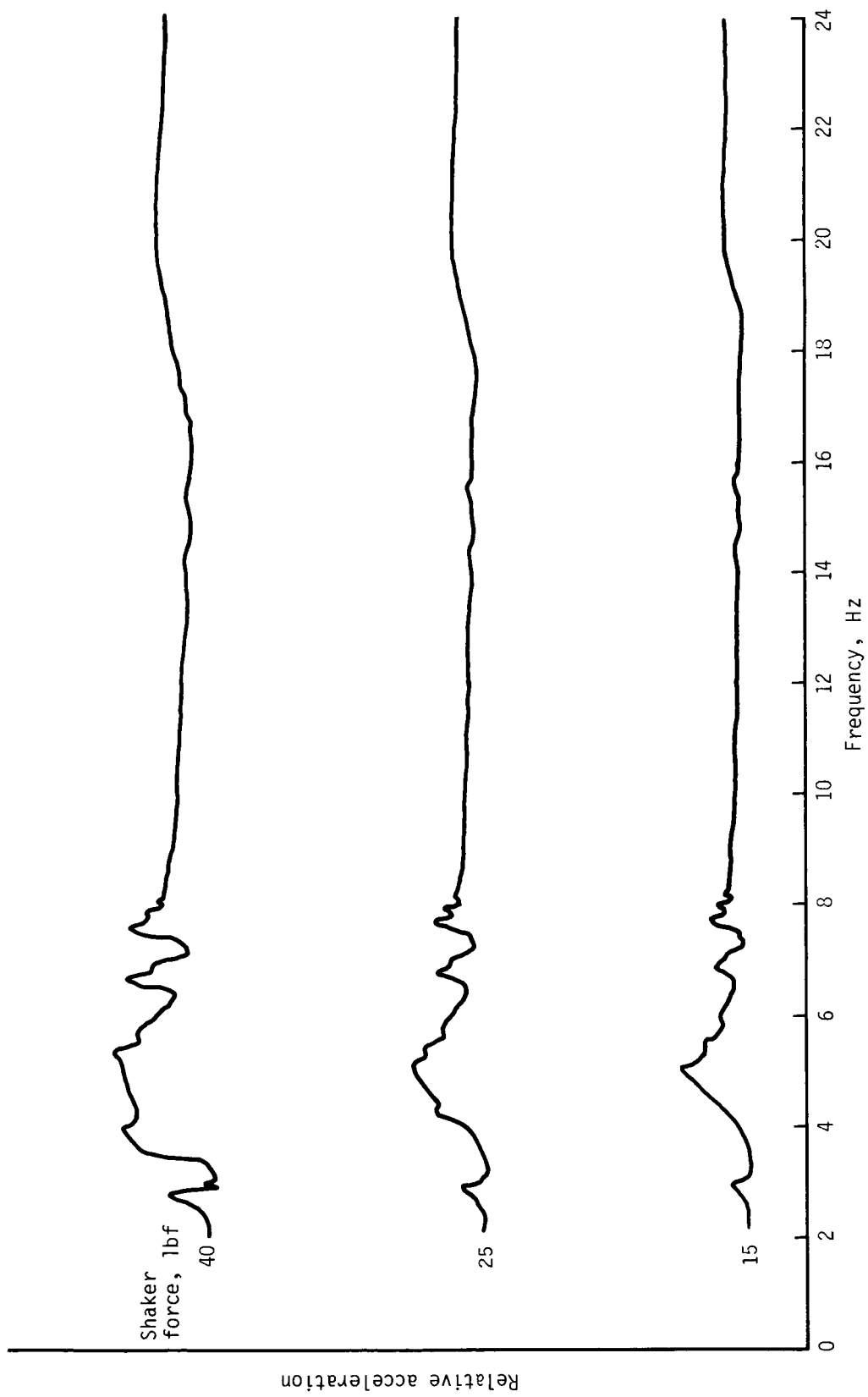


Figure A12. Frequency sweep plot for location 901V for symmetric vertical excitation, GBU-8 forward shaker location, and three force levels. Pylon bound with 450-lbf preload.

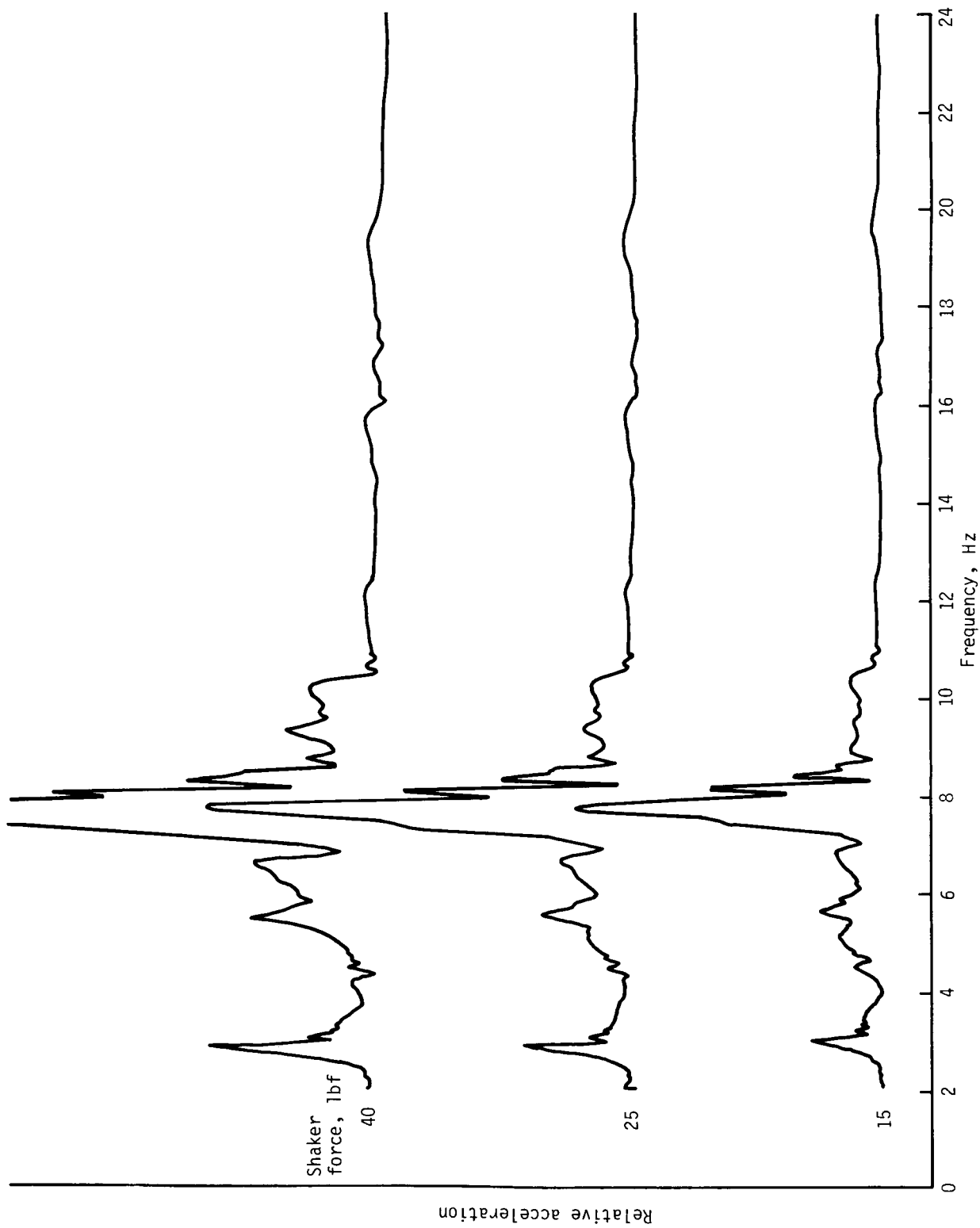


Figure A13. Frequency sweep plot for location 911V for symmetric vertical excitation, GBU-8 forward shaker location, and three force levels. Pylon bound with 450-lbf preload.

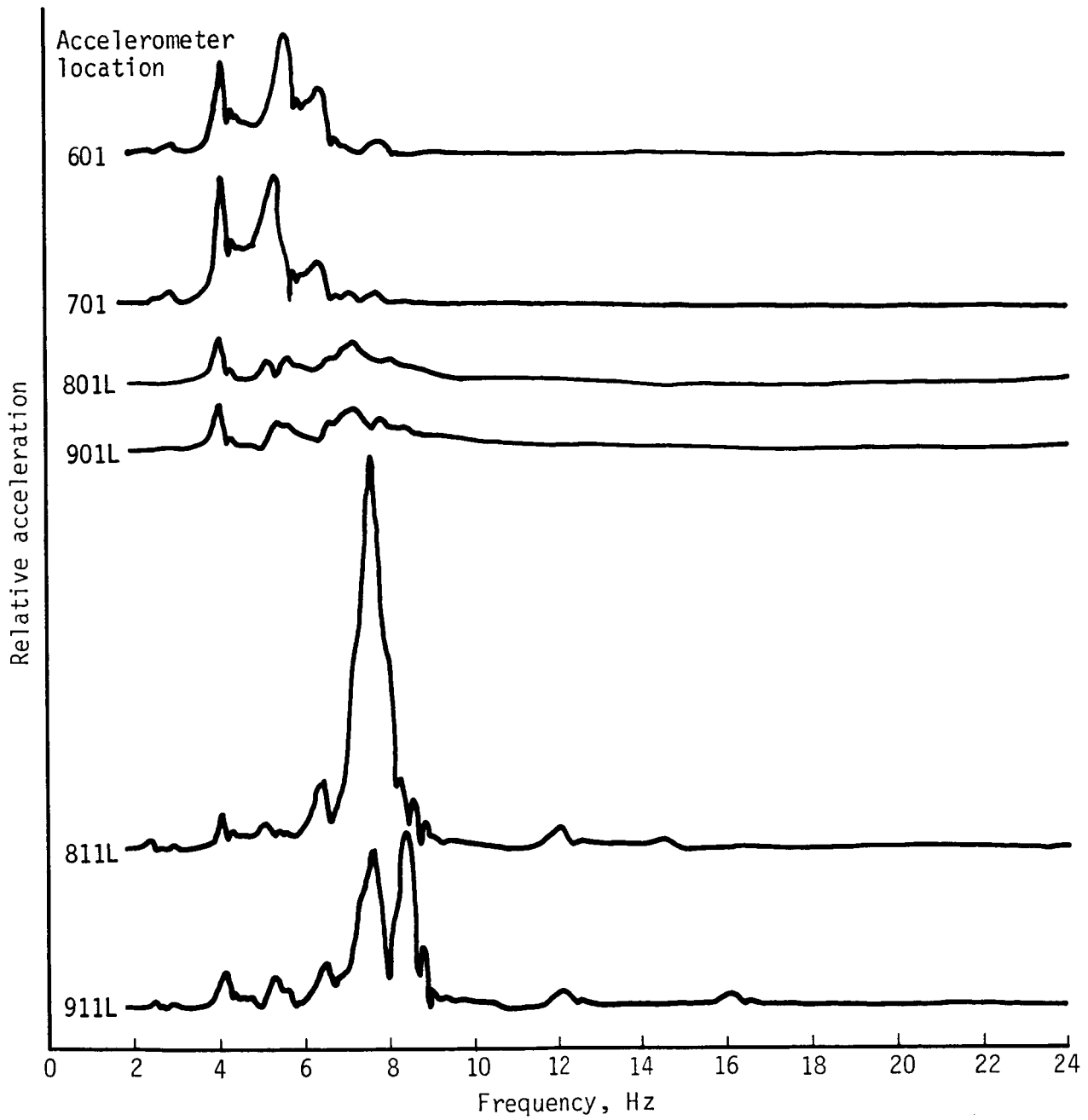


Figure A14. Frequency sweep plot for symmetric lateral roll excitation, GBU-8 forward and aft shaker locations, and force level of 15 lbf.

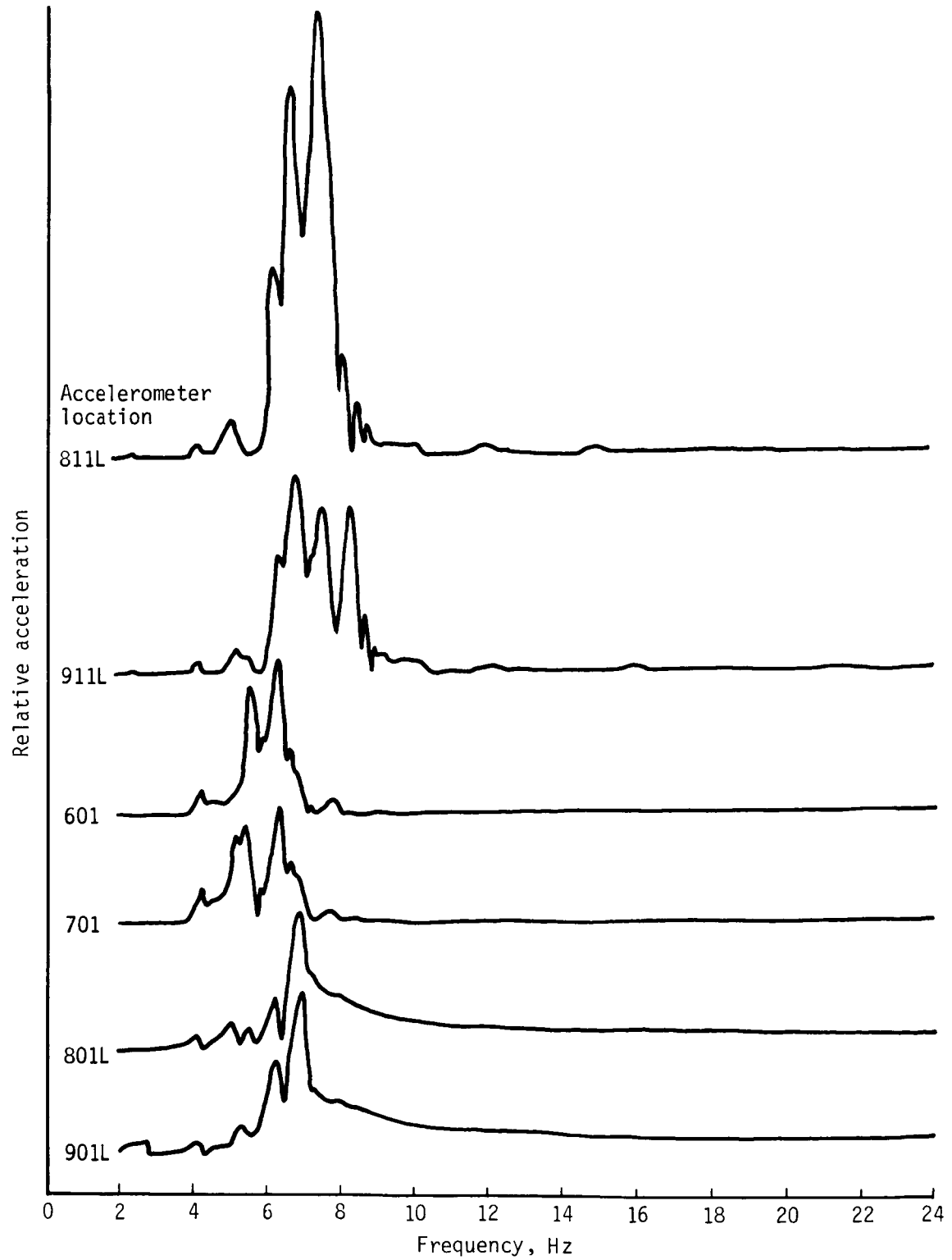


Figure A15. Frequency sweep plot for symmetric lateral yaw excitation, GBU-8 forward and aft shaker locations, and force level of 15 lbf.

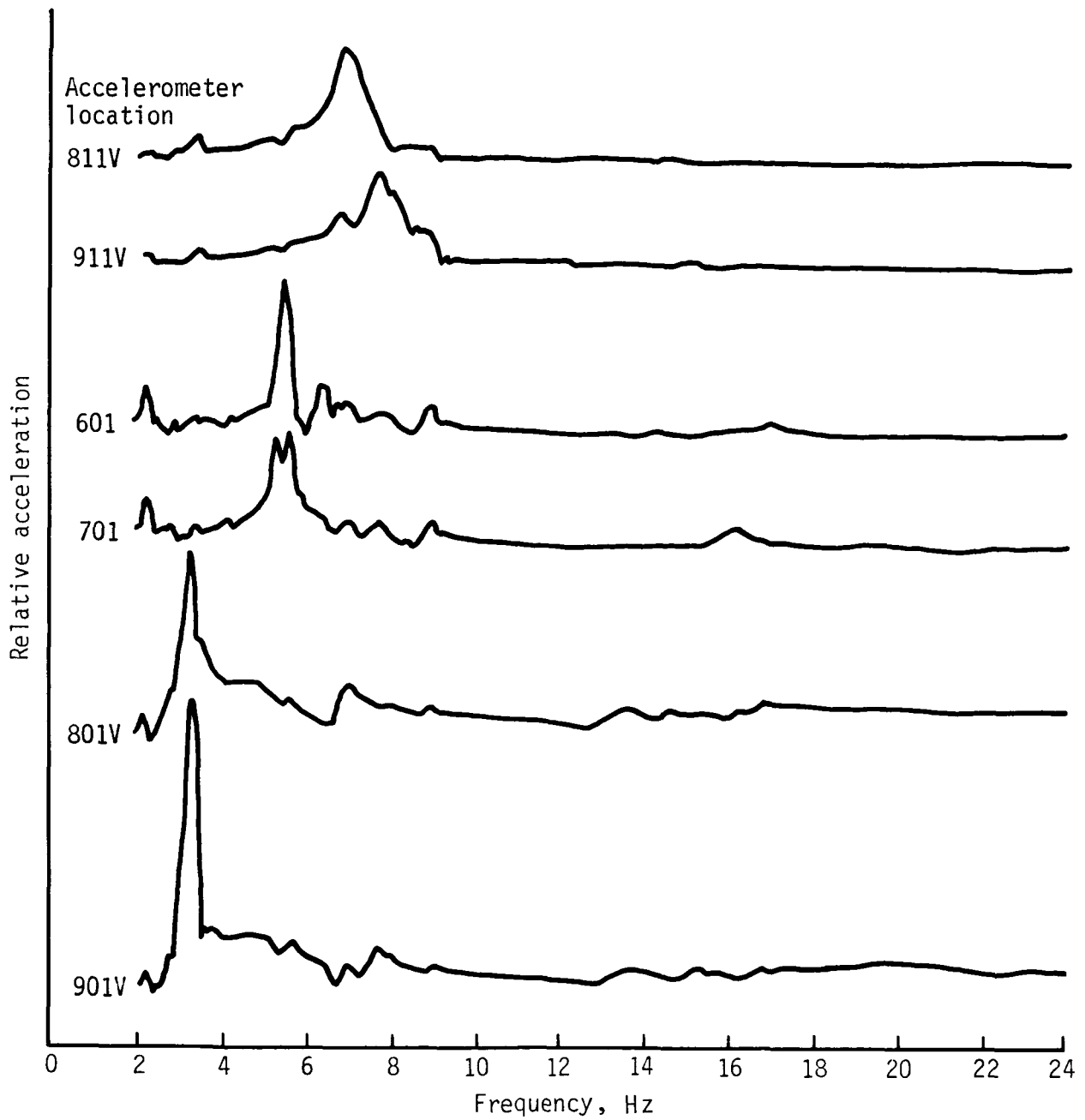


Figure A16. Frequency sweep plot for antisymmetric vertical excitation, GBU-8 forward shaker location, and force level of 40 lbf.

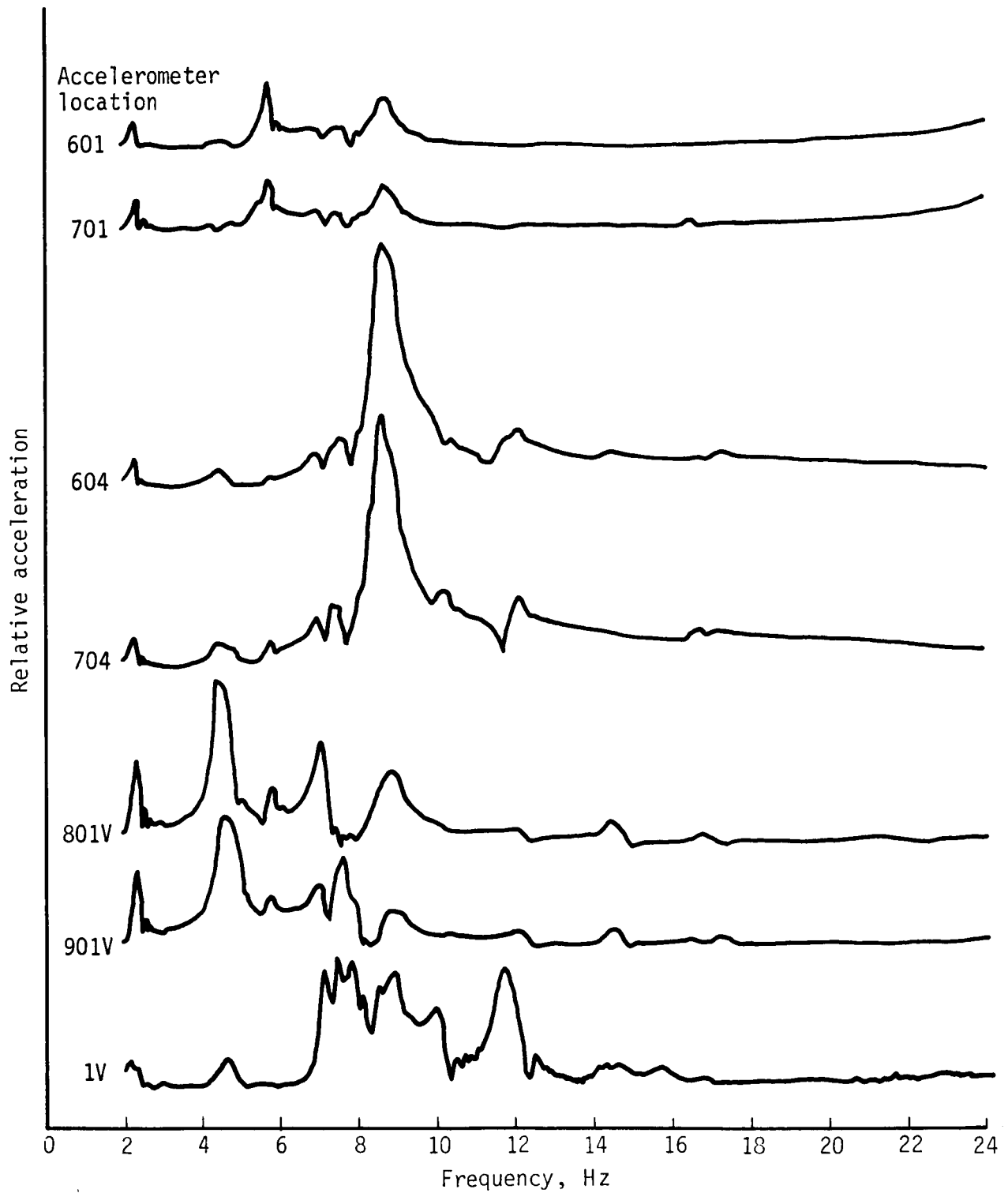


Figure A17. Frequency sweep plot for antisymmetric vertical excitation, launcher aft shaker location, and force level of 20 lbf.

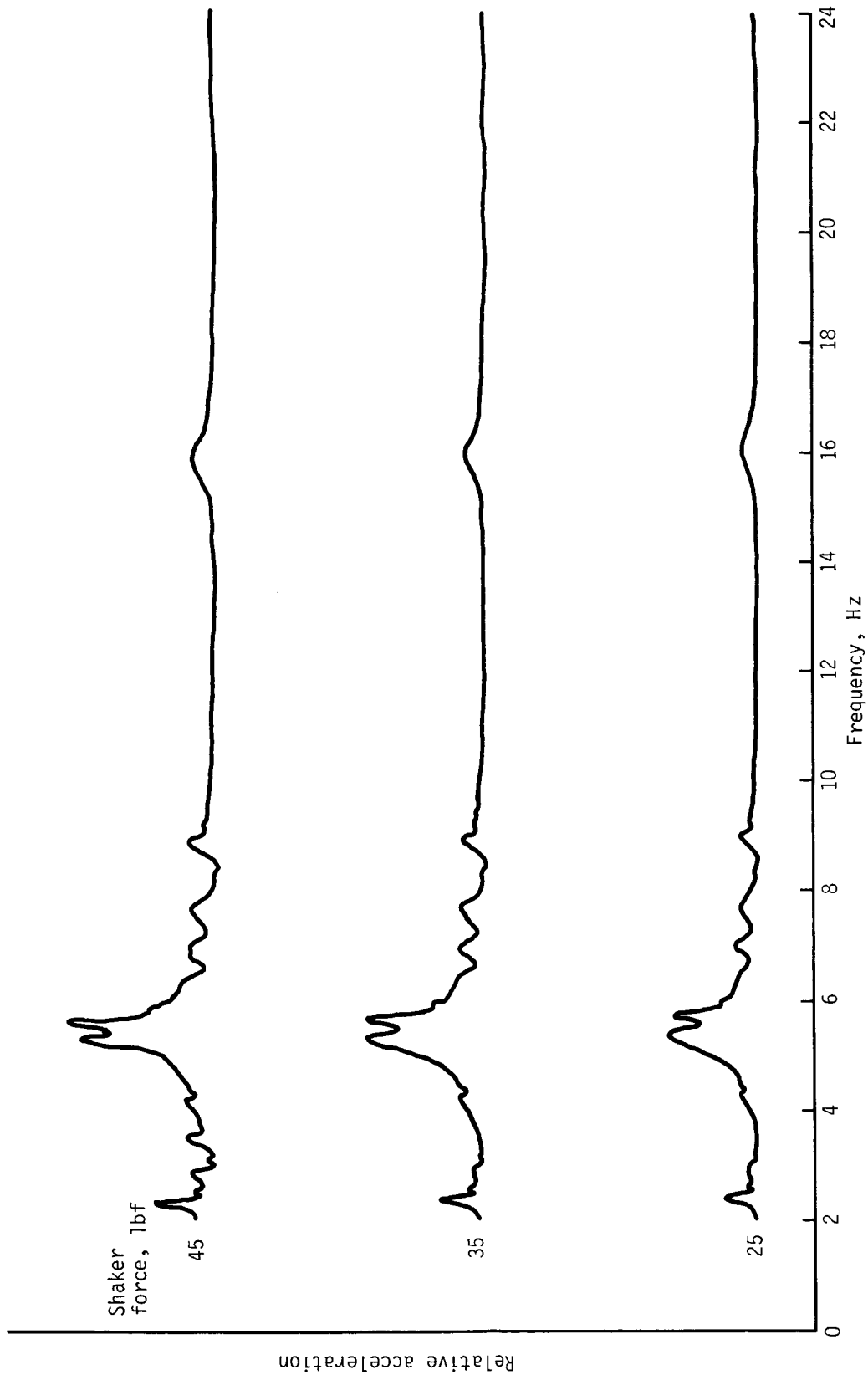


Figure A18. Frequency sweep plot at location 701 for antisymmetric vertical excitation, GBU-8 forward shaker location, and three force levels.

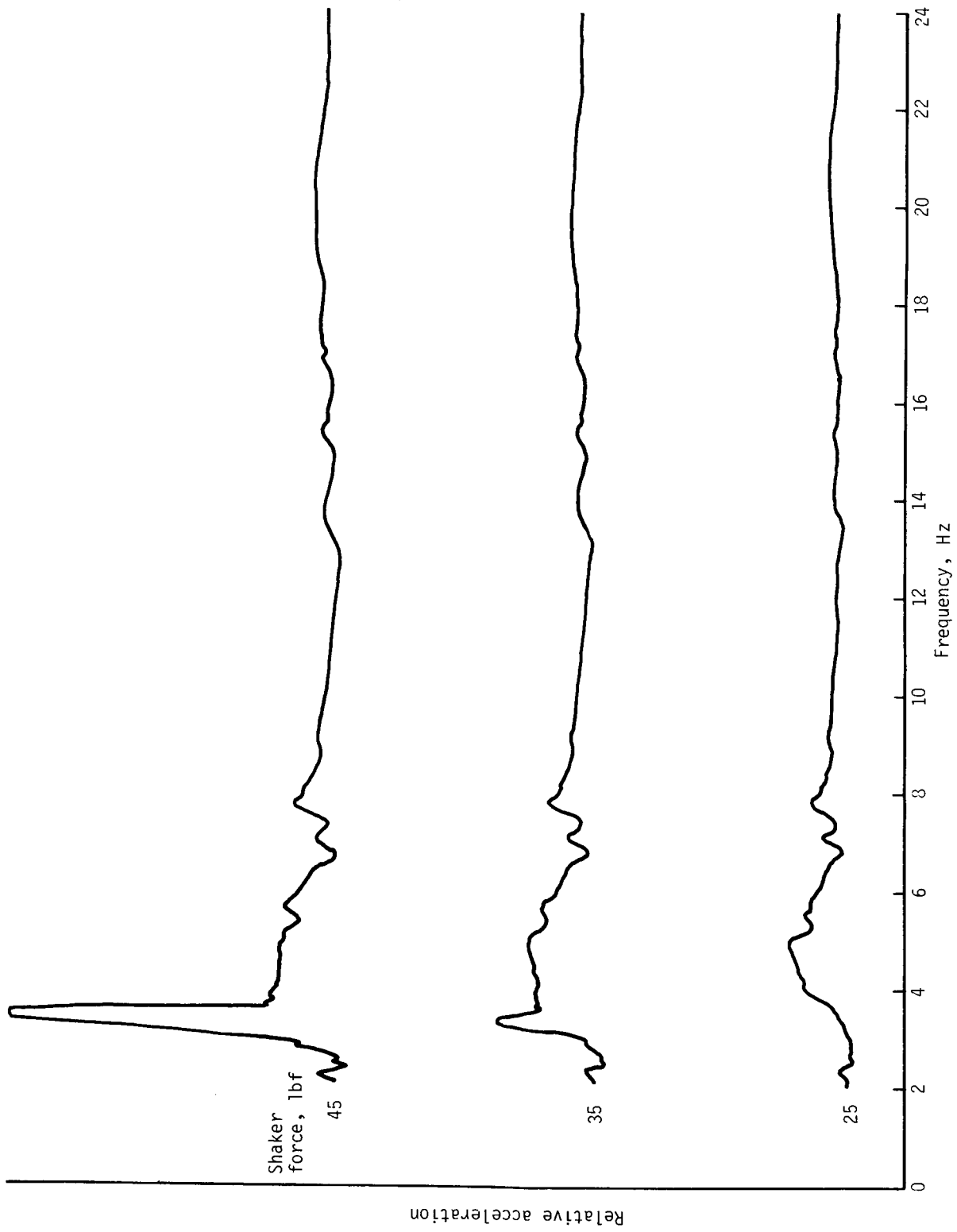


Figure A19. Frequency sweep plot at location 901V for antisymmetric vertical excitation, GBU-8 forward shaker location, and three force levels.

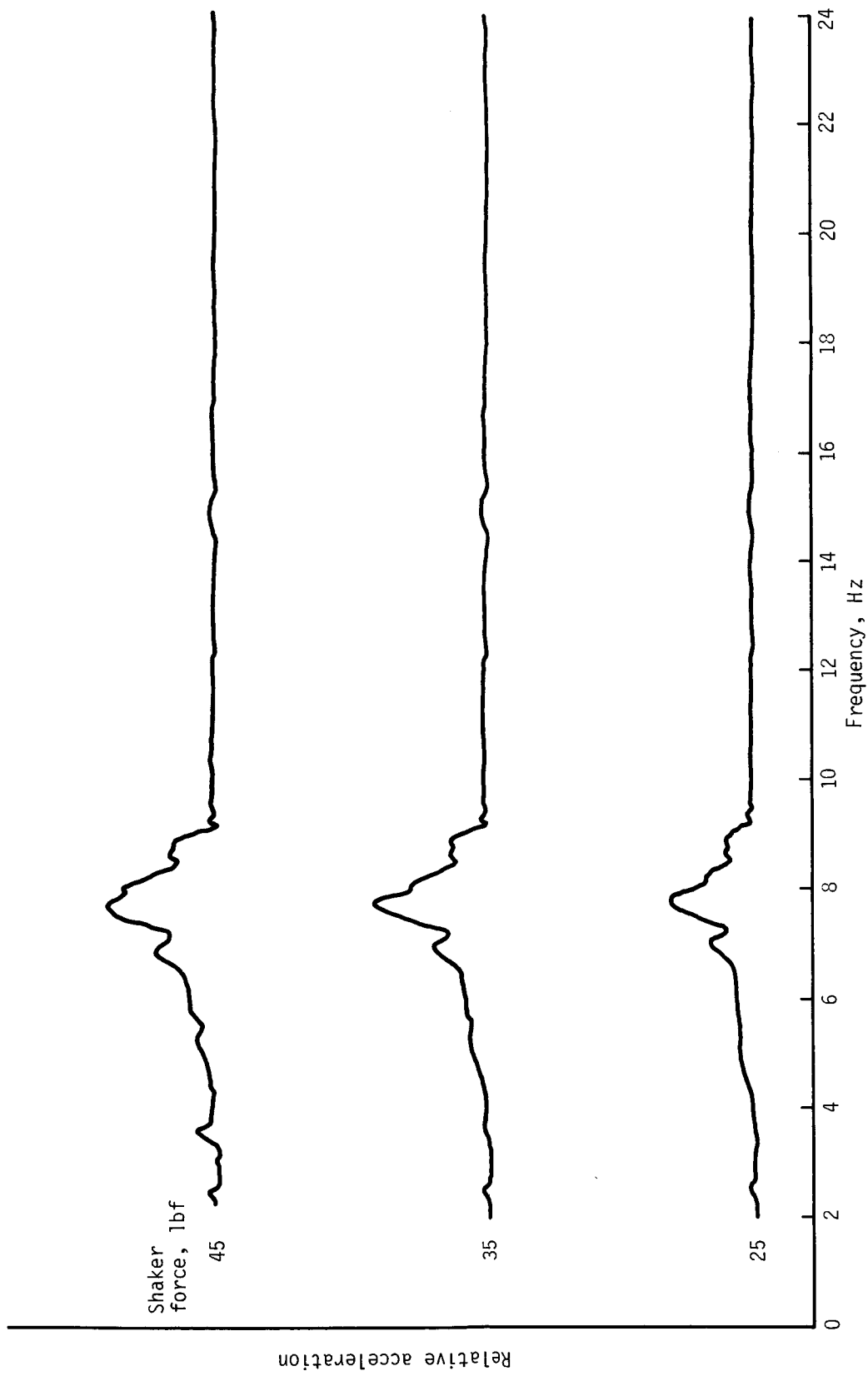


Figure A20. Frequency sweep plot at location 911V for antisymmetric vertical excitation, GBU-8 forward shaker location, and three force levels.

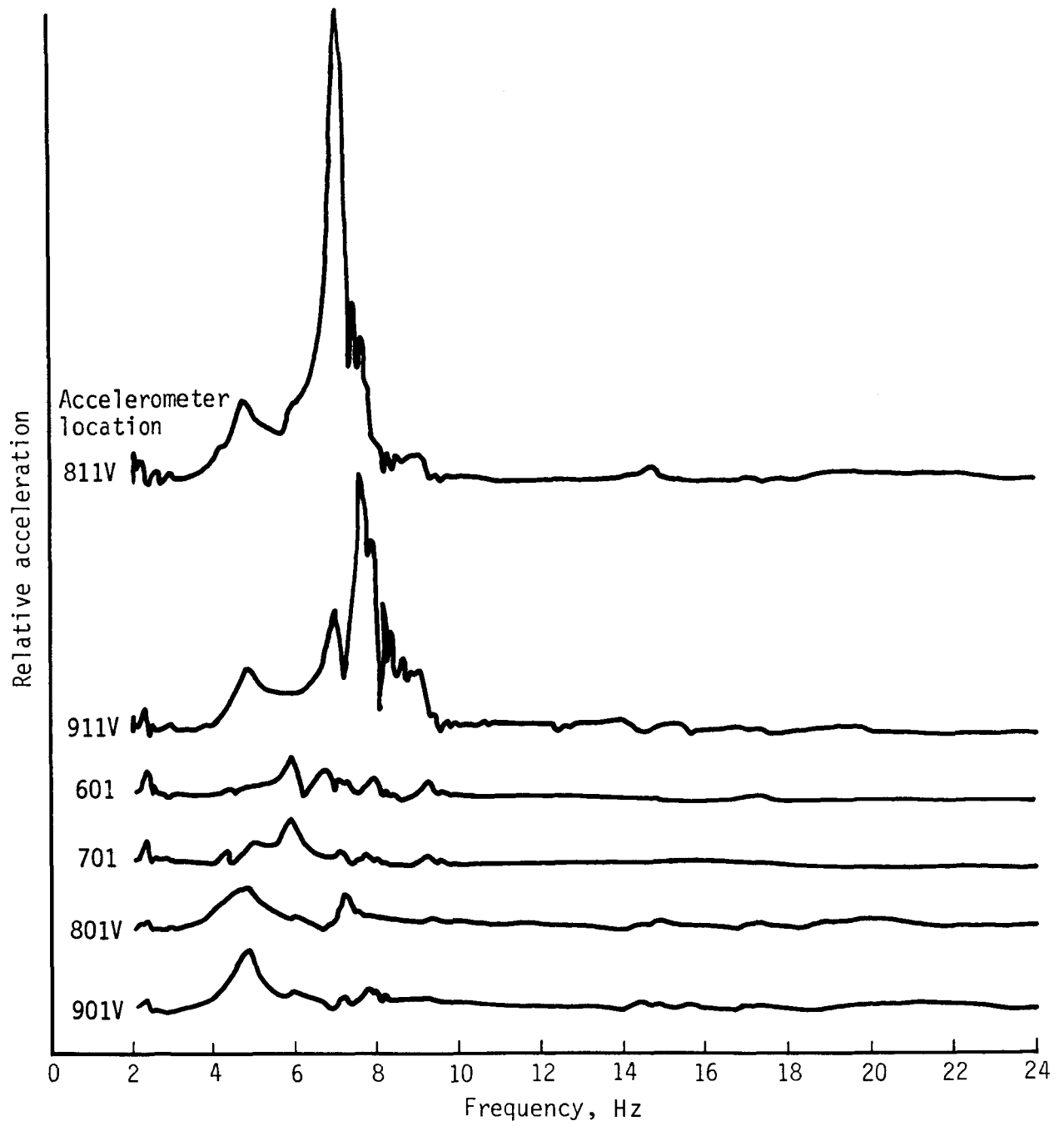


Figure A21. Frequency sweep plot for antisymmetric vertical excitation, GBU-8 forward shaker location, and force level of 15 lbf. Pylon nose up at limit.

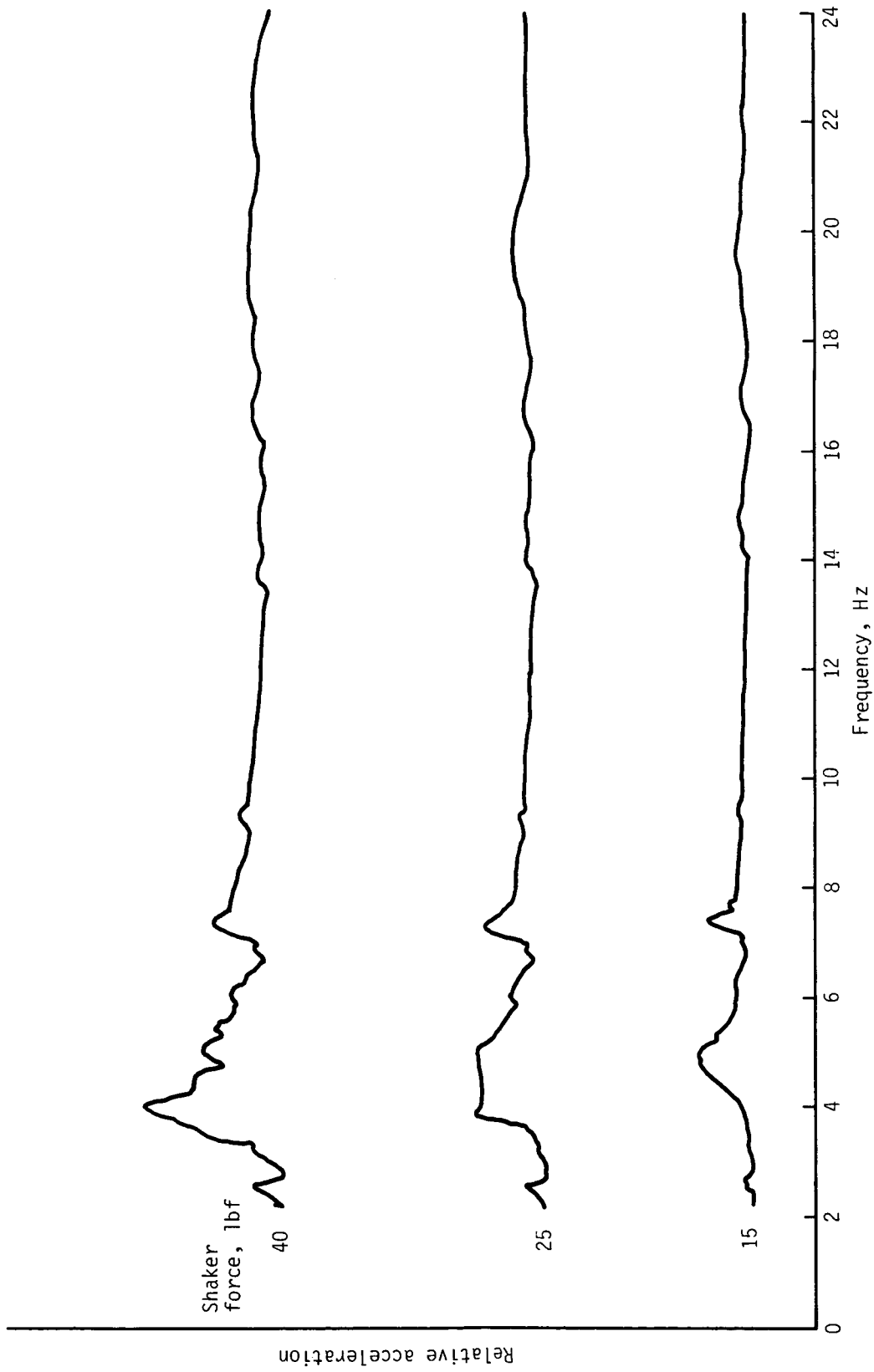


Figure A22. Frequency sweep plot at location 801V for antisymmetric vertical excitation, GBU-8 forward shaker location, and three force levels. Pylon nose up at limit.

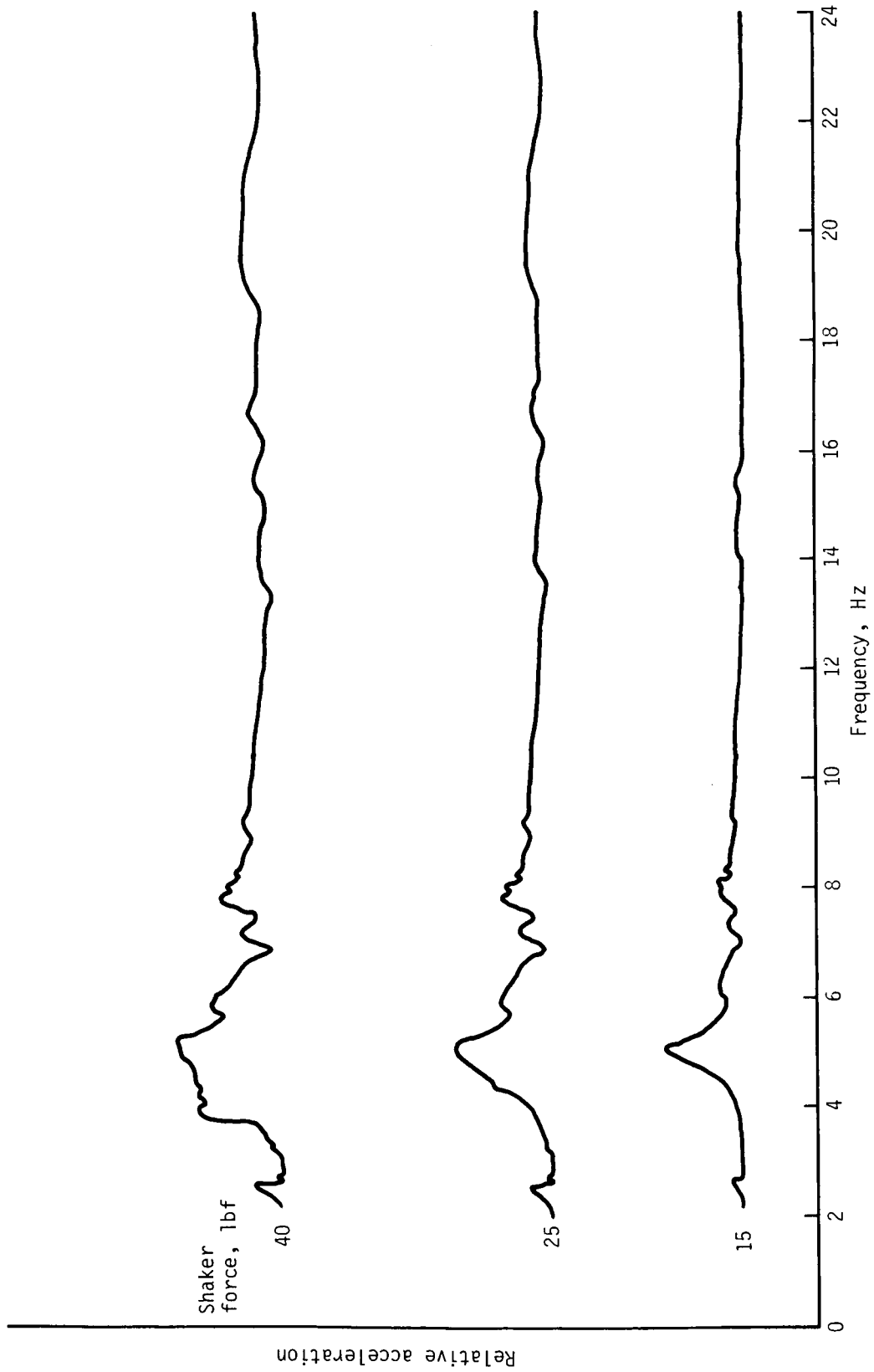


Figure A23. Frequency sweep plot at location 901V for antisymmetric vertical excitation, GBU-8 forward shaker location, and three force levels. Pylon nose up at limit.

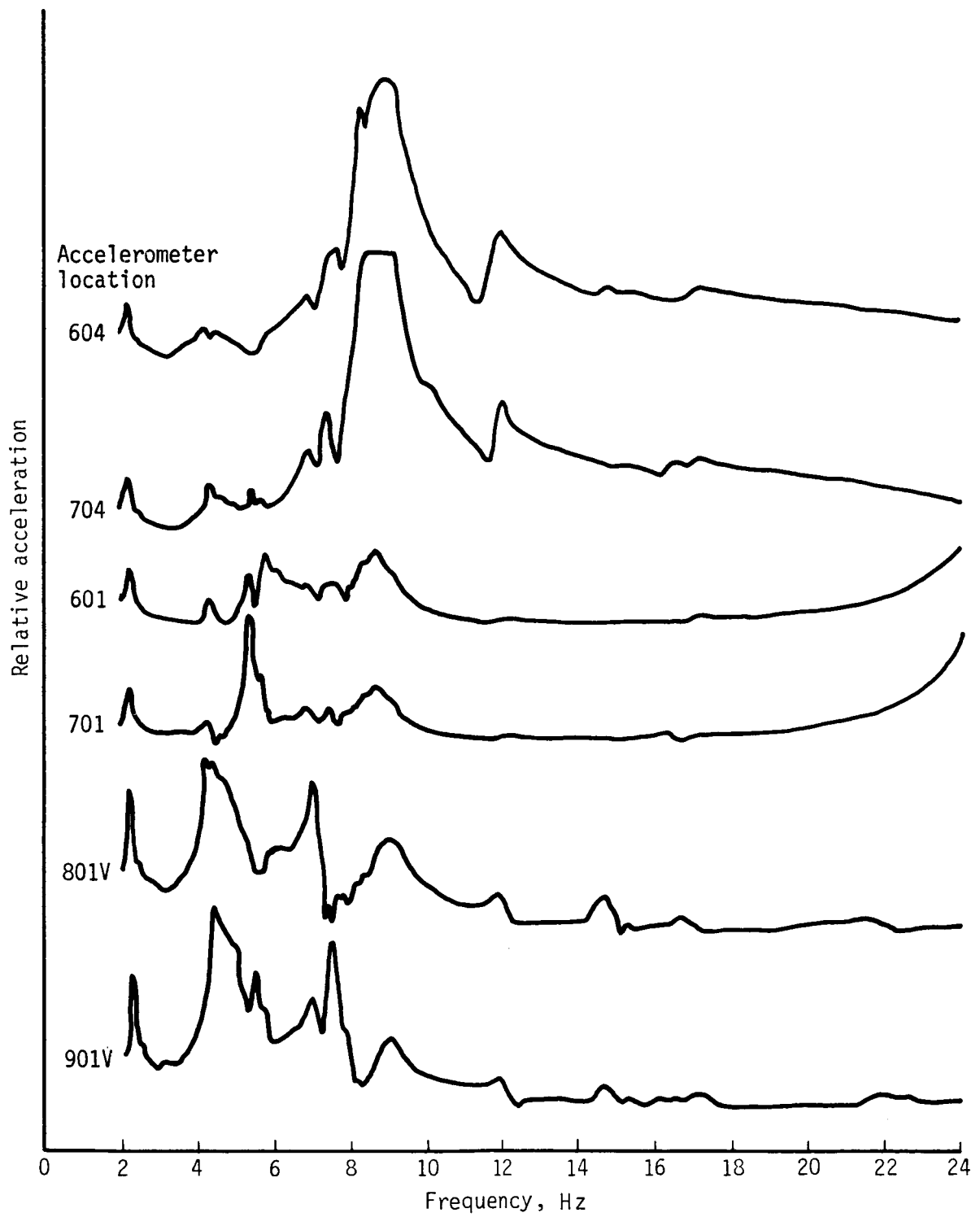


Figure A24. Frequency sweep plot for antisymmetric vertical excitation, launcher aft shaker location, and force level of 20 lbf. Pylon bound with 450-lbf preload.

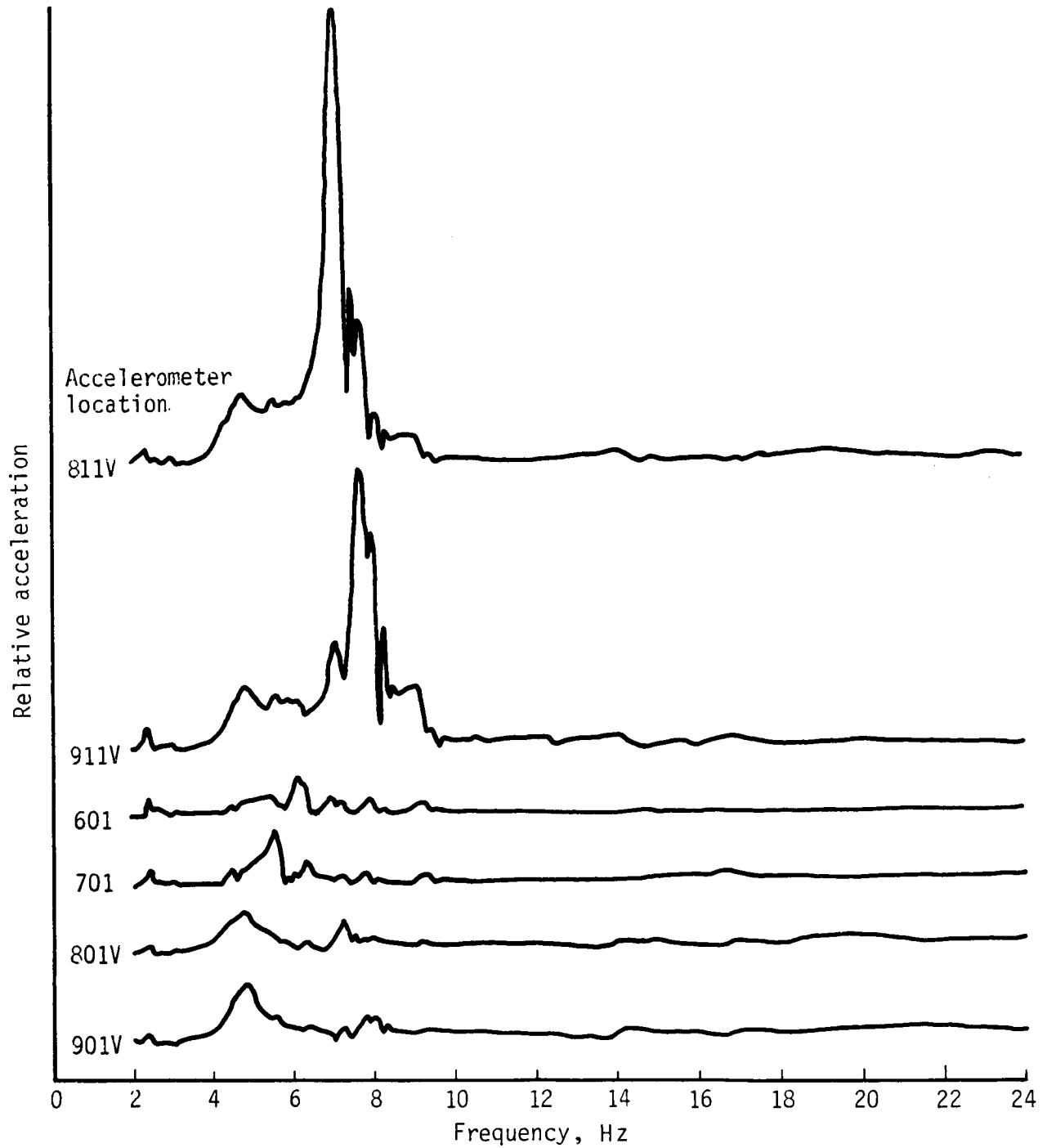


Figure A25. Frequency sweep plot for antisymmetric vertical excitation, GBU-8 forward shaker location, and force level of 15 lbf. Pylon bound with 450-lbf preload.

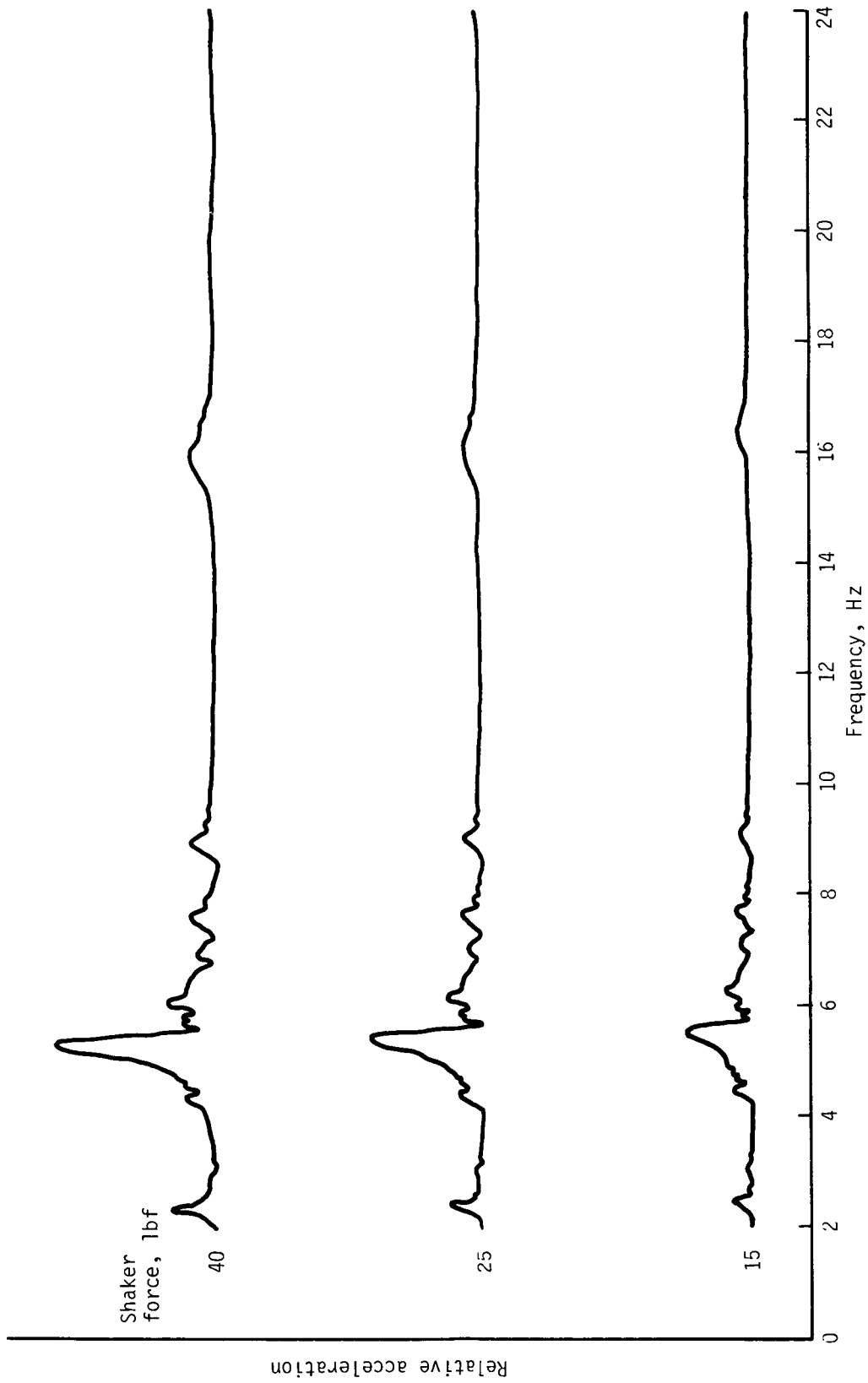


Figure A26. Frequency sweep plot at location 701 for antisymmetric vertical excitation, GBU-8 forward shaker location, and three force levels. Pylon bound with 450-lbf preload.

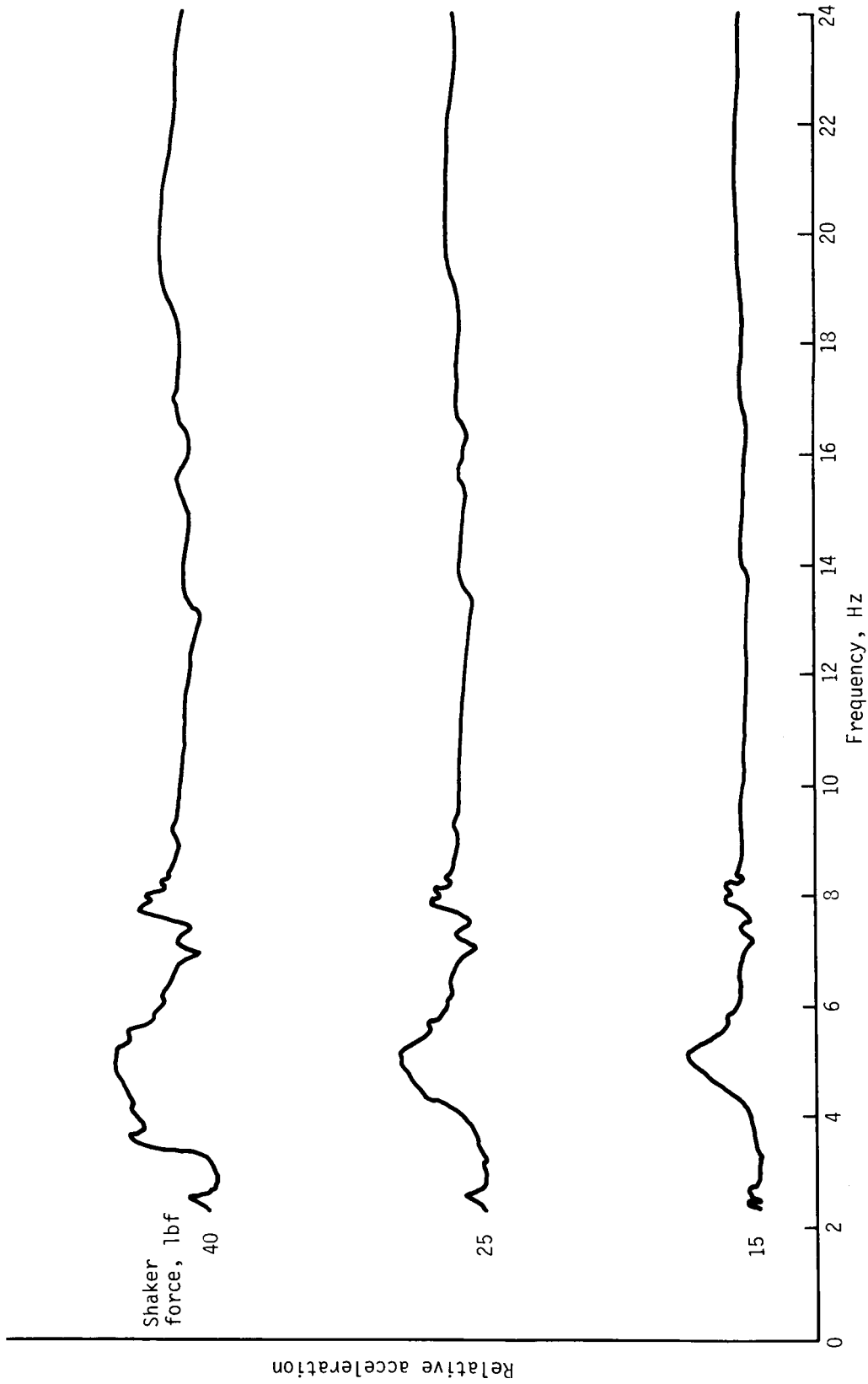


Figure A27. Frequency sweep plot at location 901V for antisymmetric vertical excitation, GBU-8 forward shaker location, and three force levels. Pylon bound with 450-lbf preload.

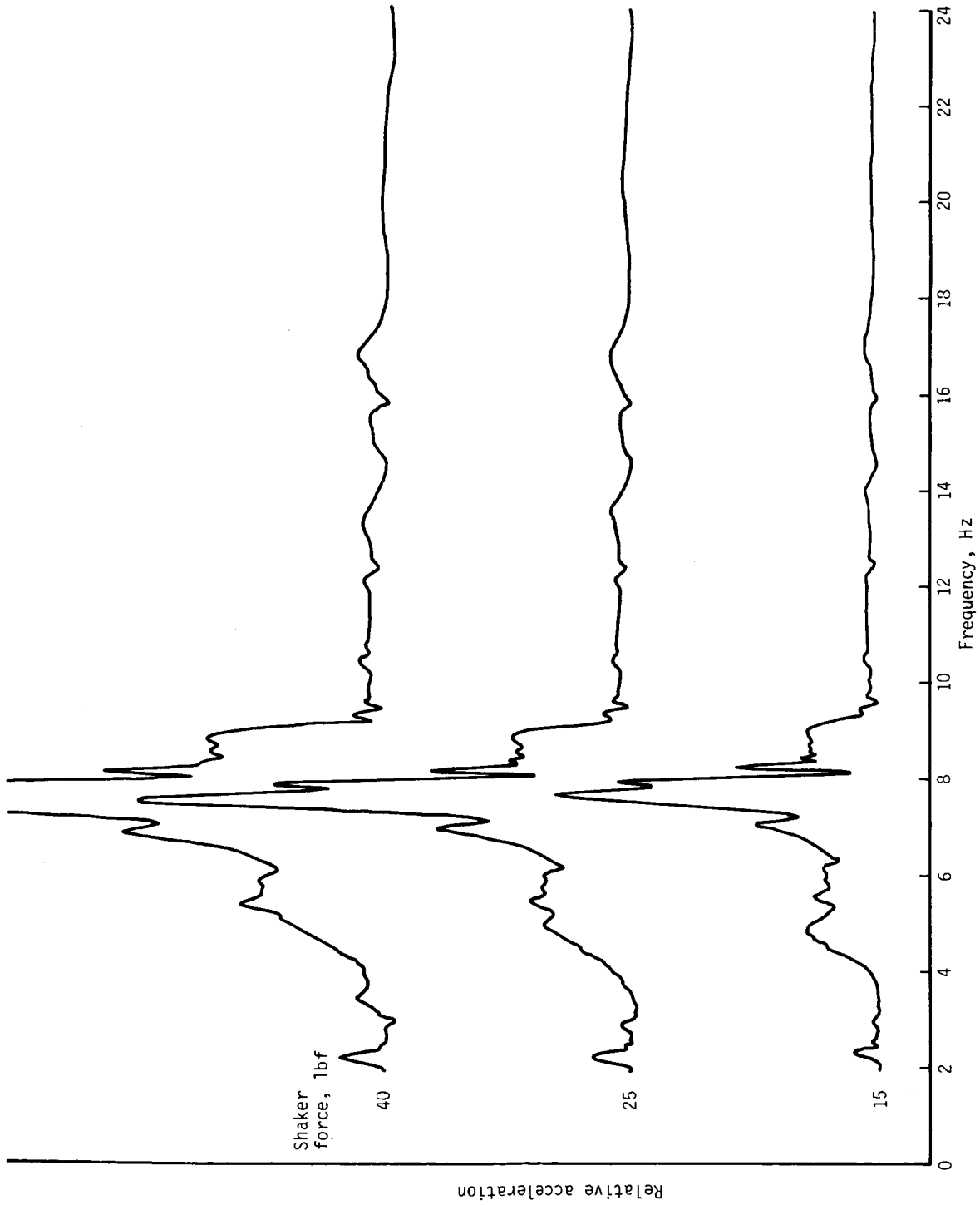


Figure A28. Frequency sweep plot at location 911V for antisymmetric vertical excitation, GBU-8 forward shaker location, and three force levels. Pylon bound with 450-lbf preload.

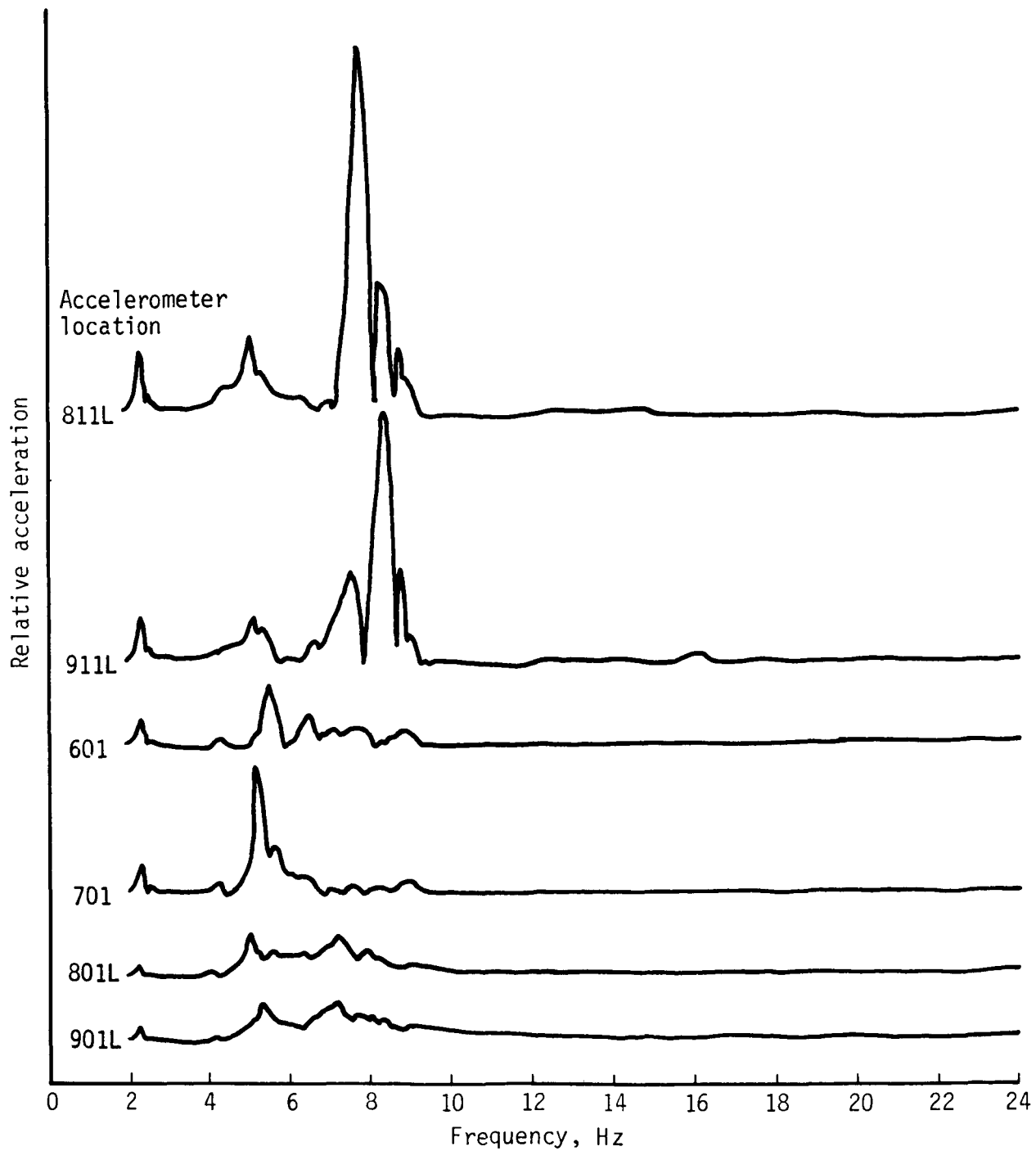


Figure A29. Frequency sweep plot for antisymmetric lateral roll excitation, GBU-8 forward and aft shaker locations, and force level of 15 lbf.

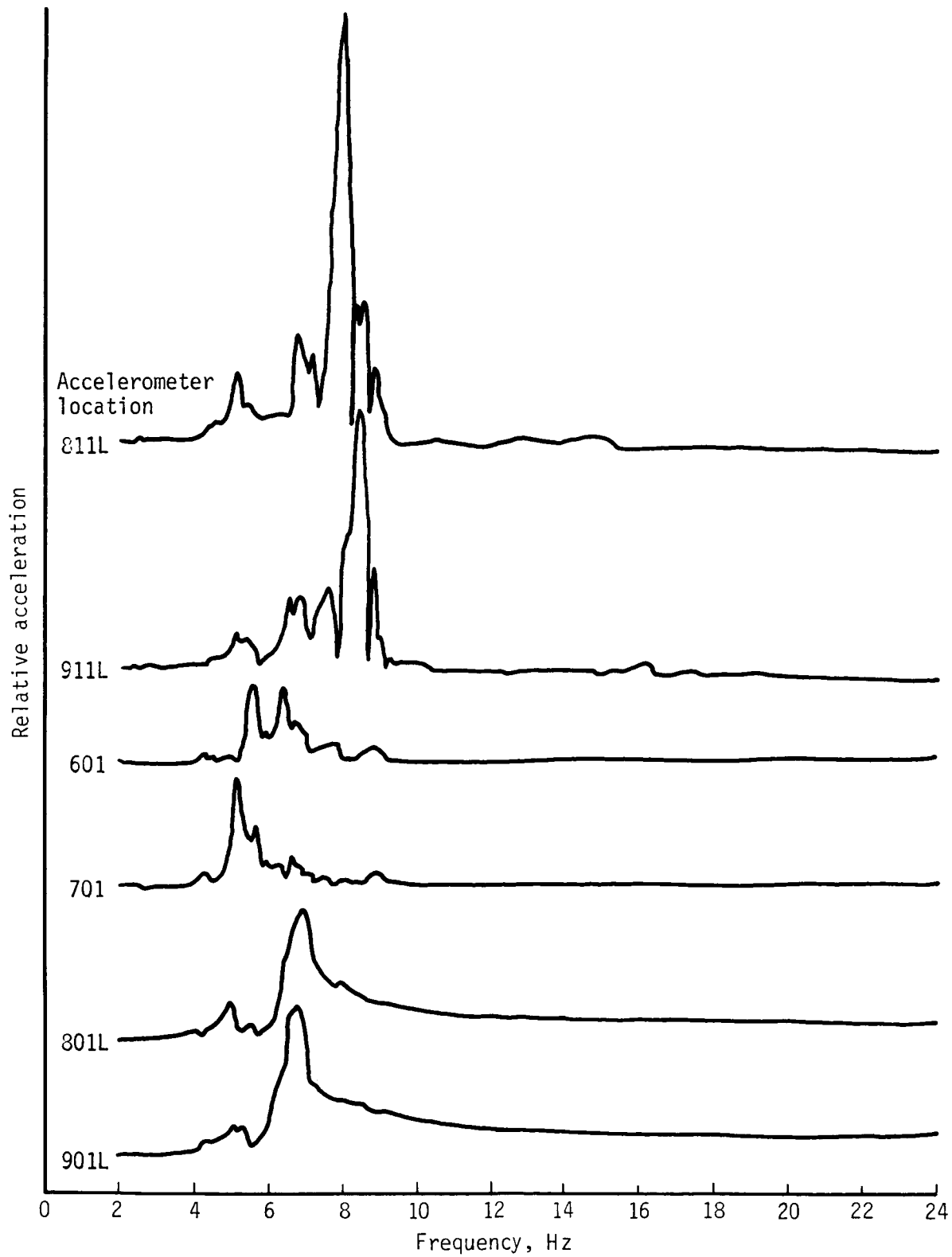


Figure A30. Frequency sweep plot for antisymmetric lateral yaw excitation, GBU-8 forward and aft shaker locations, and force level of 15 lbf.

Appendix B
Mode Shape Data

This appendix contains the measured mode shape data. The intention of the surveys was to identify the modes. Only partial surveys were accomplished

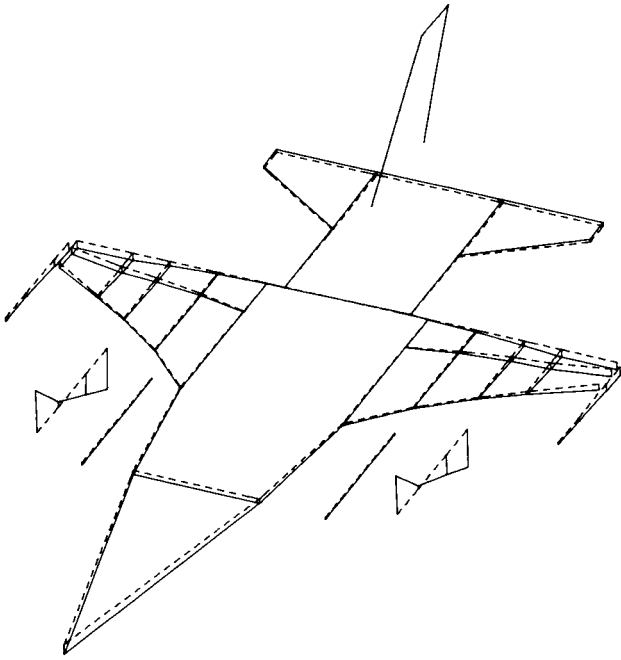
for the modes indicated by an asterisk in table BI, which lists the 13 mode shape plots presented in figures B1 and B2. The symmetric modes are given first (fig. B1) in order of increasing frequency, and they are followed by the antisymmetric modes (fig. B2) that are ordered in a similar manner.

TABLE BI. MODE SHAPE PLOTS

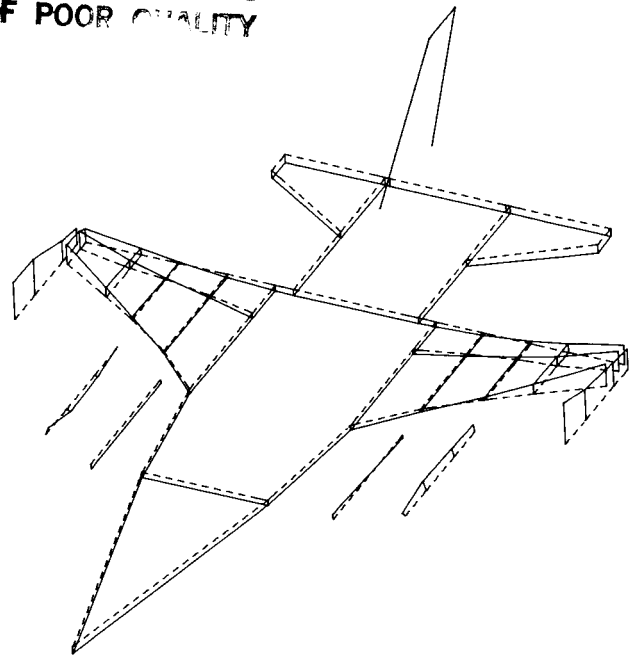
Figure	Frequency, Hz	Mode
Symmetric modes		
B1(a)	3.31	GBU-8 pitch
(b)	3.95	1st wing bending
(c)	4.65	Pylon strongback bending (pylon nose up)
(d)	*5.27	GBU-8 lateral (right)
(e)	*5.46	GBU-8 lateral (left)
(f)	6.09	Tip missile pitch
(g)	9.64	2d wing bending
Antisymmetric modes		
B2(a)	3.29	GBU-8 pitch
(b)	4.55	Pylon strongback bending (pylon nose up)
(c)	*4.94	GBU-8 lateral (left)
(d)	*5.18	GBU-8 lateral (right)
(e)	5.53	Tip missile pitch
(f)	8.66	1st wing bending

*Denotes partial survey.

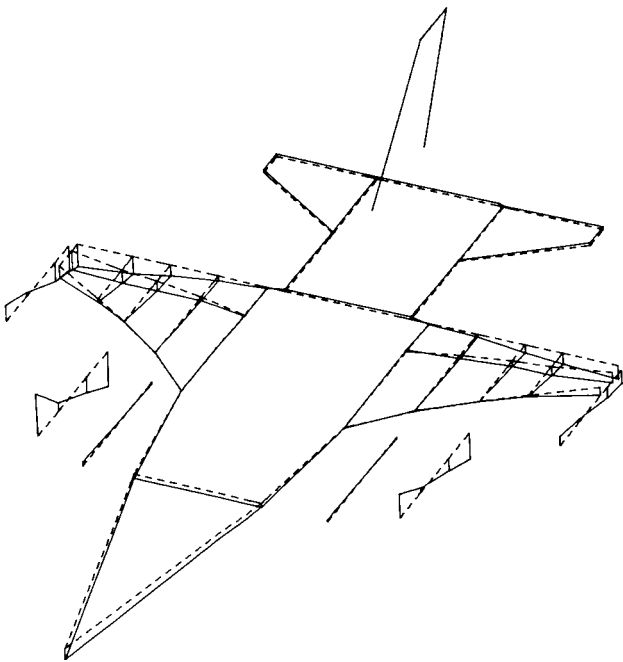
ORIGINAL PAGE IS
OF POOR QUALITY



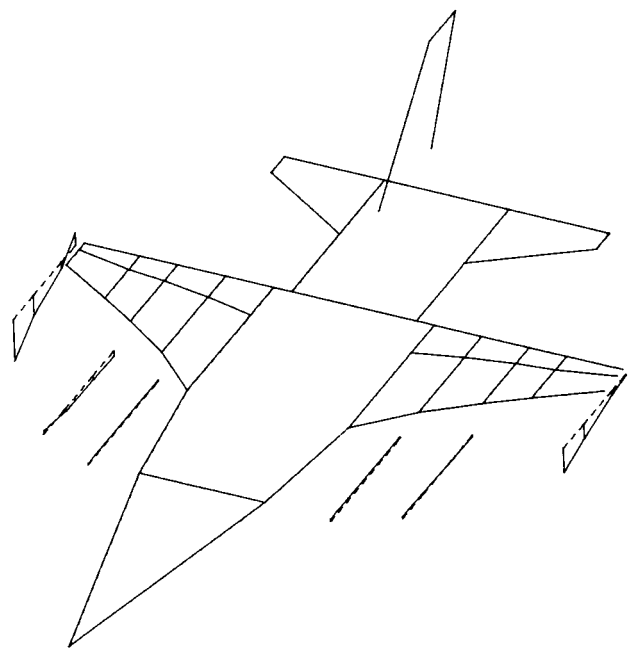
(a) Frequency, 3.31 Hz; GBU-8 pitch.



(b) Frequency, 3.95 Hz; first wing bending.

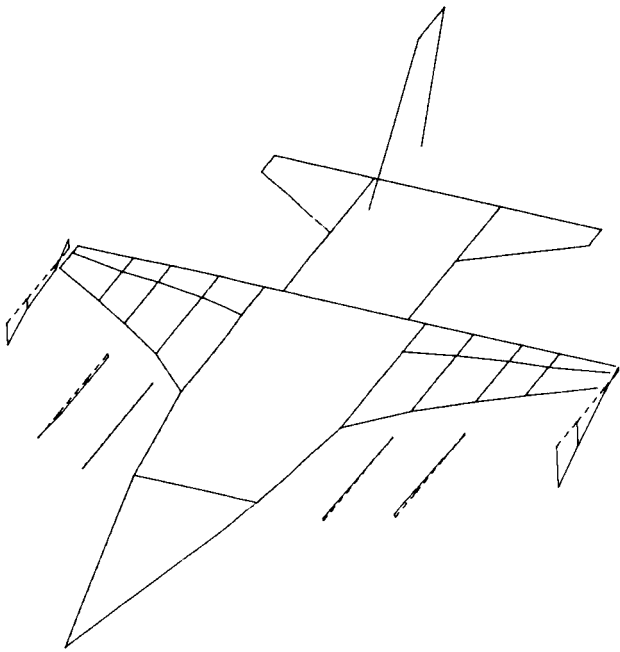


(c) Frequency, 4.65 Hz; pylon strongback bending
(pylon nose up).

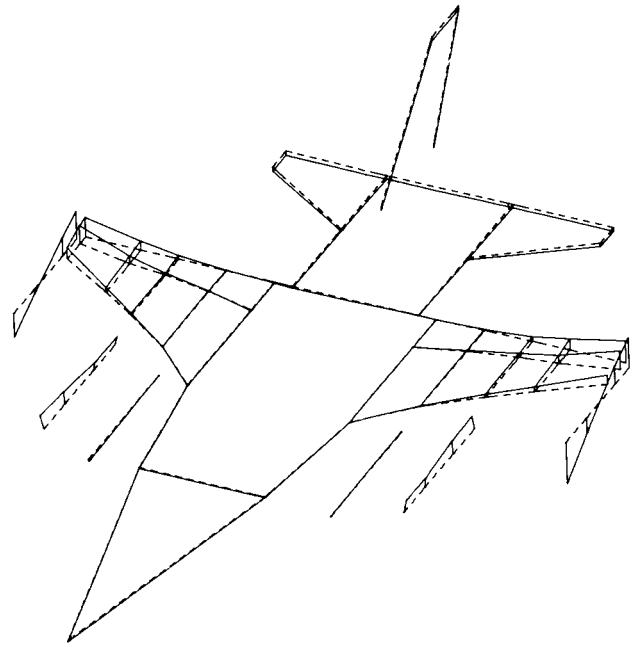


(d) Frequency, 5.27 Hz; GBU-8 lateral (right).
Partial survey.

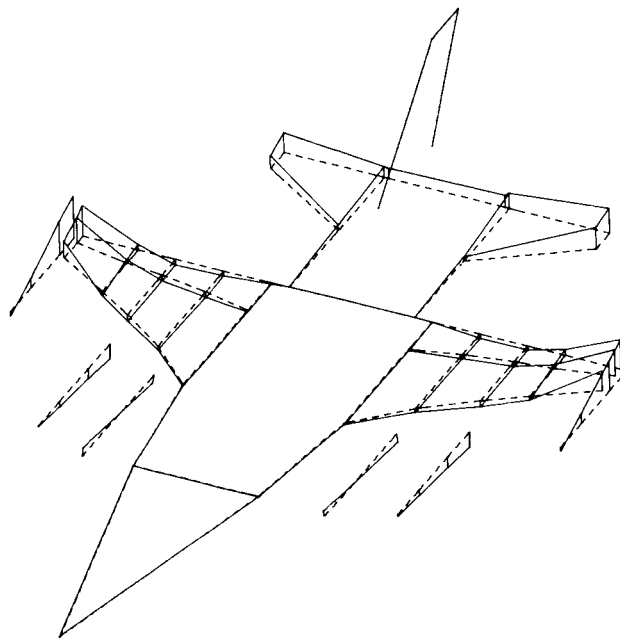
Figure B1. Symmetric mode shapes.



(e) Frequency, 5.46 Hz; GBU-8 lateral (left).
Partial survey.

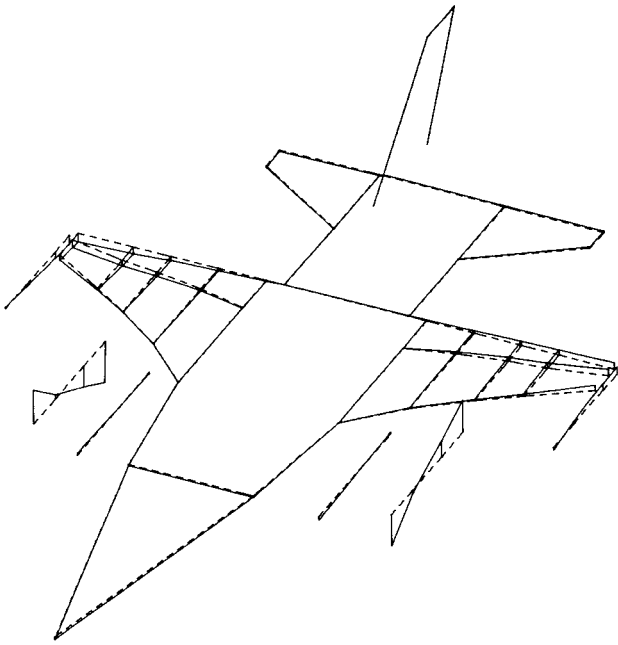


(f) Frequency, 6.09 Hz; tip missile pitch.

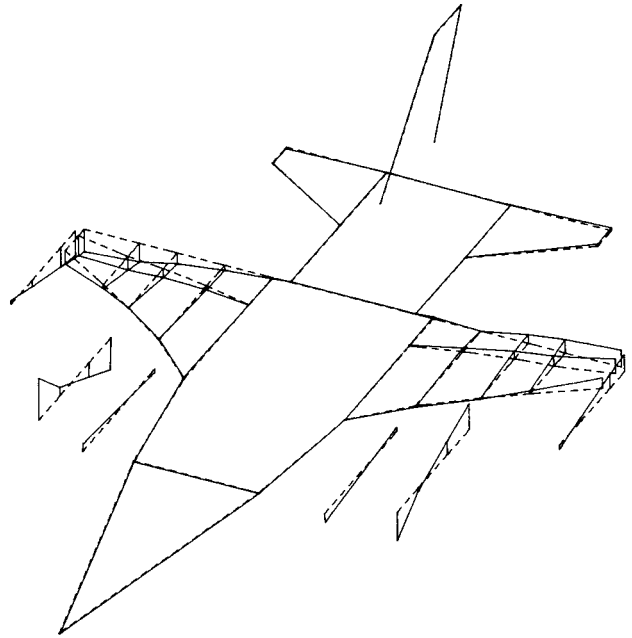


(g) Frequency, 9.64 Hz; second wing bending.

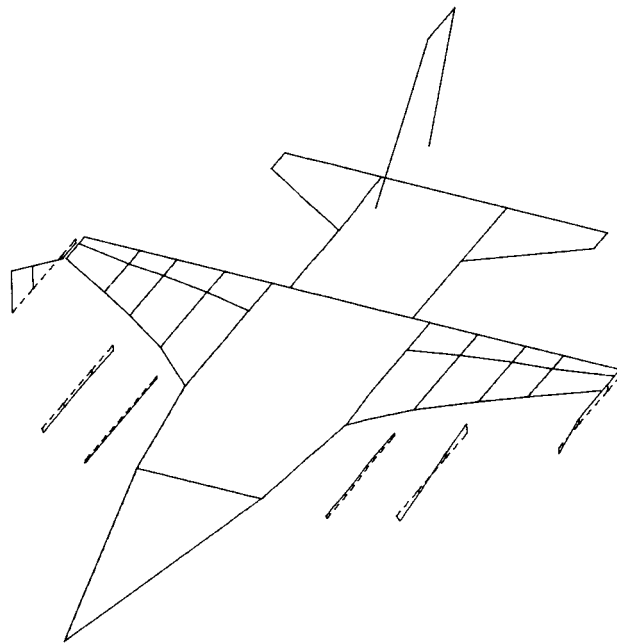
Figure B1. Concluded.



(a) Frequency, 3.29 Hz; GBU-8 pitch.

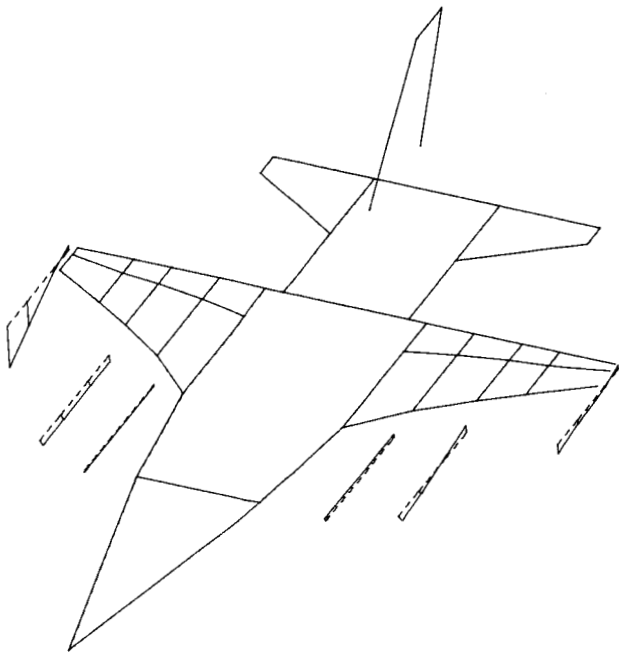


(b) Frequency, 4.55 Hz; pylon strongback bending (pylon nose up).

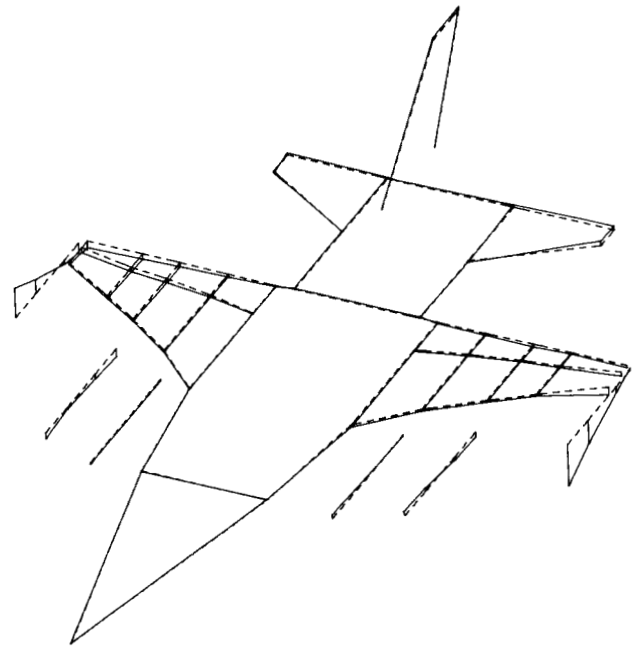


(c) Frequency, 4.94 Hz; GBU-8 lateral (left). Partial survey.

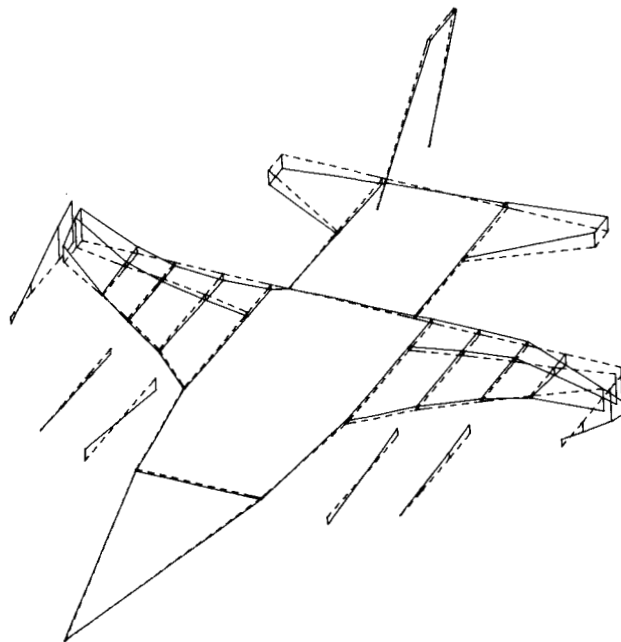
Figure B2. Antisymmetric mode shapes.



(d) Frequency, 5.18 Hz; GBU-8 lateral (right).
Partial survey.



(e) Frequency, 5.53 Hz; tip missile pitch.



(f) Frequency, 8.66 Hz; first wing bending.

Figure B2. Concluded.

1. Report No. NASA TM-87634	2. Government Accession No.	3. Recipient's Catalog No.	
4. Title and Subtitle Ground Vibration Test of an F-16 Airplane With Modified Decoupler Pylons		5. Report Date April 1986	
		6. Performing Organization Code 505-33-43-07	
7. Author(s) F. W. Cazier, Jr., and M. W. Kehoe		8. Performing Organization Report No. L-16065	
		10. Work Unit No.	
9. Performing Organization Name and Address NASA Langley Research Center Hampton, VA 23665-5225		11. Contract or Grant No.	
		13. Type of Report and Period Covered Technical Memorandum	
12. Sponsoring Agency Name and Address National Aeronautics and Space Administration Washington, DC 20546-0001		14. Sponsoring Agency Code	
		15. Supplementary Notes F. W. Cazier, Jr.: Langley Research Center, Hampton, Virginia. M. W. Kehoe: Ames Research Center, Dryden Flight Research Facility, Edwards, California.	
16. Abstract The decoupler pylon is a passive wing/store flutter suppression device. It was modified to reduce friction following initial flight tests. A ground vibration test was conducted on an F-16 airplane loaded on each wing with a one-half-full (center bay empty) 370-gal fuel tank mounted on a standard pylon, a GBU-8 store mounted on the decoupler pylon, and an AIM-9J missile mounted on a wingtip launcher. The test was conducted prior to flight tests with the modified pylon to determine modal frequencies, mode shapes, and structural damping coefficients. Data presented include frequency response plots, mode shape plots, and limited force-effect plots.			
17. Key Words (Suggested by Authors(s)) Ground vibration tests F-16 airplane Structural dynamics Decoupler pylon		18. Distribution Statement Unclassified—Unlimited Subject Category 05	
19. Security Classif.(of this report) Unclassified	20. Security Classif.(of this page) Unclassified	21. No. of Pages 63	22. Price A04